RGS16 IS A PANCREATIC REPORTER OF CHRONIC

HYPERGLYCEMIA IN DIABETES

APPROVED BY SUPERVISORY COMMITTEE

Thomas Wilkie, Ph.D. _____

Raymond MacDonald, Ph.D. _____

Ondine Cleaver, Ph.D. _____

Kosaku Uyeda, Ph.D. _____

DEDICATION

I dedicate this dissertation to my mother and father who made me the person I am. I hereby remember my late grandfather Mehmet Yaman (died on May 1, 1980) and the late brother of my aunt Harzem Nazli (died on March 27, 2009) who both died of diabetic complications. I also honor the memory of our late neighbor Saniye Menguc (died on March 29, 2003) who suffered from diabetes.

RGS16 IS A PANCREATIC REPORTER OF CHRONIC HYPERGLYCEMIA IN DIABETES

by

OZHAN OCAL

DISSERTATION

Presented to the Faculty of the Graduate School of Biomedical Sciences

The University of Texas Southwestern Medical Center at Dallas

In Partial Fulfillment of the Requirements

For the Degree of

DOCTOR OF PHILOSOPHY

The University of Texas Southwestern Medical Center at Dallas

Dallas, Texas

November, 2011

RGS16 IS A PANCREATIC REPORTER OF CHRONIC HYPERGLYCEMIA IN DIABETES

Ozhan Ocal, Ph.D.

The University of Texas Southwestern Medical Center at Dallas, 2011

Thomas Wilkie, Ph.D.

Diabetes mellitus is a collection of metabolic diseases with chronic hyperglycemia as their common syndrome. Type 1 diabetes results from pancreatic insulin producing beta cell loss due to autoimmune attack and consequent insulin insufficiency, whereas type 2 diabetes occurs as a result of somatic cell insulin resistance under metabolic stress. Therapies include insulin supplementation for type 1 diabetics and diet control and augmented insulin release for type 2 diabetics. G-protein coupled receptors (GPCR) represent the largest non-antibiotic drug targets and several family members are expressed in

beta cells. Regulators of G-protein Signaling (RGS) proteins are feedback regulators of GPCRs. Their expression can be induced by GPCR or cross-talk signals to inhibit GPCR pathway, thereby indicating when and where GPCR signaling occurs. Our studies utilizing Rgs16::GFP transgenic mouse previously showed that Rgs16 was expressed in embryonic pancreatic progenitor cells, endocrine cells, and postnatal vessel and ductal associated cells (VDAC). Euglycemic adults lacked pancreatic Rgs16::GFP expression. We investigated diabetic mice to determine if Rgs16::GFP would reactivate during beta cell expansion in adulthood. The type 1 diabetic models of beta cell death were streptozotocin (STZ) treatment and PANIC-ATTAC mice. Type 2 diabetic models consisted of *ob/ob* mice and diet induced obesity. In each case, Rgs16::GFP expression initiated in islets and VDAC after at least 6 days of chronic hyperglycemia. STZ induced Rgs16::GFP expression was reduced after lowering blood glucose levels with systematic insulin administrations. Furthermore, hyperglycemia dependent Rgs16::GFP expression required metabolic transcription factor Carbohydrate Response Element Binding Protein (ChREBP), as pancreatic Rgs16::GFP was absent in STZ-treated ChREBP KO mice. We found that Rgs16::GFP is also expressed in Pancreatic Ductal Adenocarcinoma (PDAC) tumors and primary tissue culture cells. RNA-Seq analysis revealed that cultured PDAC cells express many genes in common with embryonic progenitors of ductal and endocrine cells and identified expression of 63 GPCRs. In summary, our results suggest that Rgs16::GFP is stimulated by GPCR signals relayed from a “hyperglycemia sensor”. We propose that Rgs16 is a faithful pancreatic biomarker of diabetes and Rgs16::GFP PDAC culture and diabetic reporter mice are beneficial resources to identify ligands that stimulate beta cell expansion without promoting cancer.

TABLE OF CONTENTS

LIST OF FIGURES

LIST OF ABBREVIATIONS

ChREBP (Mlxipl): Carbohydrate response element binding protein (Max-like factor X interacting protein-like)

(d)KO: (double) Knock-out

Dpp4: Dipeptidylpeptidase-4

(e)GFP: (enhanced) Green fluorescent protein

FACS: Fluorescence-activated cell sorting

FBS: Fetal bovine serum

GAP: GTPase activating protein

Gip: Gastric inhibitory peptide

Glp1: Glucagon-like peptide-1

GPCR: G-protein coupled receptor

GSIS: Glucose stimulated insulin secretion

HAT: Histone acetyl transferase

HDAC: Histone de-acetylase

HF: High fat

i.p.: Intraperitoneal

ISX: Isoxazole

NOD-SCID: Nonobese diabetic/severe combined immunodeficient

PANIC-ATTAC: Pancreatic islet beta-cell apoptosis through targeted activation of caspase-8

PDAC: Pancreatic ductal adenocarcinoma

Rgs: Regulator of G-protein signaling

RNA-Seq: RNA sequencing

STZ: Streptozotocin

VDAC: Vessel and ductal associated Rgs16::GFP positive cell

WT: Wild-type

INTRODUCTION

Diabetes epidemic

Diabetes mellitus is a collection of debilitating metabolic diseases described by insufficient insulin action causing above normal basal glucose levels as the common syndrome of all patients (Bell and Polonsky, 2001; Guney and Gannon, 2009; Hotamisligil, 2006; Saltiel, 2001). Although the disease can manifest itself at different ages, show various degrees of severity and can occur in conjunction with other diseases, it is generally grouped under two categories: type 1 and type 2 diabetes (Bell and Polonsky, 2001). In all vertebrates, the endocrine hormone insulin is produced and secreted by the pancreatic beta cells in the Islets of Langerhans (Lacy, 1957, 1961; Langerhans, 1869; Saltiel, 2001; Weir and Bonner-Weir, 1990). Insulin lowers blood glucose by stimulating glucose uptake by peripheral tissues, such as fat and skeletal muscle, and the cessation of glucose production in liver after a meal (Chang et al., 2004; Lacy, 1975; Matschinsky, 2005; Matschinsky and Collins, 1997). Type 1 diabetes is caused by autoimmune attack and loss of insulin producing beta cells (Hotamisligil, 2006; Mathis et al., 2001). Since patients with type 1 diabetes retain proper insulin responses in their somatic cells, they supplement insulin externally to restore blood glucose to normal levels (Bluestone et al., 2010). Type 2 diabetes, on the other hand, develops over many years in humans. Type 2 is caused by insufficient insulin production that can not overcome resistance to insulin action in somatic cells of the peripheral tissues (Polonsky et al., 1996; Wellen and Hotamisligil, 2005). Somatic cells contain transmembrane receptors for the hormone insulin, which upon binding by insulin lead to activation of glucose transporters at the cell surface (Saltiel, 2001). Glucose is taken up by these transporters into the cell, thus lowering its levels in the circulating blood (Saltiel, 2001). However once glucose

uptake can no longer be accomplished at sufficient levels, it leads to elevated basal glucose concentration in the blood – the hallmark of diabetes.

The incidence of diabetes mellitus has greatly increased in developed countries in the last decades, primarily due to the increase in obesity and associated type 2 diabetes (Cowie et al., 2009; Stein and Colditz, 2004; Zimmet et al., 2001). Diabetes can be regarded as an increasing public health challenge that threatens to affect more people in the future (Saltiel, 2001; Wild et al., 2004; Zimmet et al., 2001). Metabolism has been widely studied by countless researchers for a long time and discoveries in understanding disease progression, molecular components, and energy balance together with new technologies have greatly advanced diagnosis, prognosis, and treatment strategies (Sonksen et al., 1978; Walford et al., 1978). Treatments for type 2 diabetes primarily target improving diet, increasing steady exercise, insulin therapy and augmenting insulin sensitivity and production (Ahren and Schmitz, 2004; Guney and Gannon, 2009; Moller, 2001; Saltiel, 2001). The primary treatment for type 1 diabetes is daily insulin injection but active areas of research include beta cell replacement by transplantation of islets, transdifferentiation of other cell types into insulin secreting cells, differentiated embryonic stem (ES) cells or induced pluripotent stem (iPS) cells combined with immune suppression (Bertuzzi et al., 2006; Borowiak, 2010; Couzin-Frankel, 2011; Hughes et al., 1992; Jonasson and Hoversten, 1978; Lacy, 1995; Lacy et al., 1980; Nason et al., 1988; Noguchi, 2007, 2010; Sumi, 2011; Tateishi et al., 2008; Yechoor and Chan, 2010).

Technical advancements in glucose meters have shortened measuring blood glucose levels to seconds and new coping strategies provide relief and nearly normal life standards for patients (Kuo et al., 2011; Sonksen et al., 1978; Walford et al., 1978). Nevertheless, diabetes still imposes hardships like insulin injections, dietary constraints, fatigue and potentially lethal excursions into hypoglycemia (Bluestone et al., 2010). Diabetes remains as a debilitating disease

without a certain cure, limiting patients' life, leading to organ malfunction, blindness, stroke, heart failure, and eventually to death.

This dissertation aims to contribute to pancreatic islet biology and diabetes research by introducing a novel method of identifying endogenous signals that stimulate beta cell regeneration and expansion. The reporter we use is a Regulator of G protein Signaling gene (Rgs16). The onset and progression of Rgs16 transcription makes it unique among pancreatic markers (Villasenor et al., 2010). In this dissertation, we characterize the expression of Rgs16 under diabetic conditions in several mouse models of diabetes and metabolic syndrome. We correlate the induction and continued expression of Rgs16 with blood glucose levels over time to uncover a connection with "hyperglycemia sensor" (Arees and Mayer, 1967; Leloup et al., 1998; Matschinsky, 2005; Thorens, 2001). We propose this sensor sends signals to the pancreas after it becomes apparent that insulin action is no longer sufficient to manage blood glucose levels (Delaere et al., 2010; Thorens, 2001). Target cells that express Rgs16 are islet beta cells and vessel/ductal associated cells (VDAC) in pancreas (Villasenor et al., 2010). VDAC expression was particularly fortuitous, as it led us to find Rgs16 expression in early pancreatic ductal adenocarcinoma (PDAC), the forth leading cause of cancer deaths in the USA (Aguirre et al., 2003; Ettinghausen et al., 1995; Hruban et al., 2001; Zimmerman et al., 1981). We develop a culture system using PDAC cells that complements our *in vivo* settings to test and design new and better drugs for the treatment of diabetes mellitus (Sipos et al., 2003).

Glucose homeostasis

Glucose is one of the most commonly used energy sources since the beginning of life on earth (Benzo, 1983). The utilization of this six-carbon sugar has a highly conserved evolutionary origin and its initial set of energy giving

reactions, glycolysis, involves identical steps taking place in the cytoplasm of prokaryotes and eukaryotes in both aerobic and anaerobic conditions (Meyerhof, 1927). Energy yielding reactions of this early glucose breakdown to pyruvate produce the first energy carrying compound, ATP, and electron carrier, NADH (Lohmann, 1929). The subsequent tricarboxylic acid cycle is also highly conserved in organisms and generates further NADH and metabolite intermediates that feed both catabolic and anabolic reactions in fatty acid or amino acid metabolism (Saraste, 1999). Under aerobic conditions in eukaryotes, reduced co-enzyme NADH created in the previous steps culminates in the bulk of ATP synthesis coupled to electron transport in mitochondria (Saraste, 1999). Overall, these steps of glucose breakdown and utilization produce molecular energy and metabolic precursors essential to sustain cellular reactions and much of prokaryotic and eukaryotic life (Alberts et al., 2007).

During the course of evolution, regulation of glucose metabolism inside the organism has become complex. Vertebrates evolved special features in several organs to tightly control glucose availability (Gerich, 1993). In mouse, the model organism we used throughout our work in this dissertation, organs important for the regulation of available glucose levels are indicated in Figure 1 (Cook, 1965). As carbohydrates are processed in the digestive tract and finally absorbed by the intestine, glucose is directed to liver by the portal vein. In the liver, UDP-Glucose monomers are converted to glycogen by the enzyme glycogen-synthase for short-term storage (Bollen et al., 1998; Nuttall et al., 1988; Unger, 1971). Excess glucose is a precursor for fatty acids, which are converted to triglycerides and stored in the adipose tissue for long-term availability (Alberts et al, 2007). Meanwhile, glucose is released to the blood stream and becomes available to somatic cells, such as skeletal muscle, as well as the brain and red blood cells (Saltiel, 2001). As glucose levels rise in the blood, pancreatic beta cells take up

Figure 1: Glucose homeostasis

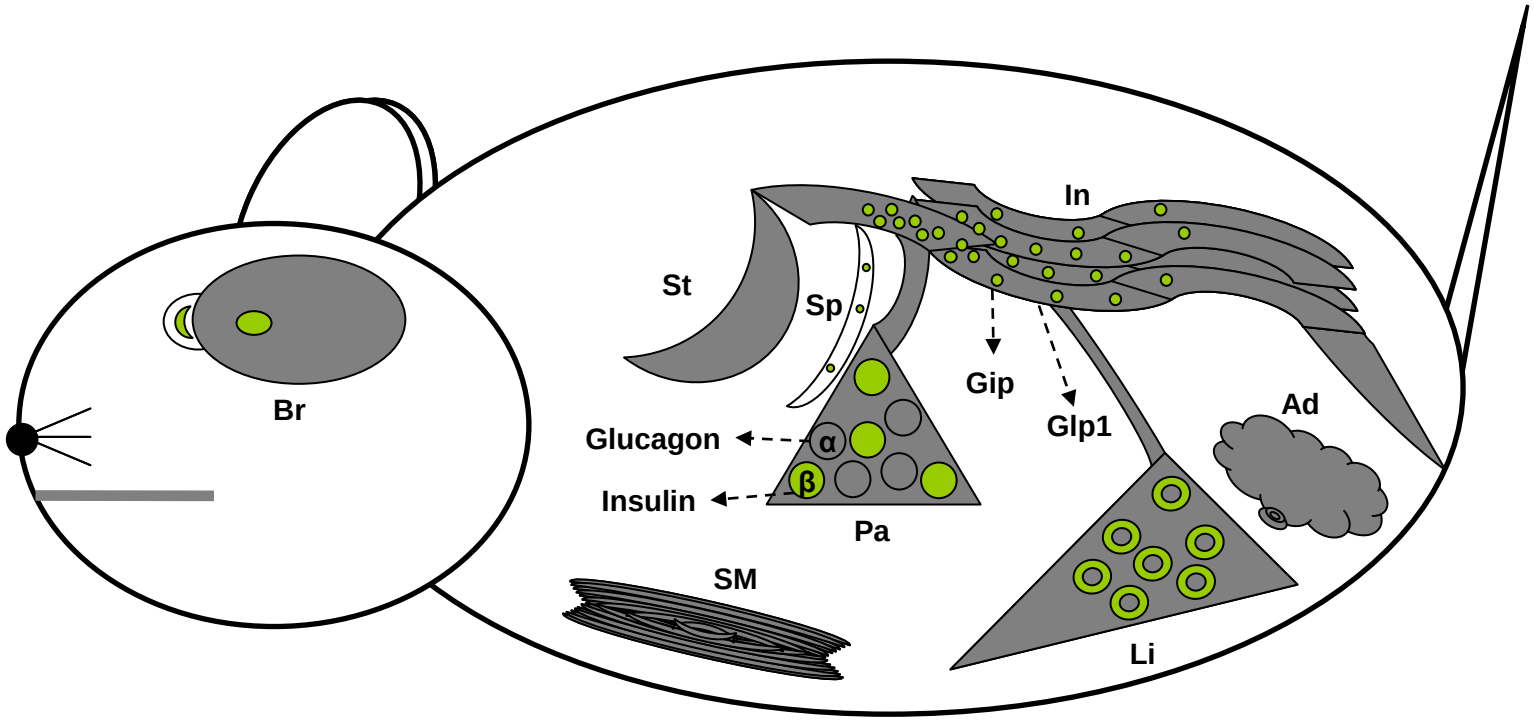

glucose and convert it to ATP (Chen et al., 1990). The increased ATP : ADP ratio causes Ca^{2+} levels inside islets to rise (Saltiel, 2001). Intracellular Ca^{2+} then stimulates the previously synthesized insulin vesicles to fuse with cell membrane and release insulin (Frankel et al., 1981; Hellman, 1975; Lacy, 1972; Siegel et al., 1980). As beta cells continue to utilize glucose for ATP production, they maintain secretion of recently created insulin at a steady state (Cherrington et al., 2002; Kanatsuka et al., 1987). Insulin release is also stimulated by intestinal hormones GLP1 and GIP (Kreymann et al., 1987; Miyawaki et al., 1999; Mojsov et al., 1986; Nauck et al., 2004; Polak et al., 1971; Sutherland and De Duve, 1948; Takeda et al., 1987; Taminato et al., 1977). Insulin dictates glucose uptake by somatic cells, while it also suppresses the release of its antagonistic pancreatic hormone, glucagon (Quesada et al., 2008; Saltiel, 2001). When glucose levels decline during the later post-prandial period, glucagon secreted from the alpha cells of the islets raises blood glucose levels by stimulating glycogenolysis which eventually yields individual glucose molecules that can enter the blood stream (Cherrington, 1999; Foster, 1984; Gromada et al., 2007; Quesada et al., 2008; Weir and Bonner-Weir, 1990). As glycogen becomes depleted, glucagon then triggers gluconeogenesis from non-carbohydrate precursors in the liver (Quesada et al., 2008). Glucagon controls glycolysis and lipolysis rates which, in turn, are important for gluconeogenesis (Foster, 1984; Unger, 1985). All these reactions

Figure 1: Glucose homeostasis
Gray structures depict organs of metabolism. Rgs16::GFP expression under various conditions is indicated as green color. Abbreviations are Br: Brain, Ad: Adipose tissue, St: Stomach, Pa: Pancreas, Li: Liver, Sp: Spleen, In: Intestine (small and large), SM: Skeletal Muscle, Ins: Insulin, Gluc: Glucagon. Tissues that are not relevant to glucose homeostasis are white. The tissues we observed with Rgs16::GFP expression are olfactory bulb (Br), hypothalamus (Br), islets (Pa), hepatocytes (Li), intestinal cells (In), and splenic cells (Sp). Endocrine hormones insulin and glucagon are secreted from pancreas, whereas Glp1 is secreted from intestine. Organ shapes, sizes, and locations are arbitrary (Cherrington, 1999; Cook, 1965; Villasenor et al., 2010; unpublished observations).

result in elevation and restoration of blood glucose levels (Cherrington, 1999; Unger, 1985). Insulin and glucagon represent the two opposite players of glucose utilization inside the body and balance each other's action in healthy energy homeostasis (Gromada et al., 2007; Klover and Mooney, 2004; Unger, 1978, 1985).

Diabetic mouse models

Glucose homeostasis is disrupted when insulin levels are no longer sufficient to stimulate glucose uptake. Hyperglycemia can result either from depletion of beta cells which are the sole source of insulin production or due to intracellular defects in insulin signaling in the somatic cells (Bell and Polonsky, 2001; Guney and Gannon, 2009; Vranic, 1992). These type 1 and type 2 diabetic conditions, respectively, are characterized by above normal physiological blood glucose concentration and require insulin treatment and dietary control.

Since the discovery of insulin and its function nearly a century ago, scientific research has focused on components and management of energy balance (Banting and Best, 1922). Insulin treatment became available by initially isolating its homolog from porcine and later by artificially producing insulin analogues using recombinant DNA technology (Chance et al., 1968). In recent years, several drugs have been designed and approved for patients with diabetes. Drugs that enhance insulin secretion have captured an important part of pharmaceutical endeavors (Ahren, 2009; Ahren and Hughes, 2005; Ahren and Schmitz, 2004; Saltiel, 2001). For initial testing of drug effects *in vivo*, scientists have relied on diabetic model organisms mimicking the human condition to study this disease.

During our studies characterizing Rgs16 gene expression, we also utilized diabetic mouse models (Figure 2) (Gannon, 2001). To mimic type 1 diabetes, we used two mouse models of beta cell apoptosis that result in insufficient insulin

Figure 2: Diabetic mouse models

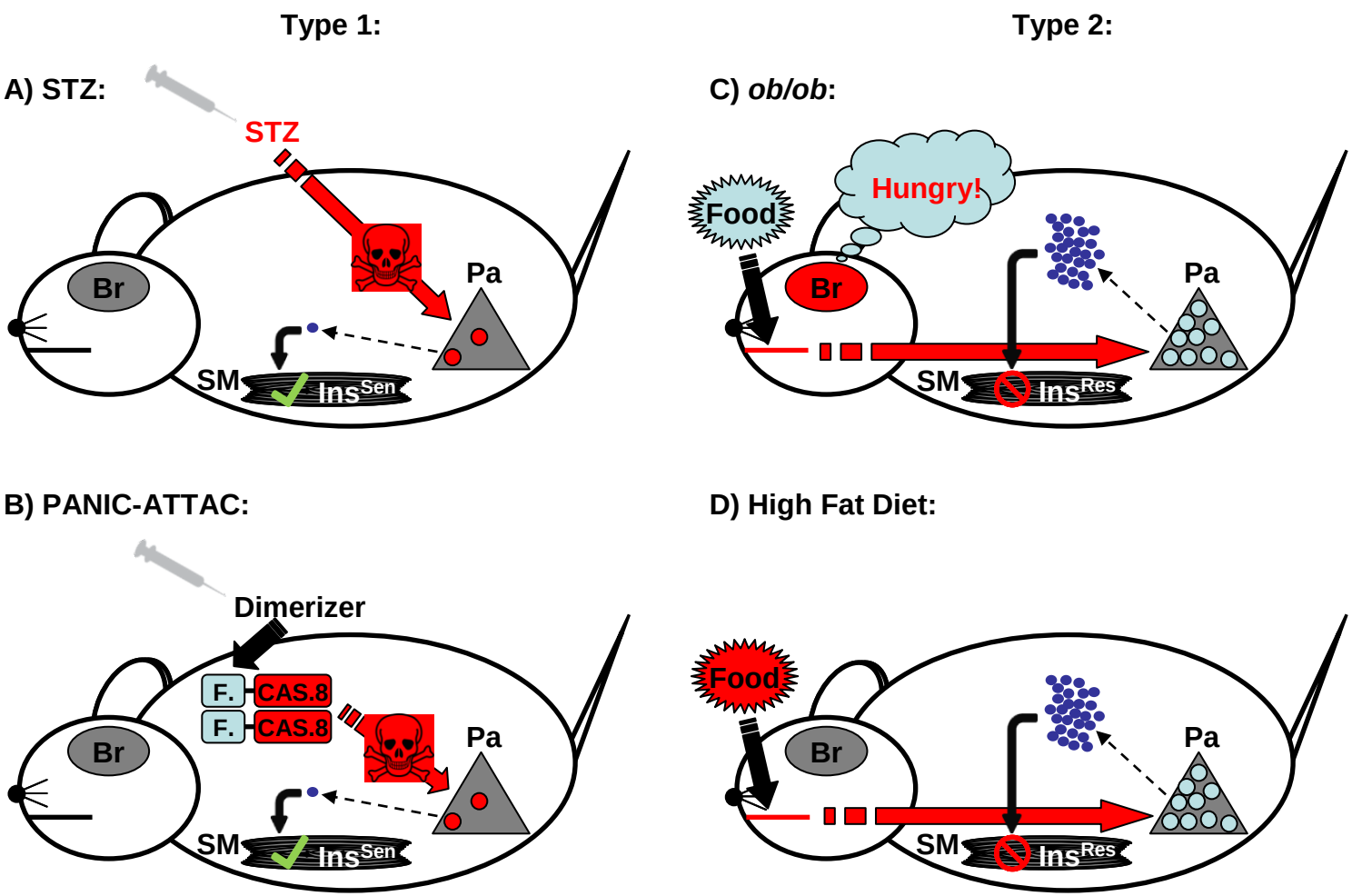

production. We used the glucose mimetic streptozotocin (STZ) treatment of mice for the fastest way of causing hyperglycemia (Figure 2A) (Brosky and Logothetopoulos, 1969; Ganda et al., 1976; Like and Rossini, 1976; Schnedl et al., 1994; Vavra et al., 1959). STZ enters pancreatic beta cells via GLUT2 transporters and causes DNA damage and presentation of auto-antigens, both of which trigger apoptosis (Huang and Taylor, 1981; Mansford and Opie, 1968; McEvoy et al., 1984; Paik et al., 1980; Rerup, 1970; Rossini et al., 1977; Schnedl et al., 1994). We also utilized another mouse model of beta cell apoptosis which differs from STZ treatment by its ability to recover normal glycemia. The "Pancreatic islet beta-cell apoptosis through targeted activation of caspase8" (PANIC-ATTAC) mouse model, created by Philipp Scherer and his colleagues, is a transgenic model in which an FKBP-fused Caspase8 gene was inserted into the genome (Figure 2B) (Pajvani et al., 2005; Wang et al., 2008). Islet specific expression is achieved by the rat insulin promoter (RIP) lying upstream of the fusion gene and restricting its expression to beta cells. CASPASE8 monomers are inactive and therefore naïve animals are non-diabetic. Injection of an agent (dimerizer) that causes pairing of 2 FKBP domains brings about dimerization of CASPASE8 monomers (Trujillo et al., 2005). Active CASPASE8 dimers initiate

Figure 2: Diabetic mouse models
Diabetic mouse models we have utilized in our studies are outlined. Red color highlights the part that causes diabetes and affects pancreatic beta cells. Skull mark indicates beta cell death. For Type 1 diabetes, STZ and dimerizer are injected intraperitoneally. Abbreviations are B: Brain, P: Pancreas, SM: Skeletal Muscle, Ins^{Sen}: Insulin sensitive, Ins^{Res}: Insulin resistant. F.CAS8: FKBP-CASPASE8 fusion protein. Dimerizing F.-CAS8 proteins are actually inside pancreatic beta cells but drawn outside due to space limitations. Small blue circles represent insulin in the blood, whereas check mark and stop symbols indicate status of intracellular insulin response. Organ shapes, sizes, and locations are arbitrary (Campfield et al., 1996; Ganda et al., 1976; Hamann and Matthaei, 1996; Pajvani et al., 2005; Schnedl et al., 1994; Tsunoda et al., 1998; Wang et al., 2008).

the apoptotic pathway inside beta cells, causing depletion of beta cells and subsequent insulin insufficiency (Trujillo et al., 2005; Wang et al., 2008).

To study type 2 diabetes, we incorporated leptin-deficient mice in our studies (Figure 2C) (Spiegelman and Flier, 2001; Zhang et al., 1994). Leptin is a hormone released by adipose tissue that suppresses hunger responses in the brain (Friedman, 2000; Friedman and Halaas, 1998). Obese, hyperphagic mice were discovered with a naturally occurring recessive point mutation in the leptin gene (Campfield et al., 1996; Hamann and Matthaei, 1996; Zhang et al., 1994). Leptin-deficient *ob/ob* animals have lack of appetite control and succumb to overeating (Friedman and Halaas, 1998). This eating-dependent obesity brings about constant burden on blood glucose levels and takes its toll on insulin signaling (Friedman, 2009; Shimabukuro et al., 1997). Animals become insulin resistant and hyperglycemic in couple of weeks after weaning. The severity of both insulin resistance and hyperglycemia increases over time (Friedman and Halaas, 1998). In addition to leptin deficiency-dependent obesity, we also used high fat diet to drive obesity in mice (Figure 2D) (Ikemoto et al., 1996; Tsunoda et al., 1998). Comparing different mouse models helped us understand the dynamics and causes of gene expression changes in terms of disease progression.

GPCR signaling

Cell signaling primarily relies on external ligands that bind to transmembrane receptors at the cell surface to initiate intracellular cascades of second messengers (Rosenbaum et al., 2009). Receptors have been grouped into families according to their conservation of structure and function. Seven-pass transmembrane domain receptors that convey extracellular ligand binding to activation of intracellular heterotrimeric G-proteins have been termed G-protein coupled receptors (GPCR) and constitute the largest family of all receptors

Figure 3: Conventional GPCR signaling

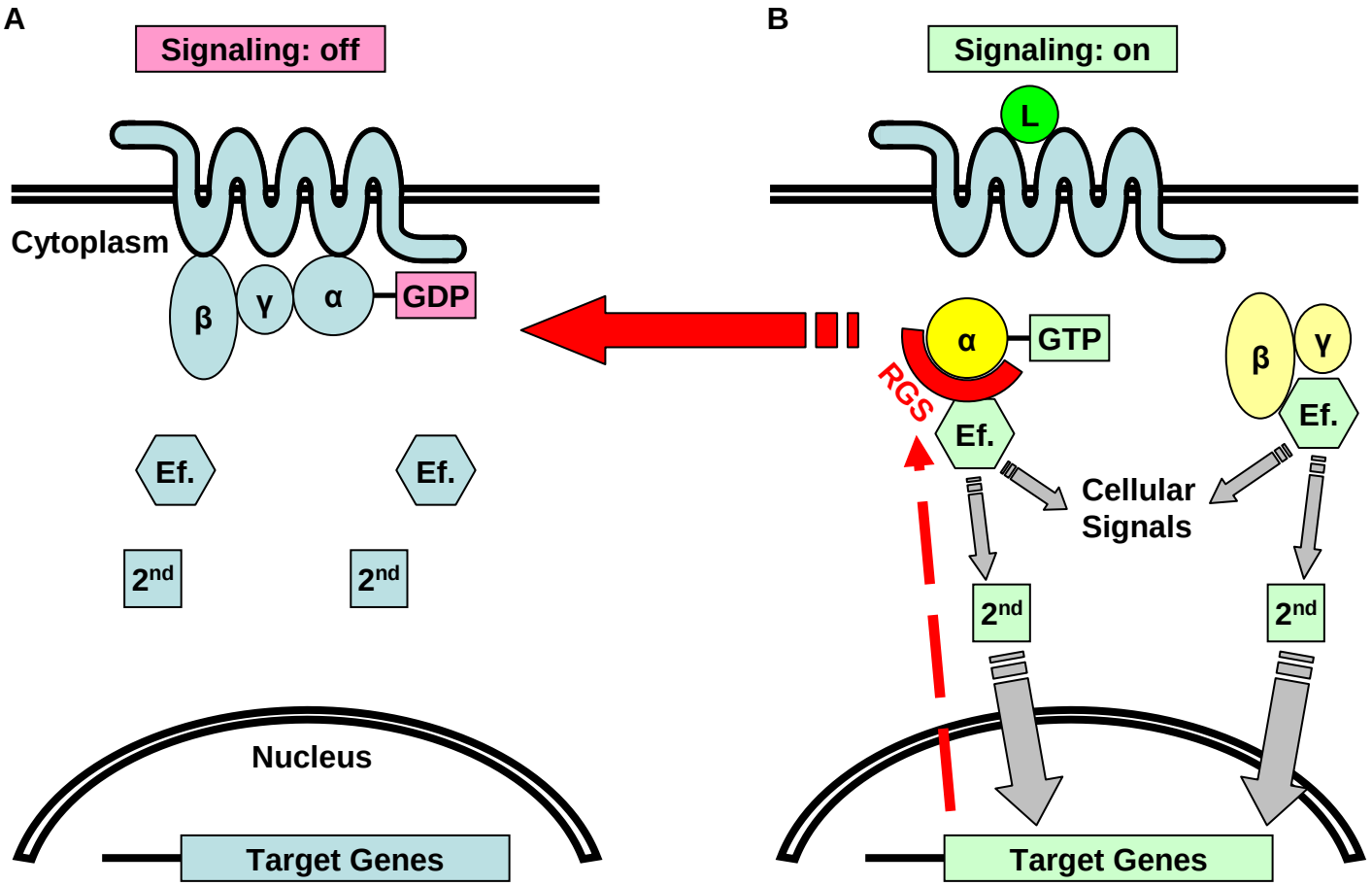

(Casey and Gilman, 1988; Freissmuth et al., 1989). G-proteins are a conserved family of intracellular proteins defined by their binding to GDP and GTP . The heterotrimeric G-protein is composed of a Gα subunit bound to GDP and associated Gβγ subunit in its inactive state (Figure 3A) (Gilman, 1984, 1987). GPCRs are guanine nucleotide exchange factors (GEFs) for the G-protein (Casey and Gilman, 1988). Ligand binding mediates a conformational change of the GPCR which allows GDP to dissociate from the Gα subunit (Dessauer et al., 1996; Kleuss et al., 1994). The high GTP : GDP ratio (about 10:1) inside the cell then maintains GTP binding over GDP to Gα, upon which Gα and Gβγ separate (Dessauer et al., 1996). Both Gβγ and Gα can then individually interact with effector proteins that amplify second messenger production inside the cell (Figure 3B) (Hepler and Gilman, 1992). G-protein interaction with effectors ceases once the intrinsic GTPase activity of Gα cleaves the γ-phosphate group from GTP, turning it into GDP (Kleuss et al., 1994). GDP-bound Gα re-associates with Gβγ subunit and returns into its original inactive state (Mixon et al., 1995). The slow GTPase activity of Gα ensures that dissociated G-protein interacts with effectors long enough to transmit the signal while enabling its recycling (Kleuss et al., 1994). Continued ligand occupation of GPCR re-initiates the G-protein turn-over and maintains a long-lasting signaling relay.

There are about ~800 GPCRs in human genome compared to ~1600 GPCRs in rodents if all olfactory receptors and rodent specific vomeronasal organ receptors are included (Dryer and Berghard, 1999; Fredriksson et al., 2003;

Figure 3: Conventional GPCR signaling
Simplified diagram of conventional GPCR signaling is shown in the on and off state on Panel A and B, respectively. Abbreviations are L: ligand, Ef.: effector, 2nd: 2nd messenger, α, β, γ: heterotrimeric G-protein subunits. Dashed red arrow indicates feedback induction of Rgs gene. Gray striped arrows indicate downstream effects, whereas red striped arrow means conversion of the signaling on Panel B back to that of Panel A (Sierra et al., 2000).

Gaillard et al., 2004; Vanti et al., 2003; Vassilatis et al., 2003). GPCRs have assumed critical roles in organisms ranging from cell migration to visual sensation and hormonal responses (Cotton and Claing, 2009; Ferguson and Caron, 1998; Maeda et al., 2003; Rosenbaum et al., 2009; Wheatley et al., 2003). GPCRs represent the largest segment of non-antibiotic drug targets as of now and the lack of information in many of orphan members could point out the room for expansion of this segment (Xiao et al., 2008). Studies in pancreatic islets have shown the expression of several GPCRs important for insulin secretion and cell differentiation (Ahren, 2009; Pennington, 1987; Regard et al., 2007). Nonetheless, much remains to be learned about their exact signaling function in beta cell physiology and expansion.

GPCR signaling is regulated at multiple steps. Ligand stability and availability controls inception and duration of signals, whereas intracellular regulators can modify GPCR and G-protein to alter their activity (Dessauer et al., 1996). Starting from unicellular eukaryotes, GPCRs have co-evolved with Regulator of G-protein Signaling (Rgs) genes, which are shown to negatively adjust GPCR signaling (Dohlman et al., 1995; Luo et al., 2001; Wilkie and Kinch, 2005). RGSs are GTPase activating proteins (GAPs) that bind and stabilize the transition state of the Gα subunit during GTP-hydrolysis (Berman et al., 1996; Hunt et al., 1996; Watson et al., 1996). By favoring a catalytic intermediate state of Gα, RGSs accelerate phosphate group cleavage and consequently the GDP-bound state of Gα up to 2000-fold (Berman et al., 1996; Natochin et al., 1998; Ross and Wilkie, 2000; Tesmer et al., 1997). This RGS-mediated facilitation of Gα inactivation prevents G-protein-effector interactions, thus inhibiting GPCR signaling. Therefore, extracellular ligands initiate the “on” state of GPCR signaling by inducing GPCRs to act as Guanine-nucleotide exchange factor (GEF), while RGS proteins accelerate transition to the “off” state by acting as GAP (Ross and Wilkie, 2000).

R4 class RGS proteins

All RGS proteins are defined by the RGS domain, a paired helical bundle of approximately 120 amino acids that conveys GAP activity (De Vries et al., 1995; Koelle and Horvitz, 1996; Popov et al., 1997; Tesmer et al., 1997). There are four main families of Gα-subunits termed Gαi, Gαs, Gαq, and Gα12. RGS proteins are GAPs for Gαi and/or Gαq proteins (Berman et al., 1996). A distantly related family of RGS Homology (RH) proteins, termed rgRGS, is Gα12-GAP (Chen et al., 2001). No Gαs-GAPs have been identified (Popov et al., 1997; Wilkie and Kinch, 2005). Rgs genes have been assigned to different classes based on amino acid sequence similarity within the RGS and flanking domains, gene structure, and cellular function (Sierra et al., 2002; Sierra et al., 2000; Wilkie and Kinch, 2005). Mammals express 4 classes of RGS GAPs, termed Rz, R4, R7 and R12 (Ross and Wilkie, 2000). These classes differ with respect to specificity in their interactions with Gα subunits, GPCRs and/or scaffolding proteins (Bansal et al., 2007; Hepler, 1999; Hollinger and Hepler, 2002; McCoy and Hepler, 2009; Sierra et al., 2000). R4 class proteins, such as Rgs16 and Rgs8, typically have a short N-terminal amphipathic helix that anchors the protein to the inner leaflet of the plasma membrane and an RGS domain (Bansal et al., 2007; Bernstein et al., 2000; Chen et al., 1999; Heximer et al., 2001; Ross and Wilkie, 2000; Saitoh et al., 2001; Srinivasa et al., 1998; Zeng et al., 1998).

The ten R4 class Rgs genes are thought to have derived via gene duplications and are found in three clusters on chromosome 1 of humans and mice, with the exception of Rgs3 (Figure 4) (Sierra et al., 2002). Although R4 class proteins have some differences in substrate specificity and receptor interactions, functional differences within the R4 class can be also conveyed by tissue distribution and temporal expression determined by cell type specific

Figure 4: R4 class RGS proteins in mice

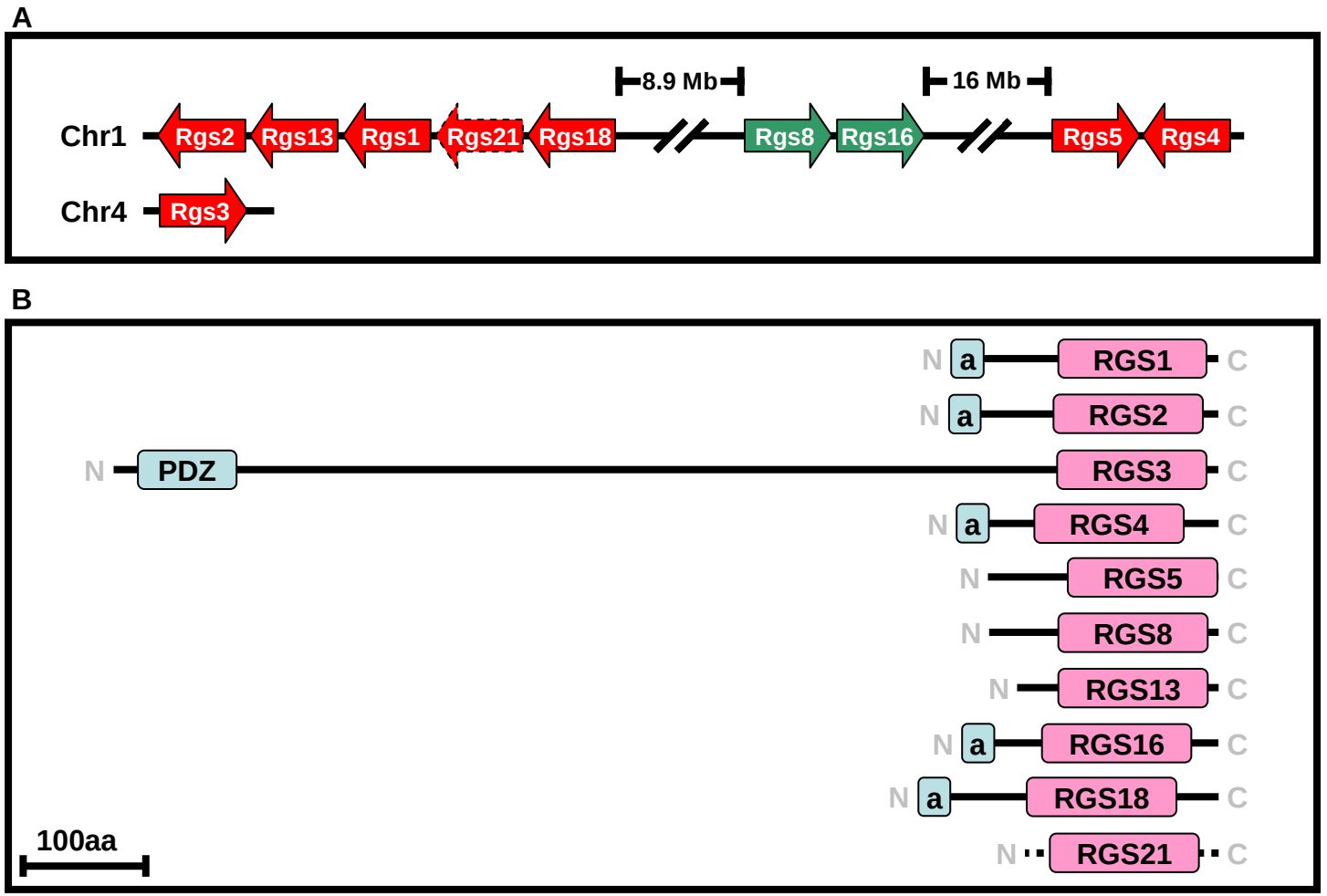

physiology (Gold et al., 1997; Mittmann et al., 2001; Neitzel and Hepler, 2006; Ni et al., 1999; Nomoto et al., 1997; Seki et al., 1998; Wang et al., 1998; Xu et al., 1999b; Yowe et al., 2001; Zeng et al., 1998). The two RGS genes of primary interest in this thesis, Rgs16 and Rgs8, are most closely related to each other among all R4 class proteins. Rgs16 and Rgs8 are tandemly duplicated in a head to tail order separated by ~43 kb (Sierra et al., 2002). Although they exhibit some differences in their expression, such as Rgs16 in suprachiasmatic nuclei (SCN) and Rgs8 in Purkinje cells of the cerebellum, they are co-expressed during pancreas development and isletogenesis, in diabetes and in liver of fasting mice (Doi et al., 2011; Gold et al., 1997; Gong et al., 2003; Grafstein-Dunn et al., 2001; Huang et al., 2006; Itoh et al., 2001; Villasenor et al., 2010). Because of their overlapping expression pattern and similar biochemical functions, Rgs16 and Rgs8 are thought to be functionally redundant in pancreas and liver (Huang et al., 2006; Villasenor et al., 2010). Identifying their unique and shared functions requires analysis of single and double knockout mice. In this thesis, we are primarily concerned with their utility as markers of GPCR signaling activity in pancreas.

Figure 4: R4 class RGS proteins in mice
Chromosomal locations of R4 class Rgs genes are shown in Panel A. Arrow directions indicate transcription direction on the forward strand. Dashed borderline indicates annotation in progress. Green colored arrows represent the Rgs8 and Rgs16 genes with GFP insertion in our reporter mice which were used for expressional analysis. Distances between Rgs gene clusters on chromosome1 are indicated in megabase (Mb) above. Arrow sizes and distances in-between are arbitrary. R4 class RGS protein lengths and domains are compared in Panel B. Proteins are aligned from N towards C terminus left to right. Pink boxes indicate the relative position of the conserved RGS domain for the labeled proteins. Dashed line indicates annotation in progress. Blue "PDZ" box shows PDZ domain. Blue "a" box shows N-terminal amphipathic helix of certain proteins. Scale bar is 100 amino acids long (Ross and Wilkie, 2000; Sierra et al., 2002).

Rgs8::GFP and Rgs16::GFP reporter mice

Rgs gene transcription can be induced by the GPCR signaling that RGS proteins feedback inhibit (Burchett et al., 1999; Burchett et al., 1998; Chakir et al., 2011; Eszlinger et al., 2004; Grant et al., 2000; Hendriks-Balk et al., 2009; Klinger et al., 2008; Miles et al., 2000; Nakagawa et al., 2001; Park et al., 2002; Romero et al., 2006; Singh et al., 2007; Stuebe et al., 2008; Taymans et al., 2003; Zhang et al., 2011b; Zou et al., 2006). Their expression can be also enhanced by non-GPCR ligands in cross-talk mechanisms (Beadling et al., 1999; Fong et al., 2000; Giorelli et al., 2002; Gunaje et al., 2011; Iwai et al., 2007; Iwaki et al., 2011; Ni et al., 1999; Panetta et al., 1999; Pepperl et al., 1998; Perrier et al., 2004; Reif and Cyster, 2000; Riekenberg et al., 2009; Takata et al., 2008; Takesono et al., 1999; Xie et al., 2010; Yang et al., 2007). As R4 class Rgs mRNAs and proteins have short half-lives, induced and ongoing transcription and consequent mRNA accumulation indicate active GPCR signaling (Burchett et al., 1998; Garnier et al., 2003; Gold et al., 2003; Huang et al., 2006; Ingi et al., 1998; Kardestuncer et al., 1998; Krumins et al., 2004; Miles et al., 2000; Pepperl et al., 1998; Siderovski et al., 1994). Rgs gene expression can be therefore utilized as reporter for when and where GPCR signaling occurs (Villasenor et al., 2010).

In order to follow Rgs gene expression, mice with an eGFP reporter transgene were constructed within the GENSAT project (Chalfie et al., 1994; Davenport and Nicol 1955; Gong et al., 2003; Heim et al., 1995; Prasher et al., 1992; Shimomura et al., 1962; Tsien, 1998). The transgene consisted of eGFP gene insertion in the 5’ mRNA leader sequence just upstream of the translation start site of Rgs8 and Rgs16 (Yang et al., 1997). The resulting transgene was recombined within a Bacterial Artificial Chromosome (BAC) and then integrated into the mouse genome (Gong et al., 2003). Thus, eGFP gene expression would be induced from the endogenous Rgs gene promoter in tissues where the relevant

endogenous Rgs gene expresses (Chalfie et al., 1994; Gong et al., 2003; Heintz, 2001); unpublished observations).

Both genes were expressed in the pancreatic bud starting from e8.5 to e9 (Villasenor et al., 2010). The expression in pancreatic progenitor cells, which give rise to all cell lineages of the adult pancreas, continued throughout the secondary transition of pancreas development, and during late embryogenesis became restricted to cells of endocrine lineage with about 2% of the GFP+ cells remaining in the ductal epithelium (Lammert et al., 2003; Villasenor et al., 2010). Rg8::GFP and Rg16::GFP expression diminished in islets within the first two postnatal weeks, but persisted in cells that are lined along the pancreatic vessels and ducts (Villasenor et al., 2010). The expression in these vessel and ductal associated cells (VDAC) also disappeared by the end of forth postnatal week. Healthy young adults were devoid of Rgs8::GFP or Rgs16::GFP expression in pancreas (Villasenor et al., 2010).

The pancreatic progenitor cell expression of Rgs8::GFP and Rgs16::GFP suggested that there were important GPCR signals active during pancreas development that have not been identified previously. Cessation of Rgs8 and Rgs16 gene expression in adult pancreas suggested that elevated expression of these genes may not be required for daily insulin release. However, extreme metabolic demand that promotes islet expansion could also re-activate these Rgs genes (Ackermann and Gannon, 2007). We therefore embarked on a study characterizing their gene expression in adult diabetic pancreas using mouse models of diabetes. We focused on Rg16::GFP expression as it was the most pronounced of the two redundantly expressed genes.

MATERIALS AND METHODS

Mouse maintenance and diet

All animals were maintained on a 12hr light and 12hr dark daily cycle at constant room temperature with lights turned on at 6 am (Zeitgeber Time 0, ZT0) and off at 6 pm (ZT12). All mice were maintained according to the rules and standards of UT Southwestern Institutional Animal Care and Use Committee. Unless otherwise noted, all mice were fed normal chow *ad libidum* and had access to distilled water. Adult mouse numbers per cage ranged between one and five. To supplement the diet with simple carbohydrates, mice were provided 5% sucrose-water along with normal chow for 2 weeks. For induction of hypoglycemia, animals were restricted fed for 1hour per day at the beginning of the dark phase for 6 days. For diet induced diabetes experiments, normal chow was replaced with either 40% kcal fat and 41% kcal carbohydrate (Teklad, #95217) or 42% kcal fat and 43% kcal carbohydrate, (Teklad, #88137) or 60% kcal fat and 20% kcal carbohydrate (Research Diets, #D12492i, irradiated) diets. Mice were fed with these high fat diets for 10 - 16 weeks. Mouse body weights as well as initial and final amounts of food were measured weekly with a scale within 0.1g accuracy.

Rgs16::GFP reporter mouse and diabetic models

Rgs16::GFP BAC transgenic mice (ICR, outbred) were obtained from M. E. Hatten (Gong et al., 2003). For analysis in leptin-deficient type 2 diabetic model, Rgs16::GFP mice were crossed with *ob/ob* mice (C57BL6 background, Jackson Laboratory) (Hamann and Matthaei, 1996). For beta cell ablation type 1 diabetic model, Rgs16::GFP mice were crossed to PANIC-ATTAC mouse model

obtained from P. Scherer (Pajvani et al., 2005; Wang et al., 2008). Adult normal glycemic PANIC-ATTAC mice were injected for 5 consecutive days with dimerizer. Glucose levels were measured weekly. Mice were sacrificed starting 1 week after the treatment. For short time points, we followed glucose and GFP expression up to 7 weeks. For middle time points, mice were sacrificed 4 months after dimerizer injection, whereas long time point mice were sacrificed 8 to 11 months post-injection. To determine ChREBP's involvement during type 1 diabetes, Rgs16::GFP mice were crossed to *ChREBP*$^{-/-}$ (129/B6) mice obtained from K. Uyeda (Iizuka et al., 2004). This cross caused a reduction in the brightness of Rgs16::GFP as we compared in the STZ model using original Rgs16::GFP and ChREBP crossed mice. It was still sufficient to make a comparison based on ChREBP genotype. For pancreas cancer studies, Rgs16::GFP mice were crossed to *Kras*$^{flox\text{-}G12D}$*; Ink4a*$^{flox/flox}$*; Ptf1a::CRE* mice obtained from R. Brekken (Aguirre et al., 2003; Chin et al., 1998; Farr et al., 1988).

Mouse genotyping

Mouse genotypes were determined with PCR of DNA extracted from digested mouse tails using high salt procedure (Emanuel, 1960). Less than 1cm long mouse tails were digested in a lysis buffer consisting of 50mM Tris-HCL at pH = 8.0, 1mM EDTA, 0.4M NaCl, 1% SDS and 0.4mg/ml Proteinase K for 2 days at 55°C. DNA was precipitated from saturated NaCl added tail digests with 100% Et-OH followed by 70% Et-OH wash. Genomic DNA pellet was dissolved in 100µl water overnight before PCR. PCR mix was prepared using HotStarTaq polymerase kit (Qiagen). All PCRs were conducted using Programmable Thermal Controller (MJ Research). All PCR programs started with 13min 93°C DNA denaturation and Taq polymerase activation period. Each PCR cycle contained

30sec denaturation step at 93°C and 72°C elongation step, whereas annealing (An) temperature and both annealing and elongation (El) durations were set according to different primer sets. After the appropriate cycles were done, PCRs were completed with an extra 2min 72°C elongation followed by cool down to 20°C. All primer oligonucleotides (IDT DNA) came as powder and stored at 25mM stock concentration in water. dNTP mix was also dissolved in water at 10mM concentration. Gα11 genotyping was sometimes used for DNA verification. KO-Rgs16 primers were used to verify the genotype of donor mice during Rgs8-Rgs16 dKO creation.

The final PCR tube contained: 2µl 10x buffer, 4µl 5x Q-solution, 0.4µl of dNTP, forward, and reverse primer each, and 0.1µl Taq polymerase all dissolved in water with 20µl total volume. Primer sequences (5' to 3') and PCR conditions along with the number of cycles and expected product lengths are listed below:

Rgs16::GFP:

Rgs16 5' forward: CACGACGTGCTGTCCTGCGTC

eGFP reverse: GTAGCGGCTGAAGCACTGCAC

Conditions: An: 61°C for 45sec, El: 50sec, 35x, product: ~300bp

Rgs8::GFP:

Rgs8 5' forward: GTAAATCCCTGCACCCAGCAG

eGFP reverse: GTAGCGGCTGAAGCACTGCAC

Conditions: An: 55.5°C for 1min, El: 1min 15sec, 35x, product: ~400bp

Rgs16 KO:

KO-Rgs16 forward: AGCACTTGCTGTAGAGGACATAGG

Rgs16 3' reverse1: AGATCAGCAGCCTCTGTTCCACAT

Conditions: An: 60C for 30sec, El: 45sec, 35x, product: ~400bp

Rgs16 WT:

WT-Rgs16 forward: ACAGCTCTGGTGATTCTGTGGGAT

Rgs16 3' reverse2: TAGGGCTTGCAGGCATTCACTACT

Conditions: An: 62C for 25sec, El: 30sec, 35x, product: ~250bp

ob/ob:

ob forward: TGACCTGGAGAATCTCT

Leptin reverse: GGAAGCCAAGGTTTCTT

Conditions: An: 51°C for 1min 20sec, El: 1min 30sec, 43x, product: 266bp

Leptin WT:

WT-leptin forward: TGACCTGGAGAATCTCC

Leptin reverse: GGAAGCCAAGGTTTCTT

Conditions: An: 53°C for 1min 10sec, El: 1min 10 sec, 43x, product: 266bp

ChREBP KO:

KO-ChREBP forward: TGATGCCGCCGTGTTCC

ChREBP reverse: GCGTTGAGCTCCTCTATTTCATCCC

Conditions: An: 56°C for 1min 25sec, El: 3min, 35x, product: ~1200bp

ChREBP WT:

WT-ChREBP forward: ACTGAGTGTCCACCTGTCTCCC

ChREBP reverse: GCGTTGAGCTCCTCTATTTCATCCC

Conditions: same as KO-ChREBP, product: ~500bp

Gα11 WT:

Gα11 forward: GACACTGCCATCTGTACAAGG

Gα11 reverse: GAGATTGACAGACGAGTTCTG

Conditions: An: 55°C for 30sec, El: 1min 15sec, 34x, product: 410bp

PANIC-ATTAC:

Caspase8 forward: GAAAGTGCCCAAACT TCACAG

Caspase8 reverse: CTTGTCATCCTTGTTGCTTACT

Conditions: An: 58C for 30sec, El: 1min, 35x, product: 621bp (done by Zhao Wang)

PCR outcome was verified by running samples in 1% agarose gel dissolved in TBE for 30min and comparing band sizes to 1kb+ ladder (Qiagen).

Aside from PCR, Rgs16::GFP copy number of heterozygous intercrosses was either assessed by olfactory bulb expression intensity of newborns from P0 to P3 or via brain quantification of the sacrificed ChREBP KO, WT or heterozygous animals. Also, genotypes of all Rgs16::GFP mice were verified by invariant intestinal GFP expression prior to assaying pancreas.

Blood glucose and insulin measurements

Non-diabetic Rgs16::GFP mice had normal blood glucose levels between 100-200 mg/dL. Therefore, we classified any value above that upper limit as hyperglycemic, rated as mild (200-300 mg/dL), moderate (300-450 mg/dL), severe (>450 mg/dL). Glucose values were measured from ~5µl tail blood using glucose strips in a glucometer (Ascentia Elite and Bayer Contour) with a read-out range of 20-600 mg/dL. Reads above upper threshold were recorded as 600 mg/dL. For insulin measurements, blood was collected and incubated at 4°C overnight. Next day, samples were centrifuged at 14000rpm for 10min at 4°C and supernatants were collected as serum. Insulin values from blood serum were measured using an ELISA kit by I. W.-Asterholm.

STZ treatments in mice

STZ in powder form (Sigma-Aldrich) was dissolved in 0.1M NaCit solution at pH = 4.5 in separate tubes before each injection with a 1mg/200µl concentration. Total amount of STZ to be injected into mice was calculated individually for each mouse by normalizing it to per kg body weight. STZ amounts and number of consecutive treatment days for dose-response experiments were the following: 40mg/kg x 1 day, 40mg/kg x 5 days, 65mg/kg x 3 days, 90mg/kg x 2 days, 175mg/kg x 1 day. Negative control NaCit only injections were done with

volumes corresponding to 175mg/kg x 1 day and 65mg/kg x 3 days. Mice were sacrificed 8 days after the STZ administration period, except for single low STZ dosage and other NaCit controls which were sacrificed at day 14. For Rgs16::GFP time course of STZ treatment (65mg/kg x 3 days), mice were sacrificed at days 2, 4, 6, 8, 10, 12, 15, and 20 post-STZ. Negative controls received 3 consecutive days of NaCit treatment with similar volumes as the STZ experimental group. STZ protocol (65mg/kg x 3 days) was also applied to male and female Rgs16::GFP mice with *ChREBP*$^{-/-}$, *ChREBP*$^{+/-}$, and *ChREBP*$^{+/+}$ genotypes. All Rgs16::GFP females were sacrificed at day 15, whereas hyperglycemia of 5 non-GFP ChREBP KO females was followed for 3 months post-STZ. Male mice with different ChREBP backgrounds were sacrificed at day 15 and 27. Two *ChREBP*$^{-/-}$ male mice were sacrificed day 55 post-STZ.

Mouse glucose and insulin injections

All glucose and insulin injections to mice were done intraperitoneally (i.p.) after dilution in PBS (Gibco). We tested the effects of both short-acting normal human insulin Humulin-R and the longer acting insulin protamine suspension Humulin-N on Rgs16::GFP. We injected mice with Humulin-R (2 IU/kg) twice daily starting from the very onset of hyperglycemia at day 2 post-STZ. We focused on day 15 comparison of STZ only and STZ + insulin groups, because that was the time interval when we observed a dramatic increase in GFP expression. Blood glucose levels of all the insulin-injected mice were measured at t = 0 min and t = 30 min at both noon (ZT6) and light-dark transition (ZT12) time points to confirm the strength and duration of insulin administration. Also, we re-adjusted the initial insulin concentration (2 IU/kg/inj) in resistant mice up to 4.5x of the starting value (9 IU/kg/inj), as we dynamically followed and responded to resistant hyperglycemia in each mouse to achieve continuous daily transient

normalizations. In separate tests, animals were given Humulin-N (2 IU/kg) twice daily for 3 days starting at day 12, for 6 days starting at day 5, and with 5 IU/kg dosage for 6 days starting at day 10 post-STZ, respectively. Glucose injection of mice either alone or with exendin-4 was done with 2g glucose/kg mouse body weight injection of 1.39M glucose dissolved in PBS. Glucose tolerance test (GTT) protocol also utilized the same amount of glucose injection, followed by blood glucose assessment at certain time points up to 10hr post-administration, except one set of Rgs8-Rgs16 dKO mice on high fat diet was subject to GTT with 1g glucose/kg mouse body weight.

Caerulein treatments in mice

Mice went through repetitive 5 caerulein (Sigma-Aldrich) administrations with 1hr intervals to induce pancreatic inflammation (Gukovsky et al., 1998; San Roman et al., 1990; Willemer et al., 1992). Each caerulein injection dosage was set as 50µg/kg mouse body weight dissolved in 100µl PBS. Mice were sacrificed at days 1, 2, 3, and 6 post-injection and their pancreata were dissected out and visualized under fluorescent microscope.

Pancreas visualization

We sacrificed Rgs16::GFP animals at various stages and pictured their pancreatic GFP expression using fluorescence microscopy (Zeiss). Animals were euthanized with CO_2 followed by cervical dislocation. Internal organs from stomach to distal colon were removed, washed twice in ice-cold PBS, and placed in trays with PBS on ice. Pancreata were dissected using fine tip forceps in ice-cold PBS under the microscope with ~10x total magnification. GFP expression was captured using a single-channel camera (Hamamatsu) in 1344 x 1024

resolution with 1 second exposure under 48x objective magnification using 1 x 1 binning and analog gain = 10, analog offset = 2 settings. The number of pictures taken varied based on pancreas size, ranging from 1 for postnatal pups to 5 fields for adults (a representative survey of ~15% of the entire pancreas). For comparison of postnatal Rgs16::GFP expression with different ChREBP genotypes, P0-P6 pups were sacrificed. Their postnatal pancreata were visualized under 96x magnification. All quantification images were saved in gray-scale 16-bit tiff image format without compression. Selected images were than pseudo-colored, undergone brightness adjustments, and converted to jpeg file format for visual presentations. Pictures for visual representation were also taken under 48x objective using a triple-channel color camera (Olympus) in 1360 x 1024 resolution and ISO 200 setting with exposures ranging between 1/6 to 1/1.5 seconds.

Image quantification

16-bit gray-scale native images were quantified using ImageJ software (Girish and Vijayalakshmi, 2004). Background intensity was subtracted from each image using a rolling ball algorithm with the ball radius set to 50 pixels. Afterwards, a variable and tight threshold was set so that all parts of the image except islet and VDAC fall below the threshold. Intensities of all particles with size ≥ 5 pixels were then summed to obtain the total light intensity per image. Averaging all image intensities from the same pancreas yielded an average GFP intensity for that pancreas, and averages of all the pancreatic values within the same group were used for comparison. For consistency of quantification, Rgs16::GFP copy number variation among *Rgs16::GFP*$^{o/+}$ and *Rgs16::GFP*$^{o/o}$ mice with different ChREBP genotypes was normalized by doubling the GFP intensity value of *Rgs16::GFP*$^{o/+}$ animals after confirming that copy number

differences of Rgs16::GFP BAC directly corresponded to a 2-fold difference in values as shown in the brain GFP quantification (Figure 12, insert). Longitudinally cut brain hemispheres were pictured under 48x magnification and with 0.1 second exposure. Brain Rgs16::GFP was quantified without background subtraction or threshold setting within a circle with 512 pixel radius selected at the center of each image. P0-P6 pancreas quantification of 96x images varied greatly because it was based on single image values and orientation of GFP+ cells within pancreas obscured accuracy of intensity comparison with this zoom level.

PDAC isolation and SCID/NOD-SCID animal treatments

Rgs16::GFP expressing PDAC primary tumor line was obtained from the late stage pancreatic tumor of a male *Rgs16::GFP; Kras$^{flox\text{-}G12D}$; Ink4a$^{flox/flox}$; Ptf1a::CRE* mouse. The large tumor was isolated from the animal and digested into single cells (L. Rivera). Cells were subcloned to enrich Rgs16::GFP expressing population (L. Rivera) and the resulting GFP+ subclone, called B12303, was propagated as the primary tumor cell line in culture. Primary PDAC cells had a doubling time of about 24hr in high glucose (25mM) media with 5% FBS. Rgs16::GFP expression was found be more pronounced at 50% FBS. Neither proliferation capacity nor adhesion strength of GFP+ and gfpNEG populations seemed to differ in PDAC culture.

One million PDAC culture cells were transplanted orthotopically into the pancreata of immunocompromised SCID recipient mice (R. Brekken) (Bosma et al., 1983). Large tumors formed within two weeks. The tumor was isolated, frozen, sectioned, stained for GFP and endothelial cell markers, and visualized (L. Rivera, data not shown).

We also used NOD-SCID mice to test blood serum derived enrichment of Rgs16::GFP *in vivo* (Bosma et al., 1983; Kikutani and Makino, 1992; Shultz et

al., 1995). PDAC culture cells with < 5% GFP+ population were resuspended at a concentration of 100,000 cells / 100µl in ice-cold PBS. Each animal was injected with 200,000 cells subcutaneously. About 3 weeks later, when the tumors on the side of the body started to reach about 1 cm^3 volume, animals were sacrificed and their isolated solid tumor was visualized under inverted fluorescent microscope.

Tissue culture PDAC maintenance

PDAC cells were grown in 10% FBS containing 25mM glucose DMEM (Gibco) with 20mM Hepes (Gibco) and 1x penicillin/streptomycin (Gibco) at 37°C and 5% CO_2. Cells were passaged by washing twice with PBS and detaching with 0.05% trypsin-EDTA (Gibco) treatment for 5 minutes. Upon quenching with 10% FBS growth media and centrifugation at 500 rpm for 5 minutes followed by aspiration of media, cells were resuspended in growth media at appropriate volume and distributed to overnight rat tail collagen1-treated (Gibco) plates at dilutions between 1:2 and 1:10. Cells retained a doubling time of 24 hours.

FACS and RNA-Seq of PDAC

PDAC cells grown on forty 10cm plates were treated with 40% FBS overnight to induce Rgs16::GFP expression (V. Pashkov). Afterwards, cells were split into 2 groups based on GFP expression using fluorescence-activated cell sorting (FACS) (UT Southwestern flow cytometry core facility). Total RNA from FAC sorted GFP+ and gfpNEG populations was isolated and prepared for RNA-Seq analysis (V. Pashkov). The results from UT Southwestern RNA-Seq core facility were normalized according to ERange method by C. Shen who calculated the gene expression levels of cumulatively 33111 entries including known genes,

predicted genes, pseudo genes, loci, and expressed sequence tags according to their reads per kilobase of exon model per million mapped reads (rpkm) (Mortazavi et al., 2008; Nagalakshmi et al., 2008; Wang et al., 2009). The cut-off value for deciding expression was set at rpkm ≥ 1 and any gene with a lower value was assumed as non-expressed in that pool. Consequently, 12546 genes were regarded as expressed in either of these PDAC populations. To see if a gene was preferentially expressed in either population, genes that had a more than 1.5-fold increase or decrease in one population over another were sorted out by taking the RNA quantitative rpkm ratio of GFP+/gfpNEG and gfpNEG/GFP+ separately.

GPCR search in PDAC RNA-Seq data

In order to obtain GPCR profiling of PDAC, a comprehensive list of all mouse genomic DNA sequences with similarity to GPCRs was compiled via BLAST search by Lisa Kinch. This list with over 1600 GPCRs was searched for gene expression from the RNA-Seq ERange data via their main and alternative symbols individually (Kroeze et al., 2003). Like before, rpkm value of 1 was set as a threshold and any gene that was below that in both GFP+ and gfpNEG populations was regarded as non-expresser. In addition, Etsuko Moriyama identified GPCRs expressed in PDAC by searching for exact sequence matches between short cDNA sequence reads and mouse GPCR libraries compiled from NCBI, Ensembl, and UCSC gene databases. Any gene missing in the first GPCR list was then additionally searched. Occasionally, a gene either could not be found or had absolute zero in the ERange list, but had high total RNA fragment counts according to Etsuko Moriyama's assessment. Such genes with high RNA counts were graphed separately and regarded as likely expressers. GPCRs without comprehensive ligand data were regarded as orphans.

GPCR search in pancreatic islet database

Alan Attie's database of pancreatic islet microarray in lean and *ob/ob* mice with C57BL6 and BTBR backgrounds was used to look for the relative expression of GPCRs in islets (Keller et al., 2008). *ob/ob* mice in the BTBR background was shown to get obesity derived type 2 diabetes, whereas *ob/ob* mice were not hyperglycemic in C57BL6 background at 10 weeks of age. The difference between these 2 backgrounds was claimed to lie in their beta cell expansion capacity, with BTBR mice being defective in comparison to C57BL6 mice, which expanded beta cells normally (Keller et al., 2008). We compiled a list of 124 GPCRs which included 63 GPCRs expressed in PDAC and GPCRs shown to be present in islets along with their family members (Ahren, 2009; Regard et al., 2007; Regard et al., 2008). With the help of M. Keller from the Alan Attie laboratory, we compared their expression in the lean and obese mice at 4 and 10 weeks of age. Differences in expression between lean and *ob/ob* mice in either background were summarized in a heat map we received from M. Keller on a logarithmic scale calculated upon normalization of the values based on all the samples from the same strain. The majority of GPCRs had constant expression level in all groups (data not shown).

ISX treatment of PDAC

N-Cyclopropyl-5-(thiophen-2-yl)isoxazole-3-carboxamide (shortened as ISX) was obtained from J. Schneider (Schneider et al., 2008). ISX concentrations spanning several orders of magnitude were obtained by 3-fold dilutions of starting 100μM master mix. DMSO as the solvent of ISX served as negative control. Total cell number and GFP+ cells among them were counted with cell counter under microscope. Representative pictures were taken with 20x objective, whereas cells

were counted with 40x objective for convenience. Multiple distinct fields were counted and averaged.

Mouse ISX injections

To test ISX under diabetic conditions *in vivo*, adult Rgs16::GFP mice were treated with STZ (65mg/kg x 3 days) and then i.p. injected with ISX dissolved in its carbohydrate based carrier cyclodextrin daily from day 5 until day 12 post-STZ. As diabetes control, NaCit-treated animals were also injected with ISX in the same time interval, whereas cyclodextrin only injections for 6 days served as control for the carrier. For day 15 post-STZ time points, ISX and cyclodextrin injections were done the same way, except they started at day 8 and day 10, respectively. Putative effects of ISX on VDAC were tested in Rgs16::GFP pups. P15 animals were i.p. injected ISX daily for 10 days and sacrificed afterwards for pancreas visualization.

HDAC inhibitor treatment of PDAC

We obtained LDR 6020 cancer cell line transfected stably with a CMV-GFP construct from E. Martinez (Johnson et al., 2008). The CMV promoter in these cells was repressed by nucleosomes and DNA hypermethylation (Johnson et al., 2008). Consequently, LDR 6020 cells did not express this GFP reporter under regular culture conditions. It was shown that HDAC inhibitors were able to abolish this repression causing enhanced GFP expression in a dosage dependent manner (Johnson et al., 2008). This cell line became our positive control for the functionality of several inhibitors of HDAC we tested simultaneously in primary PDAC. Trichostatin A (400nM), romidepsin (depsipeptide) (25ng/ml), and ISX (50μM) were dissolved in DMSO, whereas butyrate (10mM) was dissolved in

water. DMSO served as control for basal GFP level, whereas ISX was the positive control to compare GFP+ cell fraction and GFP brightness inside cells. Cells were visualized under 20x objective.

Mouse exendin-4 injections

Exendin-4 was dissolved in PBS at 25mM concentration. Exendin-4 daily dosage was set as 0.05nmol per mouse or ~5ug/kg mouse body weight. The experimental set-up involved i.p. injection of exendin-4 to mice twice daily at noon (ZT6) and light-dark transition (ZT12) for 3 or 6 days. Glucose and exendin-4 co-injected group was compared to glucose only controls to test the acute hyperglycemia coupled GFP induction potential of exendin-4. Day 1 and day 6 glucose levels and day 3 insulin levels at t = 0 and t = 1hr were compared to determine if exendin-4 stimulated insulin secretion. PBS only injections served as negative control.

RESULTS

PART 1: Chronic hyperglycemia is the primary condition driving Rgs16::GFP in islets of type 2 diabetic models

Summary: Beta cells of the pancreatic Islets of Langerhans are long lived cells with low proliferation rates in normal glycemic young adults. The absence of Rgs16::GFP in islets of normal glycemic young adults was striking, given the intense expression of Rgs16::GFP in proliferating beta cells during pancreas development and maturation. In order to determine if Rgs16 could be reactivated in islet beta cells under metabolic stress, we utilized models of type 2 diabetes induced by leptin deficiency or diet-induced obesity. Our findings indicate Rgs16::GFP is expressed in pancreatic islets in response to chronic hyperglycemia of type 2 diabetes.

1.1: Chronic hyperglycemia drives Rgs16::GFP expression in islet beta cells of obese *ob/ob* mice

We used the leptin deficient *ob/ob* mouse model to look for pancreatic expression of Rgs16::GFP. Both males and females showed elevated blood glucose levels during the second and third months of age, but increasing insulin production from expanded islets lowered blood glucose levels until massive beta cell failure in mice about 20-24 weeks of age (Figure 5A). We followed GFP expression in animals sacrificed at various ages between 5 to 24 weeks of age. Extreme and persistent hyperglycemia in *ob/ob* mice stimulated the onset and progression of Rgs16::GFP expression in pancreas, especially in mice with serum insulin levels above 35 ng/ml (Figure 5B, C). As previously reported, wild type (WT) and most *ob/+* animals were normal glycemic and did not express

Figure 5: *ob/ob* mice express pancreatic Rgs16::GFP during chronic hyperglycemia proportional to age and hyperinsulinemia.

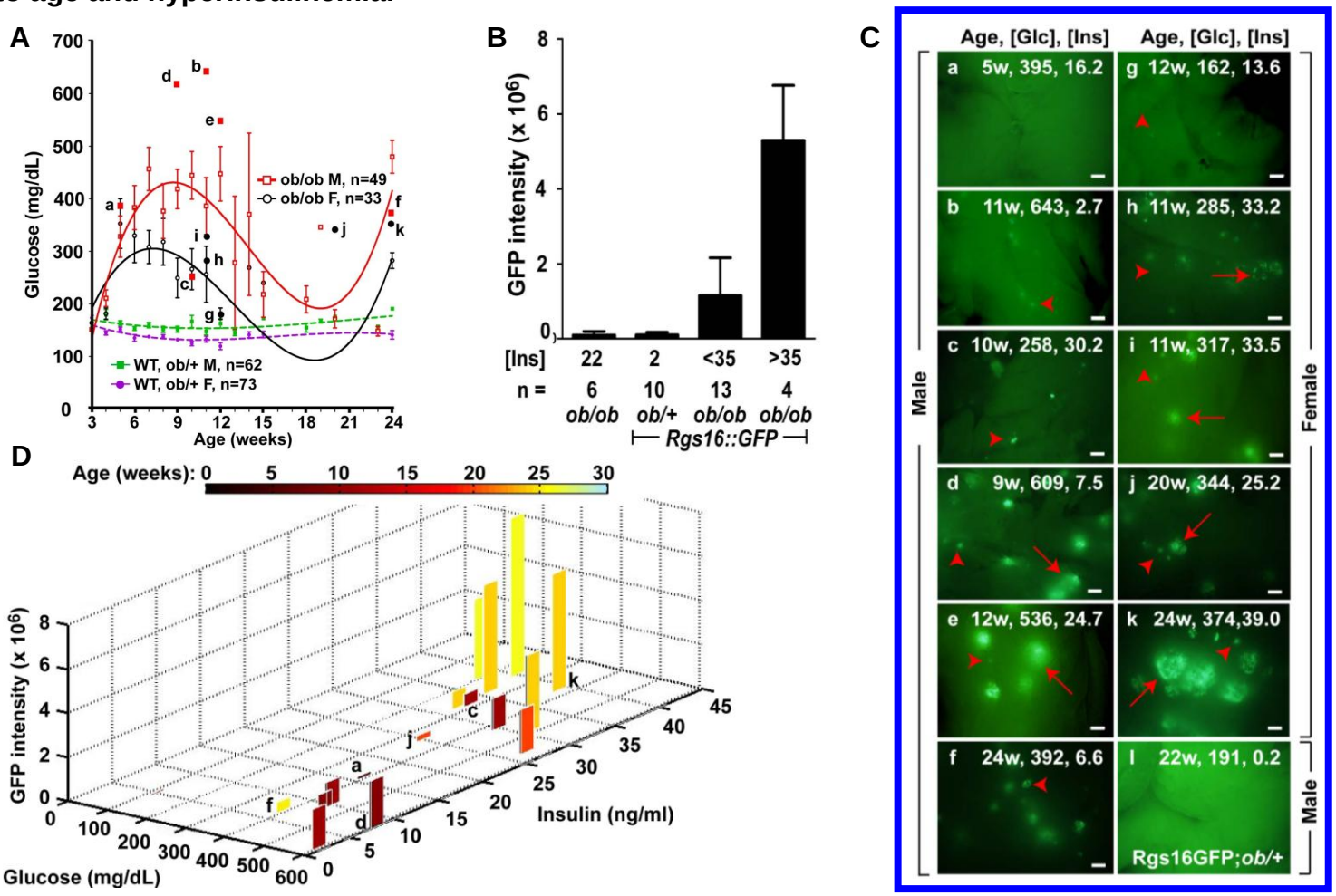

Rgs16::GFP in islets (Figure 5C). We were surprised to find that 5 week old *ob/ob* mice, which had been hyperglycemic for two weeks, did not express Rgs16::GFP in islets. GFP was not readily apparent in islets until mice were both hyperglycemic and hyperinsulinemic at about 9-12 weeks of age. Throughout the pancreas, early expression seemed to be constrained to a few cells in a few islets, but would spread to more cells and more islets at later stages (Figure 5C). Elevated blood insulin levels were suggesting past or ongoing beta cell expansion to meet the demands of peripheral insulin resistance and resultant hyperglycemia (Ackermann and Gannon, 2007). We plotted all the parameters correlating with GFP expression and noticed that increasing age, glucose, and insulin levels positively correlated with higher Rgs16::GFP expressing islet beta cells (Figure 5D). Image quantification indicated the highest GFP was in mice over 20wk of age, with at least 300 mg/dL glucose and 35 ng/ml insulin.

Based on these results, we tentatively concluded that Rgs16::GFP expression in islets was affected by multiple parameters. Although Rgs16::GFP expression in *ob/ob* mice was proportional to insulin level (Figure 5B), it was not or only weakly expressed in younger mice with very high levels of insulin between 13-33ng/ml (Figure 5C). Therefore, it seemed unlikely that Rgs16 responded to Gαq-coupled signals that enhance insulin secretion (Sassmann et al.,

---

Figure 5: *ob/ob* mice express pancreatic Rgs16::GFP during chronic hyperglycemia proportional to age and hyperinsulinemia
Panel A shows blood glucose curve of *Rgs16::GFP; ob/ob* male and female mice. Error bars are SD. Panel B compares single image GFP quantification of *ob/ob* mice with their serum insulin levels. Rgs16::GFP; *ob/+* animals are control for *ob/ob* group and non-GFP *ob/ob* animals are control for GFP expression. Error bars are SD. Panel C outlines representative GFP expression of mice and their corresponding age, blood glucose and blood insulin level in that order. Genders are indicated at the sides of the panel. Red arrows and arrow heads point to large and small islets, respectively. Correlation between GFP, glucose and insulin levels is graphed on Panel D with color spectrum indicating age in weeks (Villasenor et al., 2010).

2010; Xu et al., 1999b). Beta cell expansion is assumed to occur in response to chronic hyperglycemia (Sachdeva and Stoffers, 2009). To further investigate GPCR-regulated insulin release and beta cell expansion as potential causes of Rgs16::GFP expression, we tested wild type mice rendered insulin resistant by diet-induced obesity next. We later compared the outcome to type 1 diabetes mouse models, which are hyperglycemic because of massive beta cell death and subsequent failure to produce insulin, to type 2 diabetes.

1.2: Naturally obese mice fed normal chow can express Rgs16::GFP in islets

To determine if naturally occurring type 2 diabetic mice with WT leptin gene would express Rgs16::GFP in the pancreas, we assayed older obese mice (age ≥ 4.5mo) in our colony with normal or elevated glucose levels. These Rgs16::GFP mice had great variation in body weight and a subset was hyperinsulinemic and/or hyperglycemic (Figure 6A). We identified naturally obese mice (> 40g). Blood glucose and insulin levels were measured for 1-2 months before sacrifice. 19 of 26 mice we assayed had little or no GFP expression (< 0.2 $x10^6$), as seen, for example, in the mice labeled as 'v' to 'z' (Figure 6). Some of these mice had been hyperinsulinemic two months prior but had normal insulin levels on the sacrifice day (Figure 6C, 'w' and 'y'). 7 mice labeled 'a' to 'g' in the order of decreasing intensity expressed GFP in many islets. Their blood glucose levels were usually normal within the observation period among these mice, but 5 of them were mildly hyperglycemic at some point during their life span (Figure 6B).

Quantified GFP expression of these overweight mice was compared to their sacrifice day glucose, insulin, body weight, and age (Figure 6D, E, F, G). Of seven GFP expressing mice, two (a-b) had among the highest Rgs16::GFP expression we have ever observed (> 1.5 x 10^7), two (c-d) had obvious GFP+

Figure 6: Naturally occurring fat mice on normal chow can express pancreatic Rgs16::GFP.

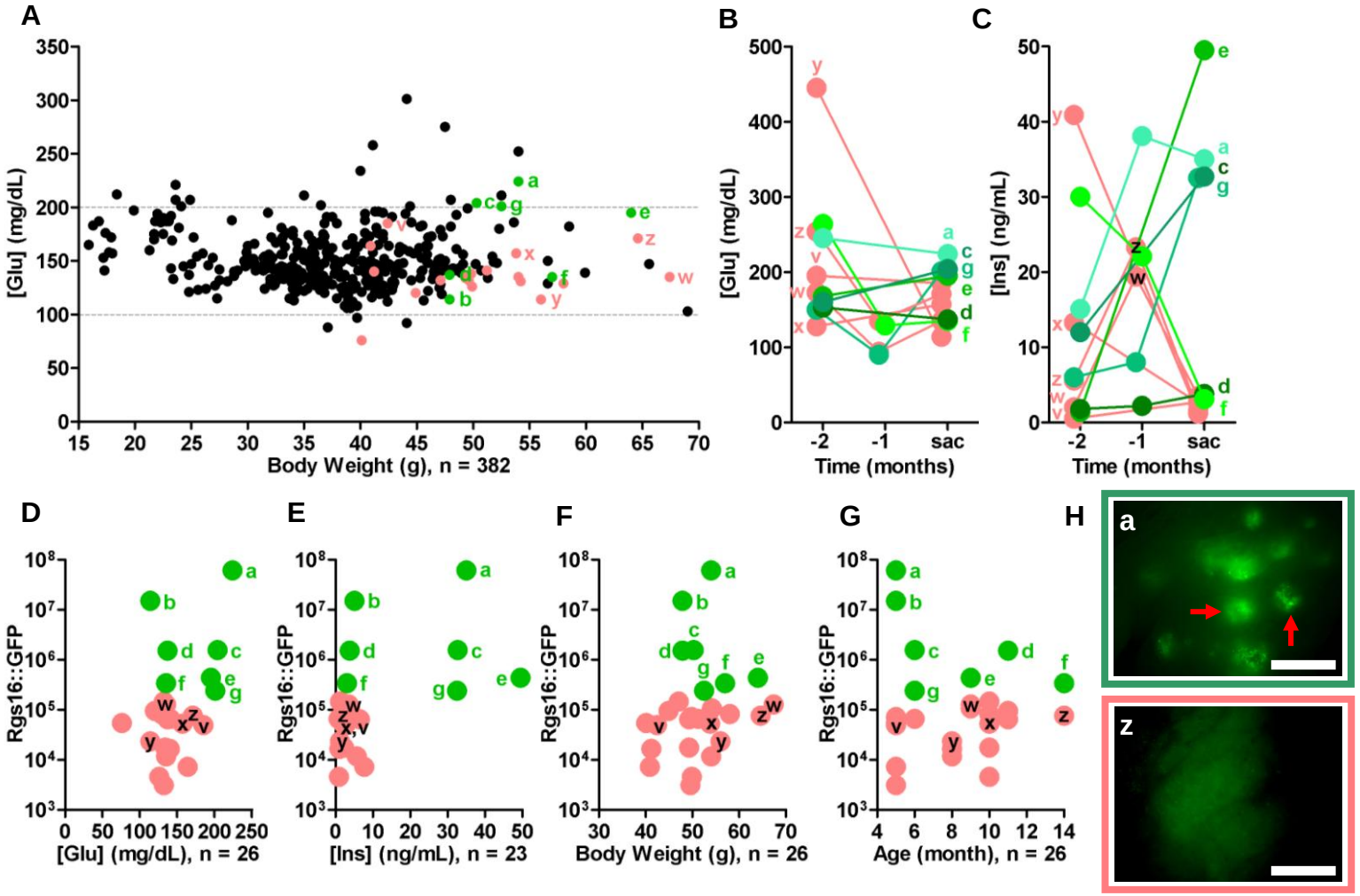

islets throughout the pancreas (~1.5 x 10^6), whereas the last three (e-g) had only moderate expression (< 0.5 x 10^6). The sacrifice day blood glucose levels of 'a', 'c', 'e', and 'g' were elevated. The GFP values were not always proportional to blood glucose concentration (Figure 6D). Insulin levels were also high in mice 'a', 'c', 'e', and 'g' corroborating the observation in *ob/ob* mice that Rgs16::GFP was most likely to be expressed in older mice when glucose and insulin levels were elevated (Figure 6E). Age and body weight values were not good predictors of expression intensity (Figure 6F, G). Mice with highest GFP tended to be around 4-6 months old, with expression being weaker in older mice that might have recovered normal glycemia after beta cell expansion.

Interestingly, we found that naturally fat mice can express as much Rgs16::GFP in islets as leptin-deficient *ob/ob* mice. Clearly, the Rgs16::GFP expression in *ob/ob* was not due to leptin deficiency but hyperglycemia. We saw that unmanipulated naturally fat mice that normalize their blood glucose levels might abolish their islet expression as with mouse 'y'. Furthermore, two GFP+ mice ('d' and 'f') had normal insulin levels at sacrifice day, indicating that insulin levels might fluctuate or that GFP expression was not solely responsive to

---

Figure 6: Naturally occurring fat mice on normal chow can express pancreatic Rgs16::GFP

Panel A shows the distribution of body weight and blood glucose levels of Rgs16::GFP transgenic adult mice from our colony with various ages (n = 382) maintained with normal chow *ad libidum*. Dotted gray lines mark the postulated interval of normal glucose concentration. 26 mice (Body weight > 40g) that were picked from that pool are colored. 7 mice with the highest GFP levels are colored green and denoted from 'a' to 'g' in the decreasing order of GFP intensity, whereas 5 GFP non-expressing mice are colored pink and denoted from 'v' to 'z' likewise. Panel B shows the glucose level course of 6 highest GFP expressing (except b at 4.8mo) and 5 GFP non-expressing mice over a 1 to 3 month time period. Panel C shows insulin level course of the same over the same time period. Panel D, E, F, and G show glucose, insulin, body weight, and age of the quantified mice at their sacrifice day, respectively. Panel H compares a pancreatic picture of mouse 'a' to that of 'z'. Scale bar is 1mm.

enhanced insulin secretion or circulating blood insulin. Hyperinsulinemia seemed to merely increase the chances of GFP expression. This was consistent with the hypothesis that Rgs16::GFP was expressed during beta cell expansion phase, rather than in islets of mice that had recovered normal glycemia but might remain hyperinsulinemic. These results showed Rgs16::GFP expression can occur in pancreas of naturally obese mice. Therefore, expression in *ob/ob* mice we previously observed was a robust and relatively uniform model of hyperphagy induced obesity, mimicking the condition of naturally obese mice with WT leptin gene.

1.3: High fat diet promotes Rgs16::GFP in islets of mildly hyperglycemic mice

Progression towards type 2 diabetes is exacerbated by chronic conditions of high insulin demand, as occurs in obesity and metabolic syndromes. After seeing Rgs16::GFP expressed in beta cells of expanding islets in *ob/ob* mice and in a fraction of older and heavier mice in our colony, we chose to determine if pancreatic Rgs16::GFP could be induced by maintaining mice on high fat diet (Ikemoto et al., 1996; Tsunoda et al., 1998). We set up recently weaned Rgs16::GFP mice either with 60% fat (60% HF), where 60% of all calories are derived from fat, or with 40% fat, 40% carbohydrate chow (40% HF). Mice continued to receive normal chow (NC) served as control. We monitored the body weight, blood glucose, blood insulin, and food consumption weekly over the course of 16 weeks (Figure 7A, D, E, F). We also gave elder adult mice either 40% HF or 60% HF (Figure 7A, B, C). Although we noticed minor spikes of blood glucose levels at isolated days within the younger groups, only couple of 60% HF mice became consistently but mildly hyperglycemic. Weight gain in the

Figure 7: 10 weeks of 60% fat diet increases the incidence of diabetes and induces Rgs16::GFP in mildly hyperglycemic mice.

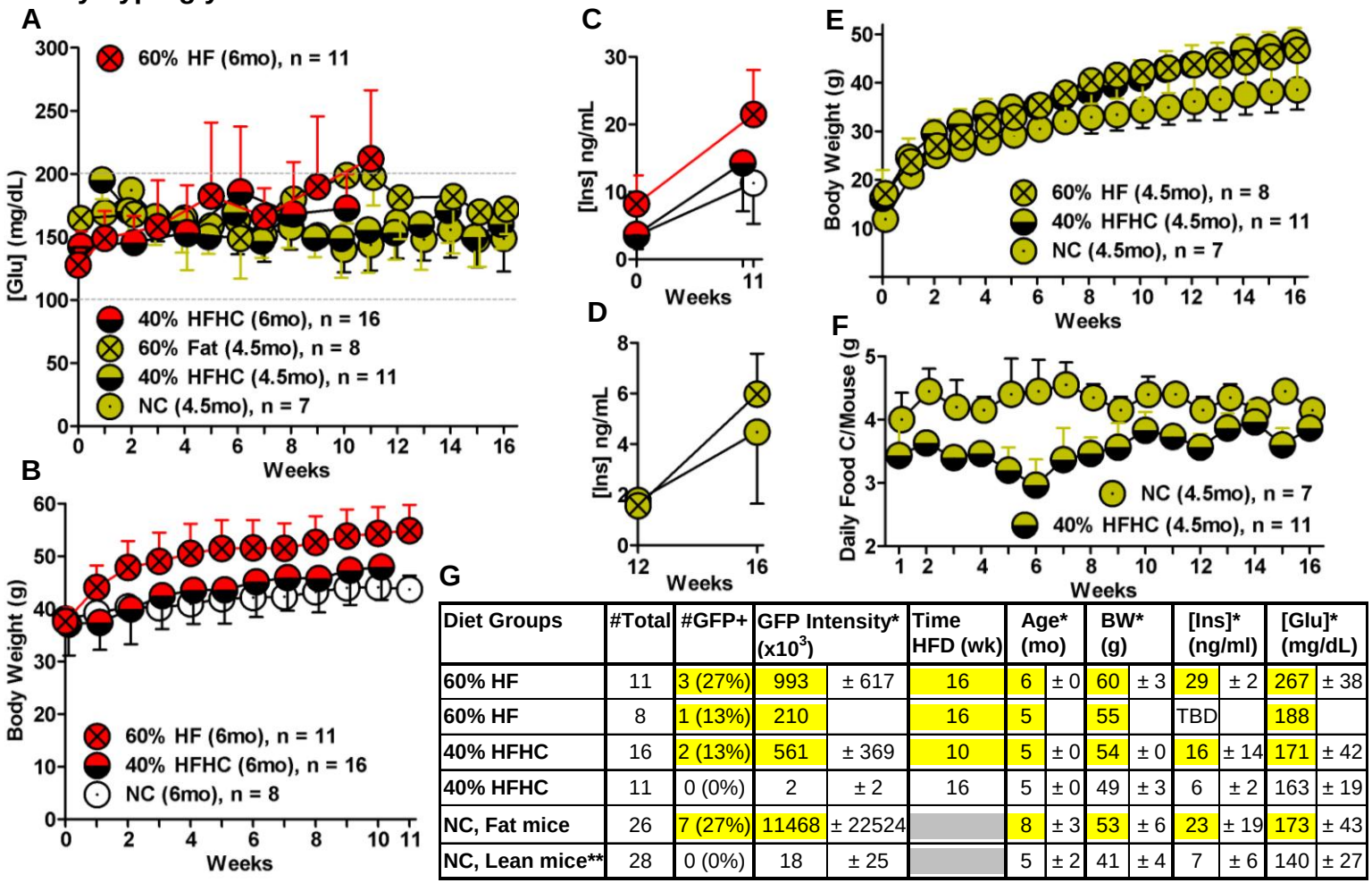

G

Diet Groups	#Total	#GFP+	GFP Intensity* ($x10^3$)		Time HFD (wk)	Age* (mo)		BW* (g)		[Ins]* (ng/ml)		[Glu]* (mg/dL)	
60% HF	11	3 (27%)	993	± 617	16	6	± 0	60	± 3	29	± 2	267	± 38
60% HF	8	1 (13%)	210		16	5		55		TBD		188	
40% HFHC	16	2 (13%)	561	± 369	10	5	± 0	54	± 0	16	± 14	171	± 42
40% HFHC	11	0 (0%)	2	± 2	16	5	± 0	49	± 3	6	± 2	163	± 19
NC, Fat mice	26	7 (27%)	11468	± 22524		8	± 3	53	± 6	23	± 19	173	± 43
NC, Lean mice**	28	0 (0%)	18	± 25		5	± 2	41	± 4	7	± 6	140	± 27

16wk 60% HF and 40% HF groups was slightly higher than NC group. 40% HF mice ate less than the NC controls suggesting a similar total calorie intake between the two groups (Figure 7F). Rgs16::GFP was not induced in either the 40% HF or NC younger mice consistent with similarities in terms of blood glucose and body weight among these two cohorts, and in most of the mice in our colony (Figure 7G). Only one mouse showed consecutive mild hyperglycemia from 60% HF group and had noticeable GFP expression. With 10 week long 40% HF and 60% HF groups that started this diet in adulthood, we observed some mice that had become hyperinsulinemic and mildly hyperglycemic towards the end of their 10wk diet period (Figure 7A, C, D). Two of 16 and three of 11 mice from the 40% HF and 60% HF groups, respectively, showed clear GFP expression and these expressers had the longest periods of mild hyperglycemia (Figure 7G). Weight gain and percentage of GFP expressing mice was greatest in the 10wk 60% HF elder group. As seen with GFP+ naturally obese mice, these results

---

Figure 7: 10 weeks of 60% fat diet increases the incidence of diabetes and induces Rgs16::GFP in mildly hyperglycemic mice
Panel A compares glucose course of different diet groups. Ages of mice at their day of sacrifice are shown in parentheses. Dotted gray lines mark the postulated interval of normal glucose concentration. Body weight course of Rgs16::GFP mice maintained on normal chow (NC), 60% fat & 20% carbohydrate (60% HF) chow, or 40% fat & 40% carbohydrate (40% HFHC) chow are indicated on Panels B and E with their corresponding controls of same age. 40% HFHC and 60% HF groups are age matched with their corresponding controls in the graphs. Panel C shows the starting and end blood insulin levels of 60% HF, 40% HFHC, and NC groups. Panel D shows the insulin level change of some younger mice from 40% HFHC (n = 3) and NC (n = 4) groups from 12th to 16th week. Panel F shows food consumption of younger 40% HFHC group and NC controls. All error bars are SD. The table on Panel G summarizes the incidence of GFP expression based on diet (yellow highlighted groups) and compares it with naturally lean or heavy mice from our colony from Figure 2. Values are shown with standard deviations where applicable. TBD: To be done. * indicates data for only GFP+ mice from that group. ** insulin values of normal chow lean group are coming from 16 mice out of 28.

confirmed that Rgs16::GFP expression could be induced by increased caloric intake but did not require leptin deficiency, as seen in *ob/ob* mice. Diet did not influence GFP levels if body weight was maintained at normal levels. 60% HF caused the greatest weight gain and was the most efficient diet for inducing Rgs16::GFP expression. Presumably, obesity promoted insulin resistance, which stimulated compensatory beta cell expansion and Rgs16::GFP expression.

1.4: Glucose supplements are insufficient to induce pancreatic Rgs16::GFP

Because Rgs16::GFP expression in islets of type 2 diabetic mice appeared to be responsive to blood glucose and insulin levels, we wanted to determine whether dietary saccharides could induce Rgs16::GFP in islets. We provided Rgs16::GFP mice either 5% sucrose-water or water *ad libidum* for 2 weeks. All mice remained euglycemic and maintained normal body weight during that period (Figure 8A, B). Both groups were fed normal chow *ad libidum*. At the end of 2 weeks, neither 5% sucrose-water nor control mice were expressing Rgs16::GFP (data not shown).

We also tested if twice daily injections of glucose (2g/kg) for six days would be sufficient to induce Rgs16::GFP in islets (Figure 8C). Blood glucose levels were elevated 1 hour after each glucose injection but returned to normal prior to the next glucose injection either that afternoon or the next morning (data not shown). None of the mice expressed GFP in islets after six days of this injection protocol.

The lack of induction of Rgs16::GFP as a result of systematic acute hyperglycemia in *ad libidum* fed mice suggested that neither transient increases in blood glucose level nor the resultant insulin secretions were sufficient to cause pancreatic GFP expression. This left us to believe that severe chronic hyperglycemia was the primary inducer of Rgs16::GFP in islets.

Figure 8: Sucrose-water and glucose injections are insufficient to induce pancreatic Rgs16::GFP in normal glycemic mice.

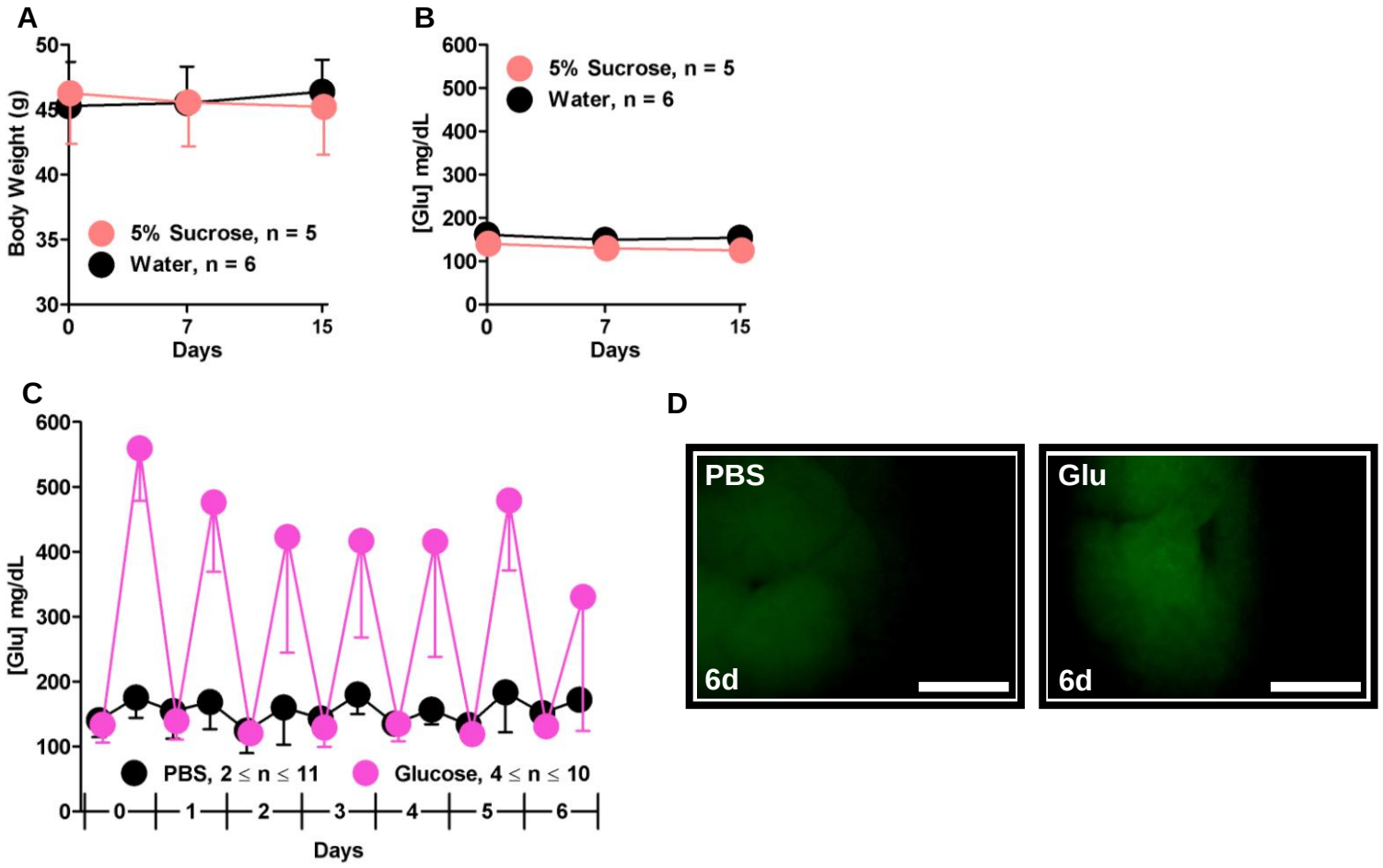

1.5: Starvation induced hypoglycemia does not stimulate pancreatic Rgs16::GFP

According to results so far, chronic hyperglycemia induced Rgs16::GFP in beta cells of islets. Because Rgs16::GFP was expressed in beta cells during embryonic and postnatal development, induction in hyperglycemic adults could be viewed as reactivation of a developmental program (Villasenor et al., 2010). The first endocrine expression of Rgs16::GFP during the secondary transition of embryonic pancreas development at e12.5 occurred in glucagon expressing cells (Villasenor et al., 2010). Therefore, we tested if stimulation of glucagon-releasing alpha cells could stimulate Rgs16::GFP in islets. We induced chronic hypoglycemia by a strenuous restricted feeding protocol that had previously been shown to promote ghrelin dependent stimulation of hepatic gluconeogenesis during starvation (Zhao et al., 2010).

Animal feeding was restricted to 1 hour per day for 6 days. These mice rapidly lost weight and became hypoglycemic (Figure 9A, B). The mice adapted to this type of starvation by increasing their food intake during the 1hr feeding period over the course of 6 days (Figure 9C). Rgs16::GFP expression was not detected in pancreata after 6 days (Figure 9D, E). This negative outcome suggested that islet GFP expression was the result of signals relayed during

---

Figure 8: Sucrose-water and glucose injections are insufficient to induce pancreatic Rgs16::GFP in normal glycemic mice
Panel A and B compare 5% sucrose containing water given Rgs16::GFP mouse ($n = 5$) body weight and blood glucose levels to those given water only ($n = 6$) over 15 days, respectively. Both groups were given normal chow *ad libidum*. Panel C compares the basal glucose level and 0-1hr glucose time course of PBS ($2 \leq n \leq 11$) or glucose ($4 \leq n \leq 10$) i.p. injected mice over 6 days. Error bars are SD. Example pictures of mouse pancreas after 6 days of daily PBS or glucose injections are shown in Panel D. Scale bar is 1mm.

Figure 9: Restricted feeding dependent hypoglycemia does not induce pancreatic Rgs16::GFP

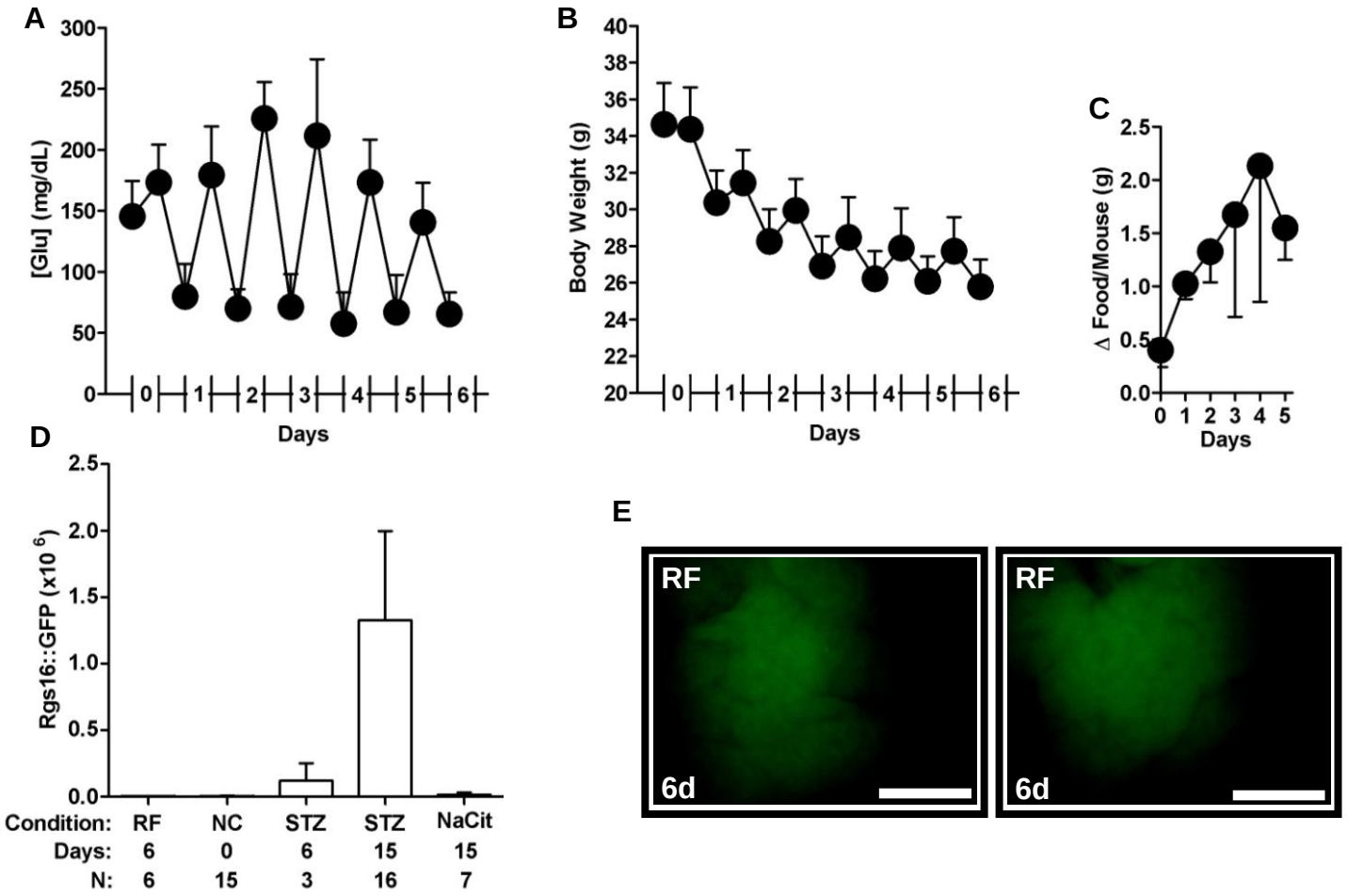

chronic hyperglycemia and not just as consequence of imbalance in glucose levels or stimulation of glucagon release from alpha cells, as occurs in response to starvation. Nonetheless, longer term experiments will be necessary to determine if alpha cell expansion induces Rgs16::GFP in pancreatic islets.

1.6: Caerulein mediated pancreatic inflammation does not induce Rgs16::GFP

Rgs16 expression was previously implicated with lymphocyte migration and homing in splenic germinal centers in an NF-κB dependent way (Hsu et al., 2008; Li et al., 2001; Xie et al., 2010). Diabetic conditions have been known to be closely tied to immune responses, such as the infiltration of T cells associated with islet loss causing type 1 diabetes (Beattie et al., 1980; Bluestone et al., 2010). We therefore asked if initiating an immune response in the acinar pancreas could induce Rgs16::GFP expression. Caerulein is a cholecystokinin mimetic and an inflammatory agent causing excess pancreatic juice secretion from acinar cells (Anastasi et al., 1967, 1968; De Caro et al., 1968; Gukovsky et al., 1998; Lampel and Kern, 1977; Niederau et al., 1985; Niederau and Grendell, 1999; San Roman et al., 1990). This initiates an immune response accompanied by swelling and edema formation (Lampel and Kern, 1977; Niederau et al., 1985).

Figure 9: Restricted feeding dependent hypoglycemia does not induce pancreatic Rgs16::GFP
Panel A shows the average blood glucose level of fasting mice before and after a 1hr normal chow restricted feeding for 6 days. Panel B depicts the body weight shift of fasting mice before and after diet. The average food consumption normalized per mouse per day during restricted feeding is shown in Panel C. Pancreas GFP quantification of restricted fed (RF) mice is compared to mice *ad libidum* fed with normal chow (NC). Mice injected with STZ at day 6 and day 15 serve as positive GFP control, whereas NaCit mice at day 15 serves as negative GFP control in Panel D. Example pictures of a pancreas at the end of restriction feeding period are shown in Panel E. Scale bar is 1mm.

Figure 10: Caerulein mediated pancreatic inflammation does not induce Rgs16::GFP

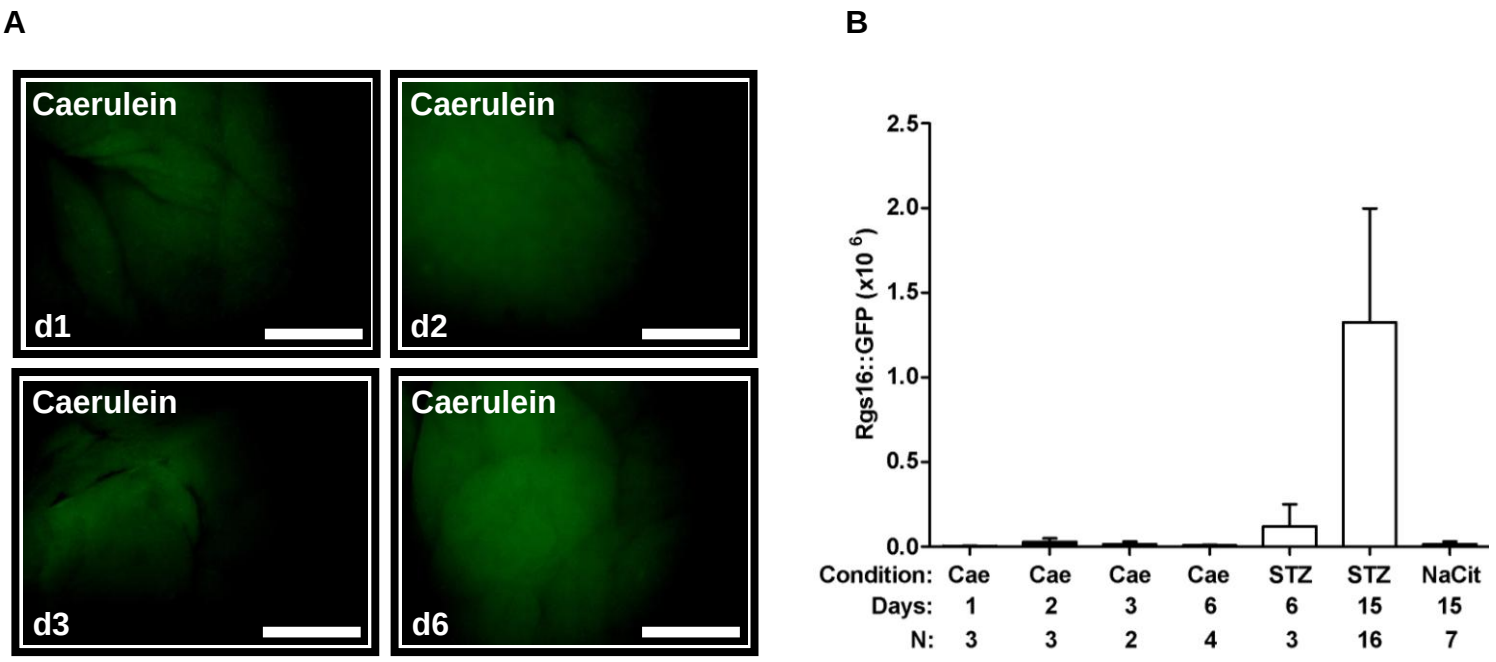

We treated mice with caerulein to induce pancreatitis. None of these mice noticeably expressed pancreatic Rgs16::GFP at any time point (Figure 10). This suggested that a general inflammatory response was not sufficient to induce pancreatic Rgs16::GFP expression. Furthermore apoptosis of acinar cells did not seem to induce GFP expression (Dittmer et al., 2008; Sasson et al., 2003). Henceforth, we focused our efforts on characterizing Rgs16::GFP under glucose stress and testing other diabetic models of chronic hyperglycemia.

Figure 10: Caerulein mediated pancreatic inflammation does not induce Rgs16::GFP

Example pictures of pancreatic Rgs16::GFP expression of normal glycemic mice treated with caerulein (50ug/kg BW x 5 times) compared at days 1, 2, 3, and 6 post-injection are shown in Panel A. Scale bar is 1mm. GFP levels are compared in Panel B. Day 6 and 15 STZ-treated and day 15 NaCit given animals are included as positive and negative control of expression, respectively.

PART 2: Chronic hyperglycemia is the primary condition driving Rgs16::GFP in islets of type 1 diabetic models

Summary: Rgs16::GFP was expressed in islets of type 2 diabetic mice, including *ob/ob*, naturally obese, or diet induced obese wild-type mice. We proposed Rgs16 was induced in response to beta cell expansion rather than signals regulating insulin release. If true, Rgs16::GFP could be initiated by any chronic hyperglycemia, including type 1 diabetes due to pancreatic beta cell depletion (Bluestone et al., 2010). Furthermore, inducible beta cell depletion would allow us to control the onset of beta cell expansion and conduct a short-term time course for Rgs16::GFP induction. We found that Rgs16::GFP is expressed in pancreatic islets during type 1 diabetes. Its intensity and onset is determined by the severity and duration of hyperglycemia. GFP expression is reduced following insulin injections that transiently restore normal glycemia and is extinguished in mice that recover normal glycemia after beta cell expansion.

2.1: Rgs16::GFP in islet beta cells of PANIC-ATTAC male mice gradually increases with duration of hyperglycemia

Initially, we utilized PANIC-ATTAC as a type1 diabetic model (Wang et al., 2008). Apoptosis in these otherwise normal glycemic mice could be triggered anytime by a drug administration that causes the FKBP-Caspase8 monomers inside the cell to form dimers and become active (Pajvani et al., 2005; Wang et al., 2008). Specific expression in beta cells was dictated by the rat insulin promoter, thus limiting the apoptotic signal to islets (Wang et al., 2008). As seen in Figure 11A, male mice became hyperglycemic after 5 consecutive days of dimerizer treatment. By contrast, most female mice remained normal glycemic. The female mice are presumably protected against apoptosis due to their higher

Figure 11: Inducible PANIC-ATTAC mice express pancreatic Rgs16::GFP in a rate proportional to the onset of hyperglycemia in male mice.

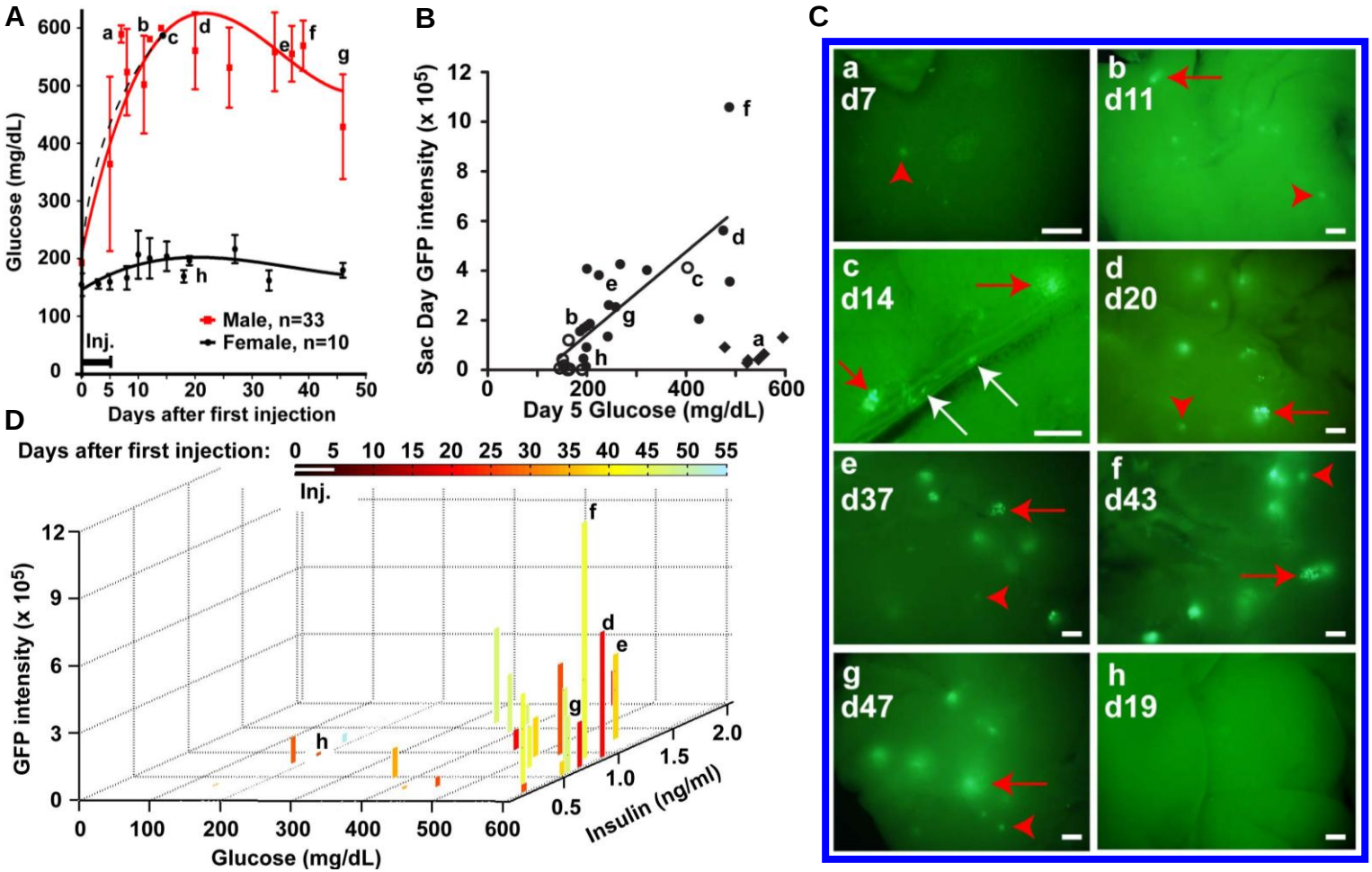

estrogen level (Le May et al., 2006; Liu et al., 2009). In the 7 week long period following induction of diabetes, male mice maintained their high glucose levels. Although the degree of beta cell apoptosis in males might be variable as seen with the large spectrum of day 5 glucose levels, all males became severely hyperglycemic within ten days.

The GFP levels of the PANIC-ATTAC mice were usually proportional to the duration of hyperglycemia, as observed previously in type 2 diabetic mice (Figure 11C). GFP expressing cells could barely be detected within the first week of hyperglycemia but spread to more islets and accumulated in more cells within islets, during following weeks. GFP intensity reflected the severity of hyperglycemia at day 5 post-dimerizer (Figure 11B). However, insulin levels were uniformly low and apparently had little or no relevance. If all parameters were considered, the highest GFP expressers corresponded to the mice with the highest glucose levels and with the longest duration of hyperglycemia (Figure 11D).

As we clearly observed that Rgs16::GFP was induced even with low insulin levels, we became more convinced that chronic hyperglycemia was the determining factor of islet GFP expression. We observed at least one

---

Figure 11: Inducible PANIC-ATTAC mice express pancreatic Rgs16::GFP in a rate proportional to the onset of hyperglycemia in male mice
Panel A shows glucose curve of Rgs16::GFP; PANIC-ATTAC male and female mice injected with dimerizer for 5 days. a, b, d, e, f, g are male and c and h are female mice. The glucose course of c is depicted with dashed black bar. Error bars are SD. Correlation of pancreatic GFP expression to the severity of day 5 hyperglycemia with linear regression curve is shown on Panel B. Filled circles are males and open circles are females. Outlier males are indicated with diamonds. Islet (red arrow for big, red arrow head for small islet) and VDAC (white arrow) expression of different mice are indicated on Panel C. Individual labels are matching to those from other panels. Scale bar is 100um. Comparison of single-image GFP quantification, glucose and insulin at sacrifice day is shown in Panel D. The number of days after 1st dimerizer injection is indicated in the color spectrum (Villasenor et al., 2010).

hyperglycemic GFP+ female, corroborating previous observations in *ob/ob* mice that islet Rgs16::GFP expression during diabetes was not gender specific. Aside from the reported protection against apoptosis, the initiation of beta cell expansion was likely to be the same in females and males (Ackermann et al., 2009; Le May et al., 2006). Because of close associations between the intensity of hyperglycemia and Rgs16::GFP in the pancreas, we postulated that a "hyperglycemic sensor" could be stimulating GPCR signals for pancreatic beta cell expansion and induction of Rgs16 transcription.

2.2: Recovery of normal glycemia in PANIC-ATTAC mice extinguishes Rgs16::GFP in islets

Upon confirmation of Rgs16::GFP expression in PANIC-ATTAC mice, the hypothesis remained that Rgs16::GFP was marking beta cells that responded to GPCR signals released during both type 1 and type 2 diabetes. It also suggested that insulin levels might not play a direct role in pancreatic GFP induction but instead respond to concomitant chronic hyperglycemia. If Rgs16::GFP induction was tied to glucose levels, then it would be interesting to know what would happen to GFP levels if mice were to recover from diabetes and restore euglycemia. With this question in mind, we looked for the outcome of recovery in PANIC-ATTAC mice (Wang et al., 2008).

Although all PANIC-ATTAC male mice became hyperglycemic within 20 days of dimerizer injection, persistence of hyperglycemia was variable. About 4 months after the initial beta cell ablation, six mice were either normal glycemic or slightly hyperglycemic (Figure 12A). By contrast, two mice continued to have severe hyperglycemia from 8 to 11 months after the initial beta cell ablation, whereas four of their littermates were normal glycemic. As the images from

Figure 12: Rgs16::GFP diminishes in recovered PANIC-ATTAC but not in hyperglycemic mice 4 - 11 months after beta cell ablation.

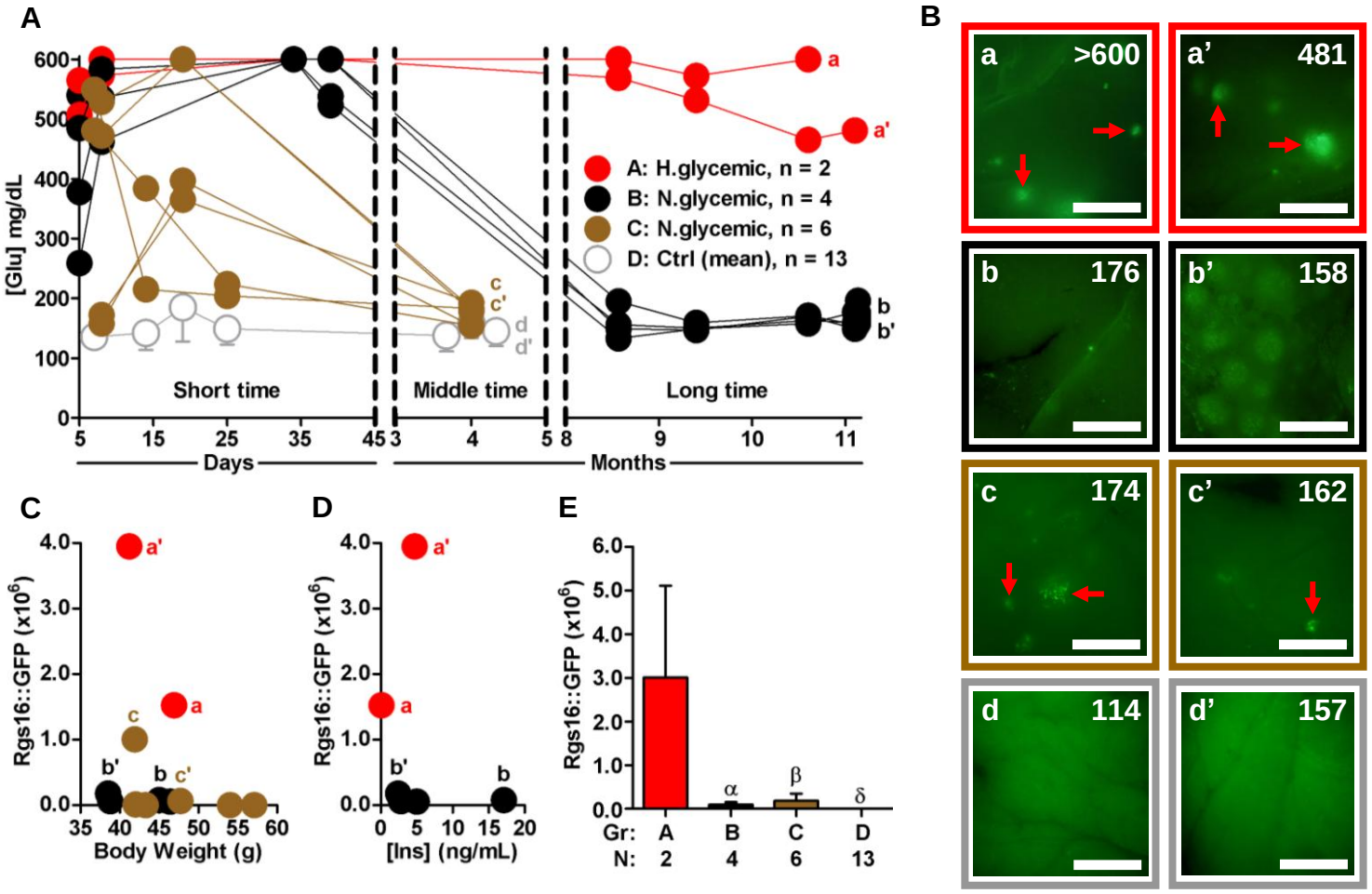

Figure 12B show, both hyperglycemic mice at 11 months, and one mouse at 4 months with slightly elevated hyperglycemia, had Rgs16::GFP expression. All euglycemic mice from either time point had little to no expression as reflected in the quantifications in Figure 12E. One normal glycemic mouse at 11 months had an isolated islet expression within a field of expanded lobe. This remnant expression suggested that Rgs16::GFP had persisted in all animals until they recovered from hyperglycemia. Body weights were similar in all groups making an underlying type 2 diabetic induction unlikely (Figure 12C). Furthermore, insulin levels did not correlate with the GFP level, as a hyperinsulinemic mouse at 11 months did not have GFP expression and the other mice all had similar insulin levels (Figure 12D). It appears that as glucose levels normalized, the signal to expand islets was extinguished explaining diminished GFP expression.

Figure 12: Rgs16::GFP diminishes in recovered PANIC-ATTAC but not in hyperglycemic mice 4 - 11 months after beta cell ablation

Blood glucose levels of PANIC-ATTAC mice after dimerizer treatment are shown in days after treatment in the short time point segment on the left and in months in the middle and long time points located on the center and right parts of Panel A, respectively. Ages range between 12-13 months for the mice at 4 months post-dimerizer time point (groups C and D) and 16-19 months for those at 11 months post-dimerizer (groups A and B). Example mice are indicated with (a, a') for hyperglycemic, with (b, b') and (c, c') for euglycemic 11 months and 4 months post-dimerizer mice, and (d, d') for the control mice respectively. Mice in groups A, B, and C are indicated with their individual glucose values, except group C mice have the average of 3 days at 4 months time point. Group D mice are non-PANIC negative control injected with dimerizer and their values are shown as mean with SD error bars. Corresponding 48x colored pancreas pictures of (a, a'), (b, b'), (c, c'), and (d, d') are shown in Panel B with sacrifice day blood glucose (mg/dL) levels top right. Scale bar is 1mm. Panels C and D compare the sacrifice day body weight and insulin levels of mice to their GFP expression. 2 mice that remained hyperglycemic in the long time course post-treatment are indicated in red color, whereas 4 normal glycemic counterparts are black. 6 normal glycemic middle time course mice are brown. Panel E compares the GFP quantification of hyperglycemic, normal glycemic, and control groups. Error bars in SD. Student's t test (unpaired, two-tailed) shows significance in-between. $p < 0.05$ (α), $p < 0.01$ (β), $p < 0.0001$ (δ).

These observations showed us that the expression of Rgs16::GFP was dynamic and closely tied to blood glucose levels. Consequently, if mice achieved euglycemia, Rgs16::GFP would no longer be induced, indicating the completion of beta cell expansion and cessation of expansion specific GPCR signals. Furthermore, abolishment of GFP as early as 4 months after inception of hyperglycemia showed that putative drugs to promote beta cell expansion could be tested in this model within this time frame. In addition, the persistence of Rgs16::GFP 11 months after beta cell death showed that the GPCR signals of beta cell expansion are continuously released as long as diabetes is untreated. As a result of all these correlations, we propose that Rgs16::GFP is a marker of beta cell expansion in both type 1 and type 2 diabetes.

2.3: STZ treatment induces pancreatic Rgs16::GFP expression coordinated with the onset and degree of hyperglycemia

Streptozotocin (STZ) treatment is a classical method for inducing rapid beta cell death (Ganda et al., 1976; Like et al., 1978; Like and Rossini, 1976). STZ has been used with different dosages to accommodate the degree of desired beta cell death either with or without hyperglycemia following its administration (Bonnevie-Nielsen et al., 1981; Leiter, 1982; Like and Rossini, 1976; McEvoy et al., 1984; Paik et al., 1980). Although recovery in the STZ model was limited to its treatment right after birth in rodents, the ease of the administration without requiring a separate transgenic mouse line like PANIC-ATTAC and the rapid apoptotic response has made it the most commonly used type 1 diabetic model (Liang et al., 2011; Thyssen et al., 2006; Wang et al., 1994).

We asked if STZ dependent type 1 diabetes could also induce Rgs16::GFP (Figure 13). We tested several dosages of STZ because high doses were lethal, caused fatty liver and chronic immune attack, whereas very low doses did not

Figure 13: STZ treatment induces rapid hyperglycemia followed by initiation of Rgs16::GFP expression in a dosage dependent manner

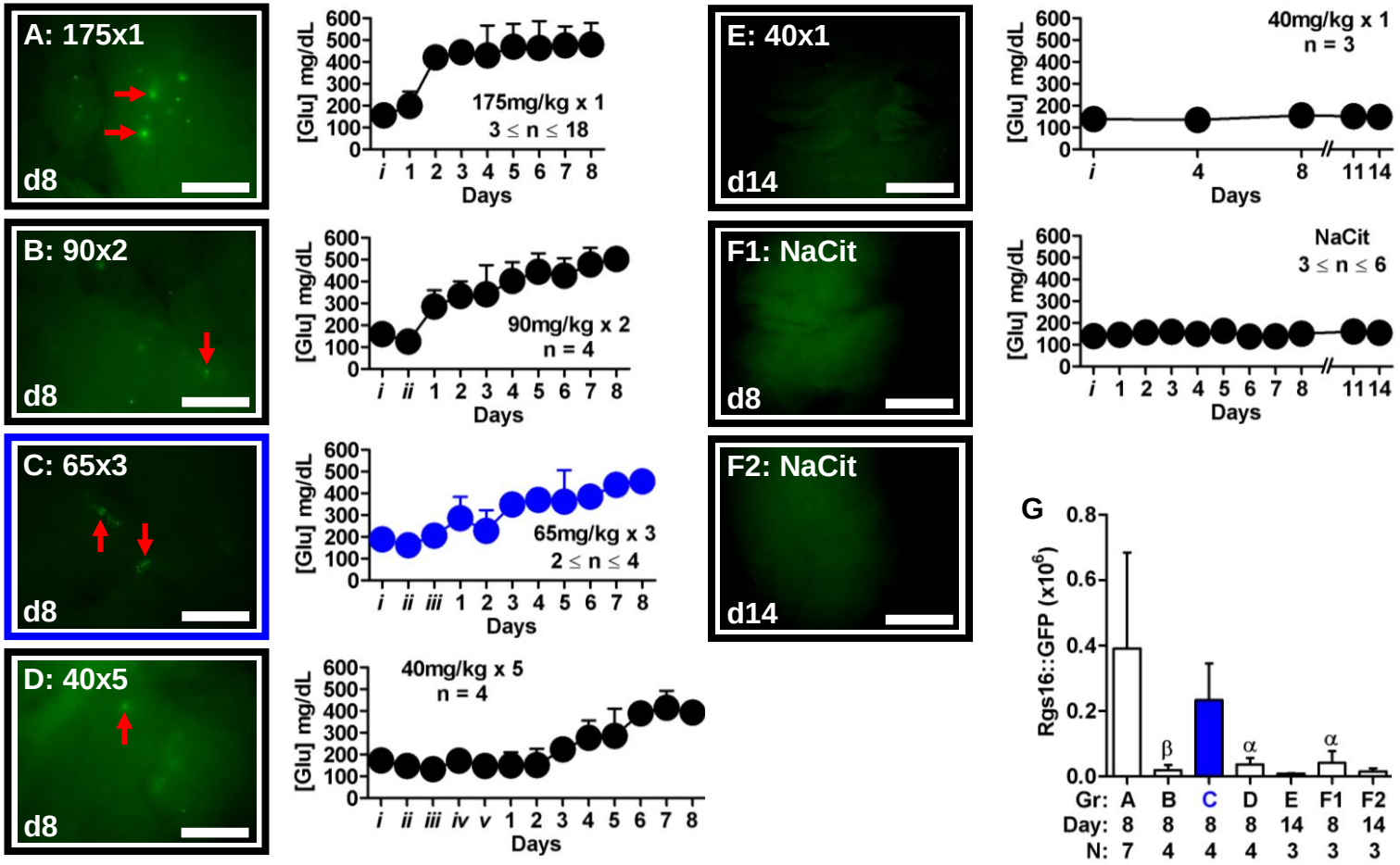

cause hyperglycemia. We measured daily glucose levels in all groups. Except for mice given a single low dosage STZ and the negative control groups, all mice eventually became hyperglycemic (Figure 13A - F2). As the panels in Figure 13 show, only two dosages were effective in inducing GFP. A single high dose STZ injection gave the highest GFP expression over a wide range, but mice were sickly, had fatty livers and undigested food in distend stomachs. 3 of them died before day 8. By contrast, mice treated with a moderate STZ protocol (65mg/kg/day for 3 days) were hyperglycemic but otherwise appeared healthy, and GFP expression in islets was the second highest among treatment groups. None of the NaCit controls and the single low dosage mice at day 14 expressed GFP, indicating that neither NaCit nor a low STZ dosage affected pancreas.

Even though all groups, except the single low dosage, had similar total injected STZ, the amount per day seemed to be the determining factor in how mice would tolerate STZ, how fast beta cell apoptosis would lead to hyperglycemia, and eventually how fast it would bring about Rgs16::GFP expression. We concluded that 3 days of STZ injection was the most effective and reliable dosage to induce Rgs16::GFP within 8 days in the pancreas without

---

Figure 13: STZ treatment induces rapid hyperglycemia followed by initiation of Rgs16::GFP expression in a dosage dependent manner
Adult Rgs16::GFP mice separated into groups for different STZ treatments are shown. Picture-blood glucose sets A, B, C, D show 175mg/kg/day for 1 day, 90mg/kg/day for 2 days, 65mg/kg/day for 3 days, and 40mg/kg/day for 5 days treatment groups at day 8 post-STZ, whereas set E with 40mg/kg/day for 1 day treatment is sacrificed at day 14. NaCit as negative control (175mg/kg/day for 1 day) is shown in the picture set F1 and F2 with day 8 and day 14 pancreas, respectively. Red arrows point GFP+ islets. Scale bar is 1mm. Columns in Panel G show average pancreatic GFP quantification for each group. Student's t test (unpaired, two-tailed) shows significance of the 65mg/kg/day x 3 days dosage (blue bar) compared to control, 90mg/kg/day for 2 days, and 40mg/kg/day for 5 days STZ groups. $p < 0.05$ (α), $p < 0.01$ (β). Error bars in all panels are SD.

accompanied side effects. We used this dosage henceforth for characterizing pancreatic Rgs16::GFP time course.

2.4: Rgs16::GFP expressing islets are progressively recruited with persistent hyperglycemia in STZ-treated mice

Mice were treated with STZ to follow the time course of hyperglycemia and pancreatic Rgs16::GFP in this type 1 diabetic model. As seen in Figure 14, basal glucose levels tended to go up starting from the third STZ day of injection. Mice invariably started to become hyperglycemic on the first day after the injection period and became more severely so throughout the 20 day post-treatment period (Figure 14).

When we looked at pancreata at various time points, there was no GFP expression at day 2 and day 4. Rgs16::GFP began to emerge by 6 days post-STZ and progressed at comparable levels up to day 12. Interestingly, expression showed a spike by day 15 suggesting an enhancement of the inducing signal between days 12 and 15. Expression remained relatively constant at day 20.

Reports tying Rgs16 to apoptosis made us consider the possibility of whether beta cell ablation mechanism or signals could be implicated with Rgs16::GFP expression (Dittmer et al., 2008; Sasson et al., 2003; Sasson et al., 2004). Similar to our previously described observations with caerulein treatments and PANIC-ATTAC mice, early mildly hyperglycemic time points after STZ derived islet apoptosis did not induce Rgs16::GFP inside pancreas. The complete lack of expression convinced us that there was not a diminishment of an acute post-apoptotic GFP induction. Therefore, we concluded Rgs16::GFP expression was not related to apoptotic mechanisms or post-apoptotic responses in diabetic pancreas.

Figure 14: Chronic hyperglycemia induces pancreatic Rgs16::GFP over time in the STZ model.

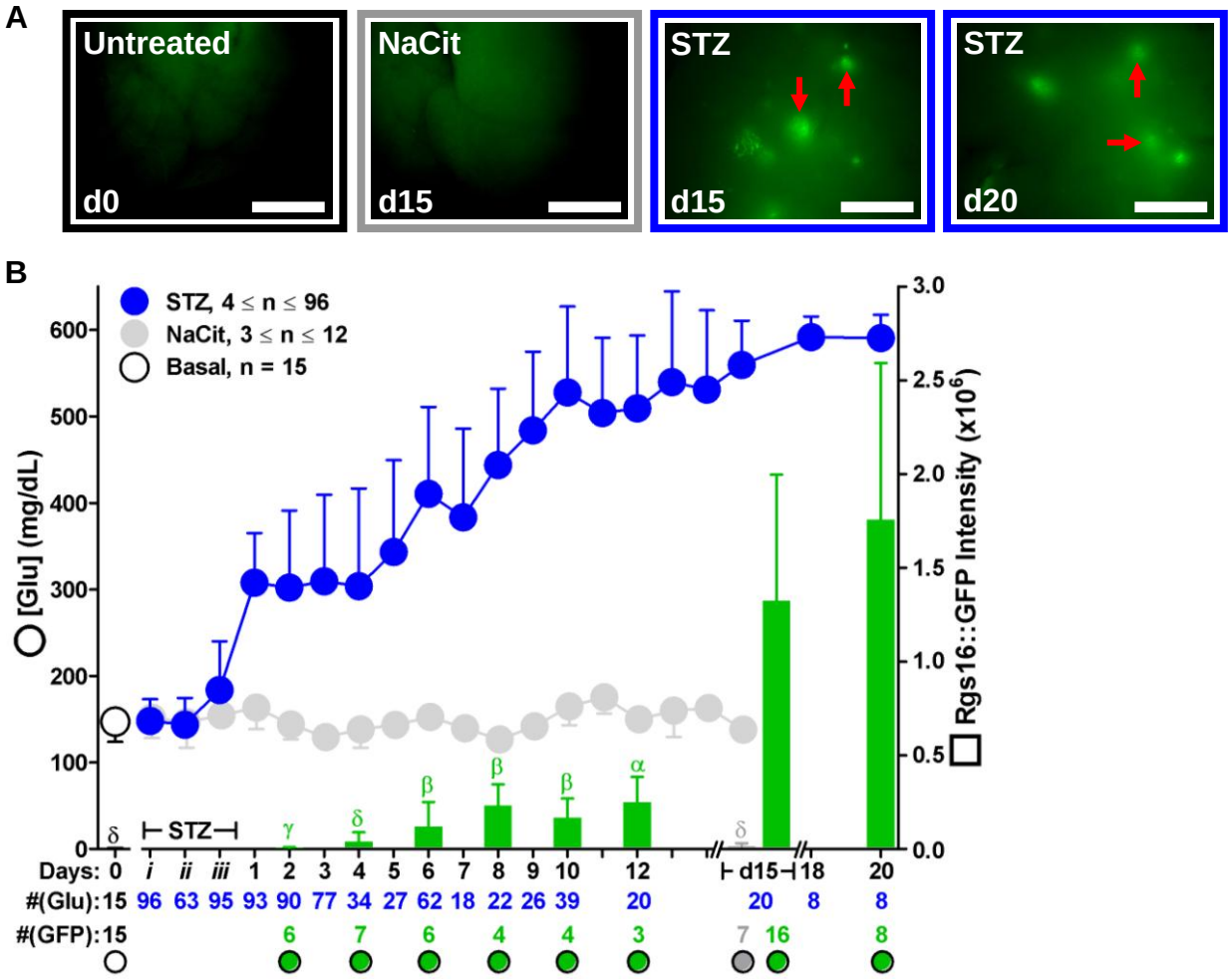

The delayed onset of Rgs16::GFP expression following initial hyperglycemia and later progression into more islets and cells mimicked the course we previously observed in both type 1 and type 2 diabetic models. As seen before, acute hyperglycemia did not have an effect on pancreatic Rgs16::GFP induction. Instead, several days of chronic hyperglycemia was required to see the earliest expression. Considering PANIC-ATTAC and STZ models together, we conclude that Rgs16::GFP would first be expressed within a week of severe chronic hyperglycemia during type 1 diabetes. Consequently, STZ treatment was a much quicker method of inducing pancreatic GFP expression than type 2 models and an easier and more uniform method of causing beta cell ablation than PANIC-ATTAC model. However, STZ could not be used as a recovery model like PANIC-ATTAC as STZ exerts broader detrimental effects that interfere with beta cell expansion *in vivo* (Barber et al., 2003; Bestetti and Rossi, 1980; Marks et al., 1993; Nishio et al., 2006; Oliver et al., 1989). Therefore, STZ would be utilized for short-term experiments to test enhancement of early signals, while PANIC-ATTAC was a more suitable model for long-term study of beta cell expansion and recovery. Day 15 was a suitable time point for testing inhibitory conditions of pancreatic Rgs16 expression via means of counteracting hyperglycemia. We also concluded that drugs that might enhance beta cell replication and Rgs16::GFP expression could be screened within 12 days of STZ

Figure 14: Chronic hyperglycemia induces pancreatic Rgs16::GFP over time in the STZ model

Untreated, NaCit and day 15 and 20 post-STZ pancreas samples are shown in Panel A. Red arrows indicate GFP+ islets. Scale bar is 1mm. The daily glucose curve (scaled to left axis) and pancreatic GFP levels at basal and days 2, 4, 6, 8, 10, 12, 15, and 20 (scaled to the right axis) of male Rgs16::GFP mice treated with STZ are shown in the composite graph of Panel B. Untreated Rgs16::GFP mice have normal basal levels (circle) and NaCit-injected animals (gray dots) are negative control for STZ. Error bars are SD. Statistical significances between day 15 GFP and other groups are calculated via Student's t test (unpaired, two-tailed). $p < 0.05$ (α), $p < 0.01$ (β), $p < 0.001$ (γ), $p < 0.0001$ (δ).

administration in Rgs16::GFP reporter mice. The STZ protocol (65mg/kg x 3 days) thereby provided us not just confirmation of Rgs16::GFP induction during type 1 diabetes but also an *in vivo* assay to test stimulatory and inhibitory conditions and compounds of beta cell expansion signals.

2.5: Insulin injections interrupt the persistent chronic hyperglycemia and thereby islet expression of Rgs16::GFP in STZ-treated mice

The STZ model of type 1 diabetes was most efficient for inducing Rgs16::GFP following hyperglycemia. Thus, we used the STZ model to test signals that might be established during hyperglycemic demand on the pancreas. If mice normalized blood glucose levels over time as in PANIC-ATTAC, inducing signals and thereby GFP expression would also diminish. We wanted to see the direct consequence of reducing hyperglycemic demand on GFP expression. In order to test that, we decided to inject insulin to STZ-treated hyperglycemic mice.

When we monitored blood glucose levels before and after insulin injections, we noticed that glucose levels normalized for only about 4 hours a day (data not shown). On average, resting blood glucose levels in the insulin-treated STZ mice were significantly lower than STZ only counterparts at day 15 as seen in the pancreas pictures on Figure 15A and GFP quantification on Figure 15B. Mice with the highest amount of insulin injections and most consistent normalizations of blood glucose had the lowest GFP levels. We concluded that relieving mice from ongoing hyperglycemia, even very briefly each day, could repress pancreatic Rgs16::GFP expression.

We also tested intermediate-acting Humulin-N, insulin-protamine suspension, starting at later days of post-STZ treatment to exert a longer duration of normalized blood glucose levels. In these trials, pancreatic GFP level was only

Figure 15: Daily insulin injections lower blood glucose levels transiently and are sufficient to suppress Rgs16::GFP in STZ given mice.

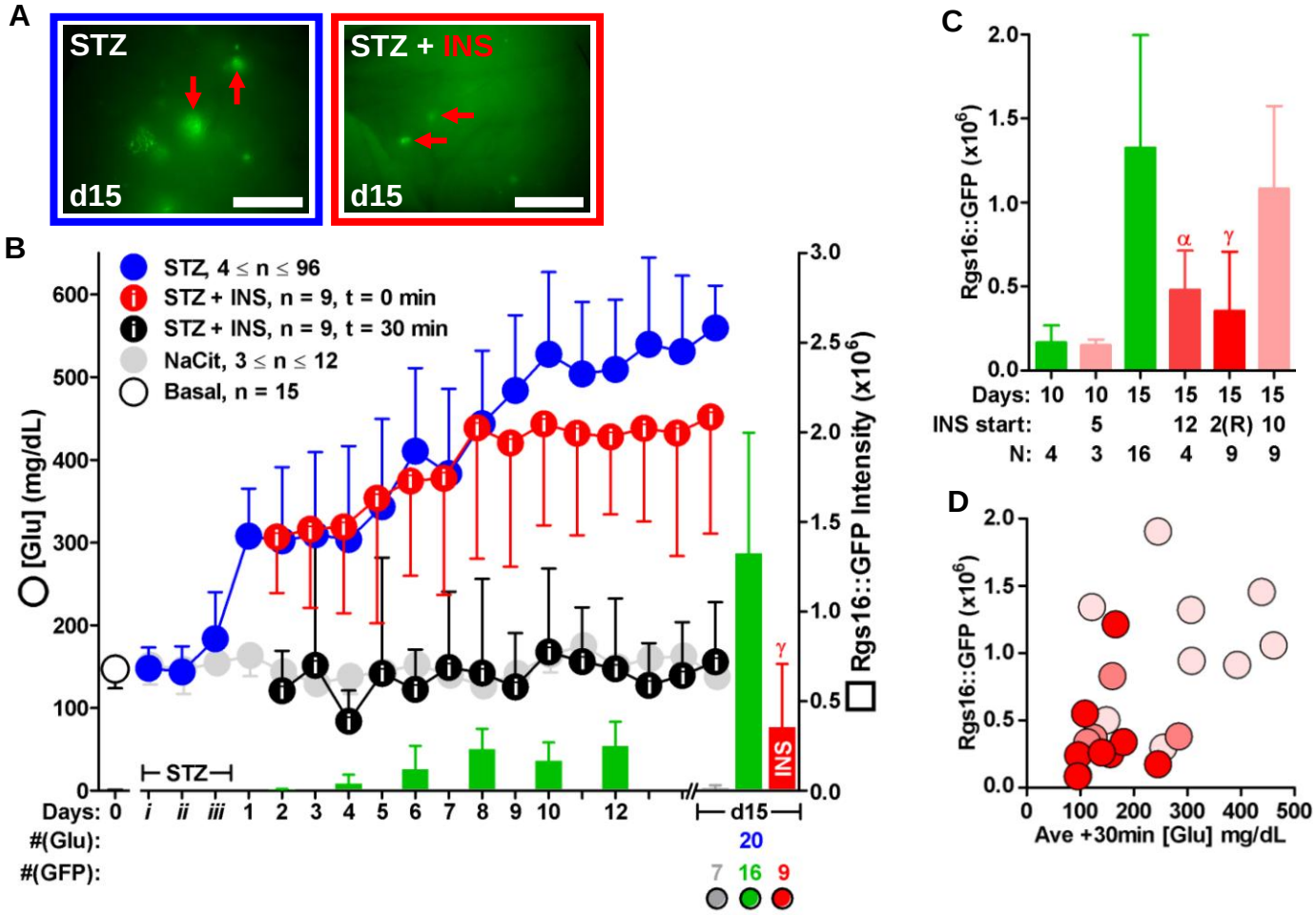

significantly reduced if normalization of blood glucose levels were successful at t = 30min (Figure 15C, D).

Our insulin administrations to STZ given mice together showed that the early signal to induce Rgs16::GFP in the pancreas can be interrupted by transiently lowering blood glucose levels. This gave a more definite answer to the question whether glucose and insulin together were affecting a signal that turns on Rgs16::GFP. When insulin administration was insufficient to lower glucose, it did not lower GFP. On the other hand, we achieved significant reductions of pancreatic GFP if we could consistently normalize glucose levels after insulin injections. Taken together, insulin injections had only inhibitory effects on pancreatic Rgs16::GFP. However, rather than acting as a ligand to inhibit Rgs16::GFP, it exerted its effect by lowering blood glucose levels via cellular glucose uptake.

Based on the positive correlation between pancreatic Rgs16::GFP and glucose levels in the STZ model, as well as previous results in other diabetic

---

Figure 15: Daily insulin injections lower blood glucose levels transiently and are sufficient to suppress Rgs16::GFP in STZ given mice
Insulin-injected mouse pancreas is compared to STZ only pancreas in Panel A. Red arrows indicate GFP+ islets. Scale bar is 1mm. The glucose curve (scaled to left axis) and day 15 pancreatic GFP levels (scaled to the right axis) of male Rgs16::GFP mice treated with STZ are shown in Panel B. Basal glucose levels (red dots with "i") of insulin group animals and their levels 30min after insulin injection (black dots with "i") are indicated separately. Untreated Rgs16::GFP mice have normal basal levels (circle) and NaCit-injected animals (gray dots) are negative control for STZ. Error bars are SD. Statistical significance between day 15 GFP and insulin-injected (Humulin-R) day 15 group (INS) is calculated via Student's t test (unpaired, two-tailed). Panel C compares STZ to STZ+INS group of mice at day 10 and day 15. Insulin injection start days are shown below the graph. All insulin types are Humulin-N except mice from Panel B. $p < 0.05$ (α), $p < 0.001$ (γ). Day 15 STZ mice treated with insulin are graphed according to t = 30min insulin levels in Panel D. Red dots are mice from the INS group of Panel B. Bright reds are injected from day 12 and faint reds are injected from day 10 twice daily with Humulin-N.

models, we propose that Rgs16 is under control of signals that are created or enhanced based on the duration and severity of hyperglycemia. This idea suggests there is a "hyperglycemia sensor" that can detect and distinguish normal oscillations in circulating glucose levels from sustained hyperglycemia (Delaere et al., 2010; Thorens, 2001). This detector then initiates or impacts signals involving beta cell expansion under metabolic demand. Rgs16::GFP would then be induced within this beta cell proliferative state to feedback regulate associated GPCR signaling inside islets. Although it is possible that "the hyperglycemia sensor" could be directly regulating beta cell expansion, it is also possible that distinct but coordinated signals stimulate beta cell proliferation and induction of Rgs16 (Matschinsky, 2005; Thorens, 2008). Nevertheless, either possibility still points out that Rgs16 is downstream of signals from the "hyperglycemia sensor" (Thorens, 2008). Given that we have detected Rgs16::GFP in islets of normal glycemic mice under metabolic stress, such as early type 2 diabetes induced by HF diet, it is possible that the read-out from the hyperglycemia sensor is integrated with sensors for insulin or other metabolic hormones and/or nutrients. Although the location of the sensor is not known, work by others suggests arcuate nuclei of hypothalamus (Arees and Mayer, 1967; Leloup et al., 1998; Ngarmukos et al., 2001; Nishio et al., 2006; Thorens, 2001). The heterogeneous distribution of Rgs16::GFP expressing islets and GFP+ cells within the islets is consistent with signals coming from the peripheral nerve terminals inducing beta cell expansion (Leloup et al., 1998). In any case, all these possibilities require elaborate testing in the future.

PART 3: ChREBP is required for Rgs16::GFP in islets of STZ-treated hyperglycemic mice

Summary: Analysis of Rgs16 KO and inducible transgenic mice with liver-specific Rgs16 expression showed Rgs16 inhibits hepatic fatty acid oxidation during fasting (Pashkov et al., 2011). Rgs16 transcription was glucose-dependent and downstream of the transcription factor Carbohydrate Response Element Binding Protein (ChREBP) (Pashkov et al., 2011). ChREBP was first discovered as the glucose-dependent factor driving lipogenic gene transcription in liver after feeding (Ishii et al., 2004; Kabashima et al., 2003; Kawaguchi et al., 2002; Kawaguchi et al., 2001; Ma et al., 2006; Ma et al., 2005; Yamashita et al., 2001). Although direct binding to Rgs16 promoter was not detected, ChREBP was required for maximal Rgs16 transcription in liver and in cultured hepatocytes, revealing an unexpected function of this transcription factor during a long fast (Davies et al., 2008; Pashkov et al., 2011). Recently, ChREBP was found to regulate gene transcription in a glucose dependent manner in isolated pancreatic beta cells or beta cell lines as well (Boergesen et al., 2011; Cha-Molstad et al., 2009; da Silva Xavier et al., 2006; da Silva Xavier et al., 2010; Gao et al., 2010; Noordeen et al., 2010). We investigated type1 diabetic ChREBP KO mice and found that they lacked Rgs16::GFP induction during chronic hyperglycemia after STZ-treatment. We propose ChREBP is either required in beta cells or for the development and/or function of a “hyperglycemia sensor” that transmits signals to the pancreas and induces Rgs16 expression.

3.1: Rgs16::GFP expression is absent in STZ-treated ChREBP KO mice

Under normal conditions, Rgs16::GFP animals with ChREBP KO or WT genotype were normal glycemic with no differences in body weight as expected,

as previously reported (Iizuka et al., 2004). ChREBP KO animals were reported to have mild defects in their glucose stimulated insulin secretion (GSIS) and therefore we confirmed their Rgs16::GFP expression status before STZ administration. As seen in Figure 12, there was no GFP expression in normal glycemic ChREBP KO animals without manipulation. A distinction between genotypes was seen in the first 6 days after STZ injection, where KO animals became hyperglycemic faster than heterozygous and WT controls. This tendency could be caused by their compromised GSIS or increased sensitivity to apoptosis. After 6 days, and for as long as 27 days post-STZ, hyperglycemia was indistinguishable in ChREBP KO, heterozygous, and WT mice.

Despite prolonged hyperglycemia, Rgs16::GFP was not expressed in ChREBP KO mouse pancreas at day 15 post-STZ. By contrast, WT pancreas had Rgs16::GFP expression as expected (Figure 16). Interestingly, expression in ChREBP heterozygous mice was about half the intensity of their WT siblings. Initially, we considered that ChREBP activity could be copy number dependent. We also investigated pancreata at a later time point to understand if Rgs16::GFP was completely abolished or had a long delay in the initiation of expression. Since GFP persisted at least to day 20 post-STZ in the ICR background mice, we assayed ChREBP KO mice at day 27 post-STZ. All animals continued to be severely hyperglycemic. WT animals expressed pancreatic GFP at the same high level, whereas ChREBP KO mice still did not express GFP. Surprisingly, GFP levels in heterozygous ChREBP mice were on average much lower at day 27 compared to WT. Absence of GFP expression in several heterozygous animals suggested expression could not be maintained with single ChREBP gene copy. These results showed that Rgs16::GFP induction required ChREBP.

This is the first report that ChREBP contributes to early phase beta cell expansion GPCR signal feedback response. Since we experimented with whole-body KO animals, it was not apparent whether ChREBP expression in pancreas or

Figure 16: Rgs16::GFP expression in STZ model is absent in ChREBP KO mice

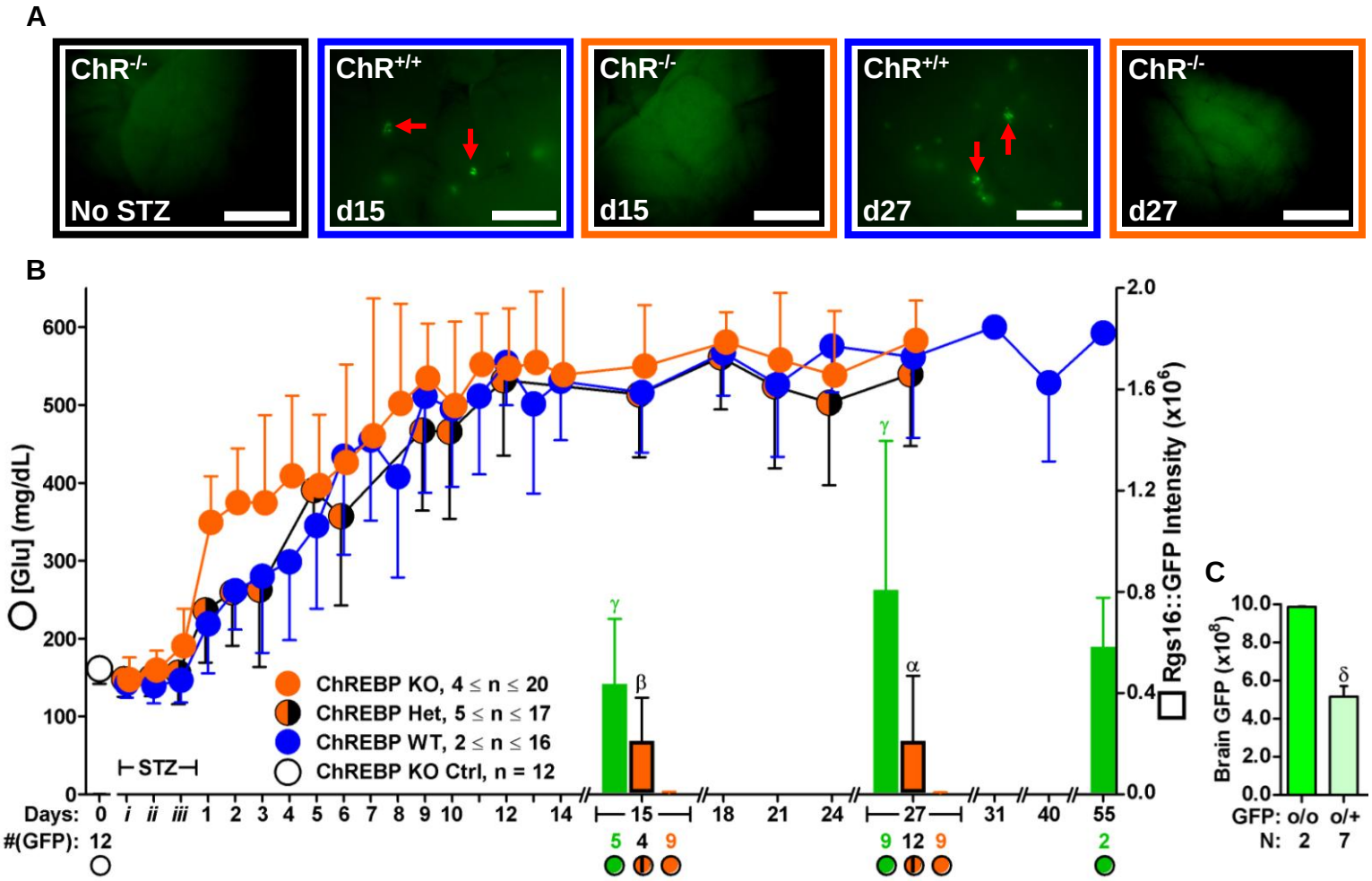

elsewhere was crucial for Rgs16::GFP induction. It was also not conclusive if loss of ChREBP was affecting beta cell specific diabetic response or if it was involved at some regulatory stage of hyperglycemic signals. The latter idea raised the possibility of an association between ChREBP and signals mediated by the "hyperglycemia sensor". On one hand, ChREBP might be important for initiating signals from the sensor, on the other hand it could be critical for the transcriptional response to those signals in beta cells. Answers to these questions will require tissue specific inducible ChREBP KO animal models, where we could compare STZ driven Rgs16::GFP responses.

3.2: ChREBP is not required for Rgs16::GFP in beta cells during neonatal isletogenesis

The lack of Rgs16::GFP expression in the absence of ChREBP *in vivo* raised the question if pancreatic Rgs16::GFP expression was absent during embryogenesis and postnatal isletogenesis in ChREBP KO animals. We knew that *Rgs16::GFP; ChREBP*$^{+/+}$ animals continued to express GFP until the end of weaning. This possibility of ChREBP affecting pancreas developmental

---

Figure 16: Rgs16::GFP expression in STZ model is absent in ChREBP KO mice

Pancreatic sample pictures of male Rgs16::GFP mice with ChREBP WT and KO backgrounds at day 15 and 27 post-STZ are shown in Panel A. Red arrows indicate GFP+ islets. Scale bar is 1mm. The daily glucose curve (scaled to left axis) and pancreatic GFP levels at days 15, 27, and 55 (scaled to the right axis) of male Rgs16::GFP mice treated with STZ in *ChREBP*$^{+/+}$ ($3 \leq n \leq 10$), *ChREBP*$^{+/-}$ ($5 \leq n \leq 10$) and *ChREBP*$^{-/-}$ ($4 \leq n \leq 15$) backgrounds are shown in the composite graph in Panel B. Untreated *ChREBP*$^{-/-}$ mice ($n = 12$) serve as basal GFP control. Brain quantification showing the difference of GFP expression between *Rgs16::GFP*$^{o/o}$ and *Rgs16::GFP*$^{o/+}$ mice at day 15 STZ is displayed in Panel C. Error bars are SD. Statistical significances are calculated with Student's t test (unpaired, two-tailed). $p < 0.05$ (α), $p < 0.01$ (β), $p < 0.001$ (γ), $p < 0.0001$ (δ).

necessitated us to check early GFP expression in the developing pancreas of ChREBP KO pups. As seen in Figure 17A, GFP was equally expressed in ChREBP KO and WT pups. Intensity of expression, number and distribution of GFP+ islets looked indistinguishable between ChREBP KO and WT pups.

Postnatal Rgs16::GFP induction seemed to be independent of ChREBP and metabolism. Since these mice were normal glycemic, their beta cell expansion could be assumed to progress normally either with or without the ChREBP gene. As depicted in models of Figure 17, one explanatory idea could be that beta cell expansion was autonomous during postnatal development where Rgs16::GFP inducing signals were generated independently of the "hyperglycemia sensor". Although we do not know how postnatal signals differ from those created during diabetes, they clearly did not require ChREBP. This suggestion contrasts the adult situation, where signals to induce Rgs16::GFP were ChREBP dependent. We hypothesized that the diabetic beta cell expansion stimulus to dormant pancreas might come from the brain (Figure 17B). ChREBP-independent postnatal induction of Rgs16::GFP is consistent with the role of ChREBP as a transcription factor of metabolism rather than the development. However, requirement of ChREBP for the development of the "hyperglycemia sensor" can not be ruled out.

3.3: **Pancreatic Rgs16::GFP is reduced in female mice that resist STZ driven hyperglycemia**

Females resist beta cell driven apoptosis (Balhuizen et al., 2010; Kumar et al., 2011; Le May et al., 2006; Liu and Mauvais-Jarvis, 2009, 2010; Rossini et al., 1978). We observed this phenomenon in dimerizer-injected female PANIC-ATTAC mice where all but one continued to be normal glycemic. Rgs16::GFP expression in this outlier resembled that of a male mouse and therefore hinted that

Figure 17: Neonatal Rgs16::GFP expression in ChREBP KO mice is unaffected.

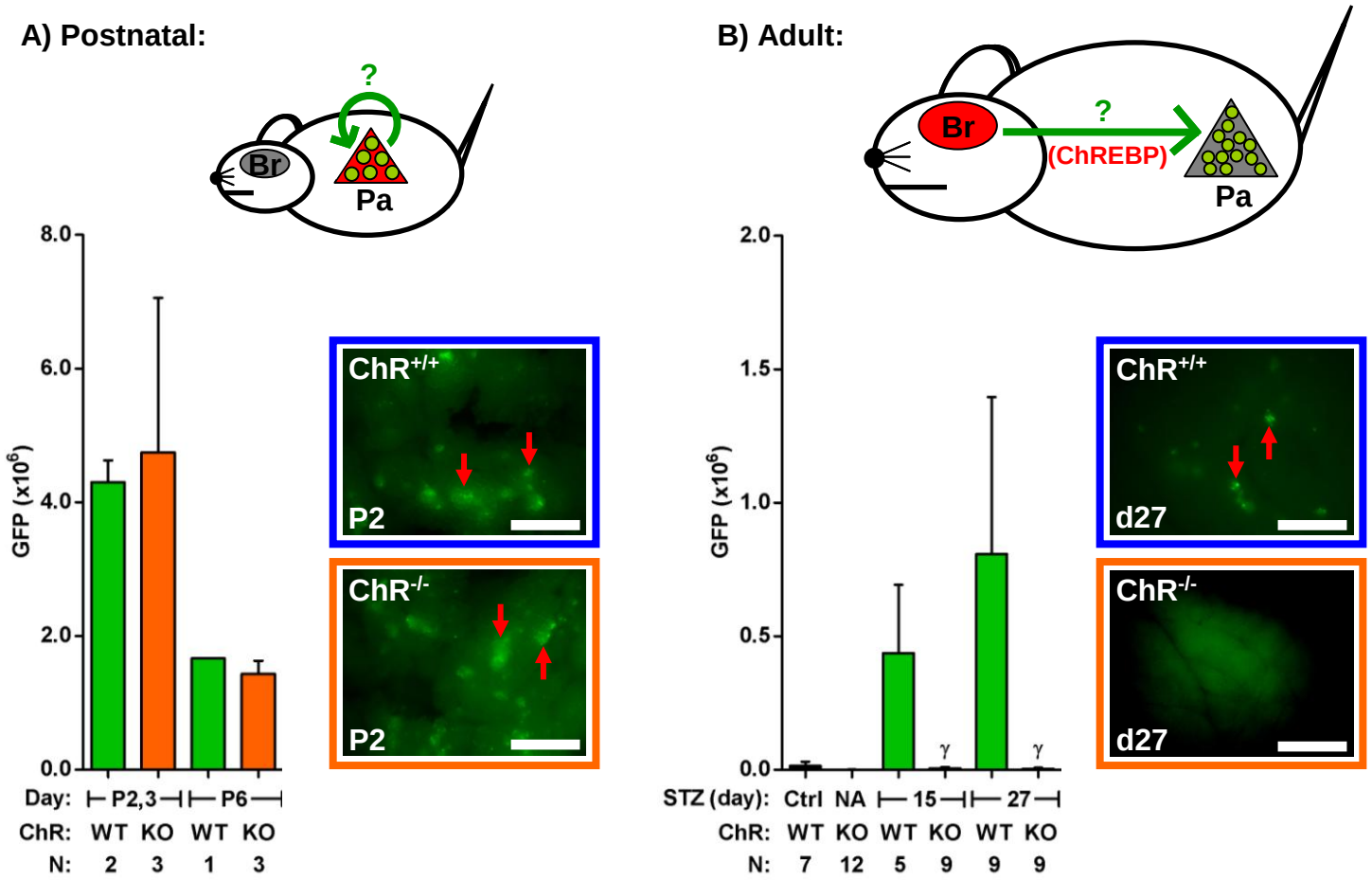

the difference between male and female response to type 1 diabetes induction might merely lie in their estrogen dependent protection against apoptosis (Liu et al., 2009).

We hypothesized that Rgs16::GFP female mice would have less or no expression than males if STZ treatment could not exert its effect. When Rgs16::GFP females were treated with STZ, they continued to be normal glycemic during the early days post-STZ. The first increase in glucose level became visible at day 4 with one and at day 5 with another female. At day 15 post-STZ, only 3 females had history with hyperglycemia with only 1 of them reaching high levels whereas the rest of the females never showed even slight hyperglycemia (Figure 18B). When we looked at the pancreata of all the female mice, we only saw a noticeable expression in one female that had the longest duration and highest value of hyperglycemia (Figure 18A).

This clear deviation of glucose curve and GFP values of female mice from males was expected according to the data about estrogen derived protection against apoptosis and consistent with our observations in PANIC-ATTAC (Villasenor et al., 2010). The variation among females could be attributed to variances between their estrogen levels at the time we started STZ treatment

---

Figure 17: Neonatal Rgs16::GFP expression in ChREBP KO mice is unaffected

Panel A shows example 1-picture GFP quantification and pictures of post-natal ChREBP WT and KO animals. Panel B shows GFP quantification at day 15 and day 27 post-STZ (65mg/kg/day x 3 days) Rgs16::GFP animals with ChREBP WT and KO backgrounds. Ctrl mice are NaCit-injected day 15 *ChREBP*$^{+/+}$*; Rgs16::GFP* mice. Also, 12 untreated *ChREBP*$^{-/-}$*; Rgs16::GFP* mice serve as basal GFP control for STZ groups and are indicated as NA. Statistical significances are calculated with Student's t test (unpaired, two-tailed). $p < 0.001$ (γ). Models suggesting the source of induction signal in postnatal mice and STZ model are shown above graphs and pictures in Panel A and B, respectively. Abbreviations are Br: Brain and Pa: Pancreas. Red arrows indicate GFP+ islets. Scale bar is 0.5mm for Panel A and 1mm for Panel B.

Figure 18: Pancreatic Rgs16::GFP is reduced in female mice that resist STZ driven hyperglycemia

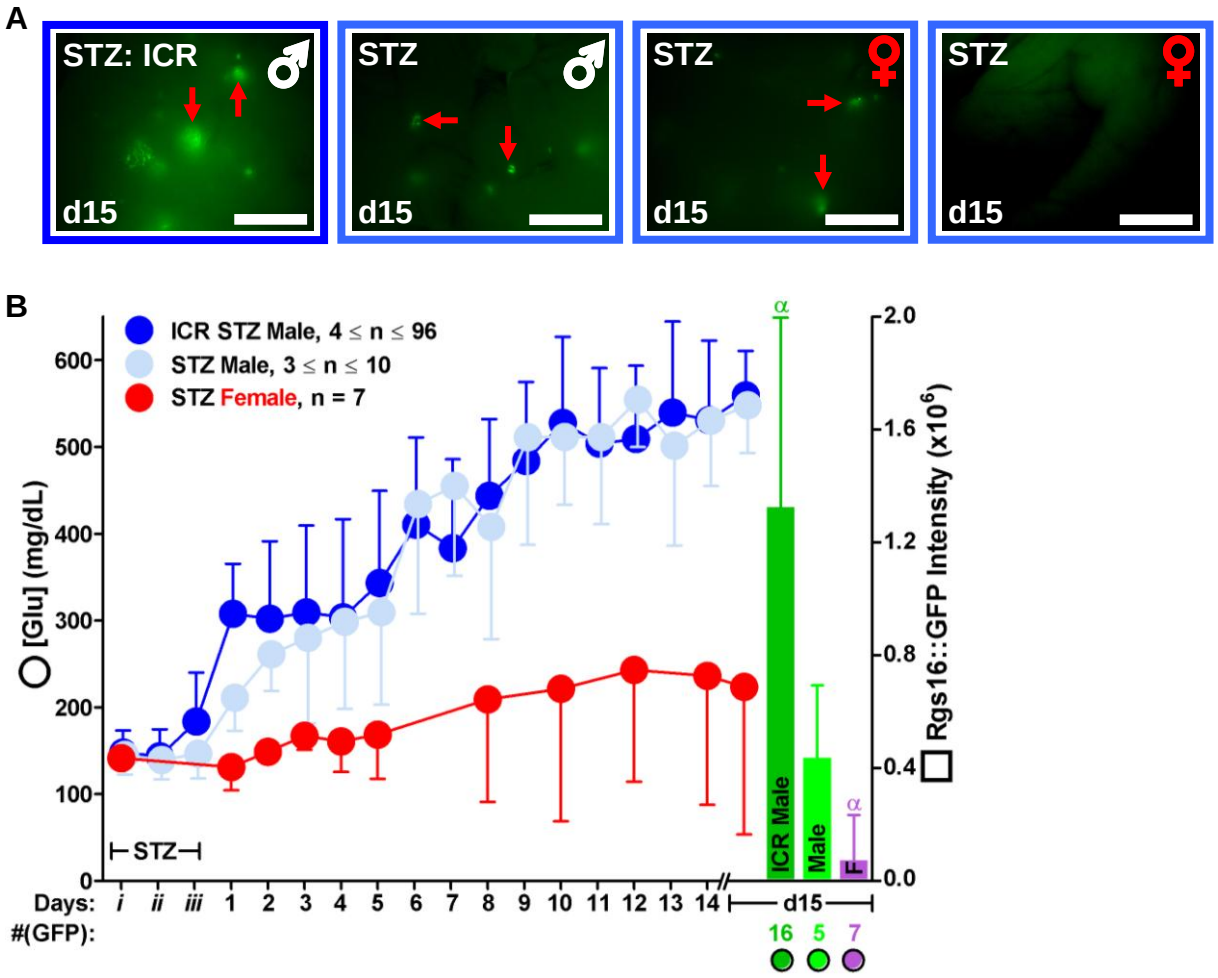

(Balhuizen et al., 2010; Liu and Mauvais-Jarvis, 2010). Nevertheless, the expression in the STZ administered hyperglycemic female confirmed that Rgs16::GFP induction was not gender specific but responded to blood glucose level. Based on this outcome, we postulated that females in the appropriate phase of the estrus cycle could serve as diabetic controls for testing drugs that enhance GFP expression.

3.4: STZ induces chronic hyperglycemia but not pancreatic Rgs16::GFP in ChREBP KO female mice

The intriguing resistance of females against hyperglycemia raised the possibility of the estrogen playing a role in the mechanism of ChREBP dependent "hyperglycemia sensor" (Ackermann et al., 2009; Liu and Mauvais-Jarvis, 2009). As seen with ChREBP KO male mice becoming hyperglycemic faster than WT counterparts, we speculated whether GSIS defects of ChREBP KO mice would counteract the protection of females (Iizuka et al., 2004). In that case, it would be interesting to see if estrogen in hyperglycemic females would induce Rgs16::GFP under diabetic conditions in ChREBP KO background (Balhuizen et al., 2010).

We administered STZ to Rgs16::GFP female mice with ChREBP KO and heterozygous backgrounds (Figure 19). After about a week, some heterozygous

---

Figure 18: Pancreatic Rgs16::GFP is reduced in female mice that resist STZ driven hyperglycemia

Representative images of day 15 male and female pancreata from mice with different strains treated with STZ (65mg/kg x 3 days) are shown in Panel A. Red arrows indicate GFP+ islets. Symbols at right hand corner indicate gender. Scale bar is 1mm. The glucose curve (scaled to left axis) and day 15 pancreatic GFP levels (scaled to the right axis) of male ICR strain Rgs16::GFP mice and mixed background male and female Rgs16::GFP mice treated with STZ are shown in Panel B. Error bars are SD. Statistical significances of GFP values between mixed background males vs. females or ICR males are calculated with Student's t test (unpaired, two-tailed). $p < 0.05$ (α).

Figure 19: Rgs16::GFP is not turned on in ChREBP KO hyperglycemic females

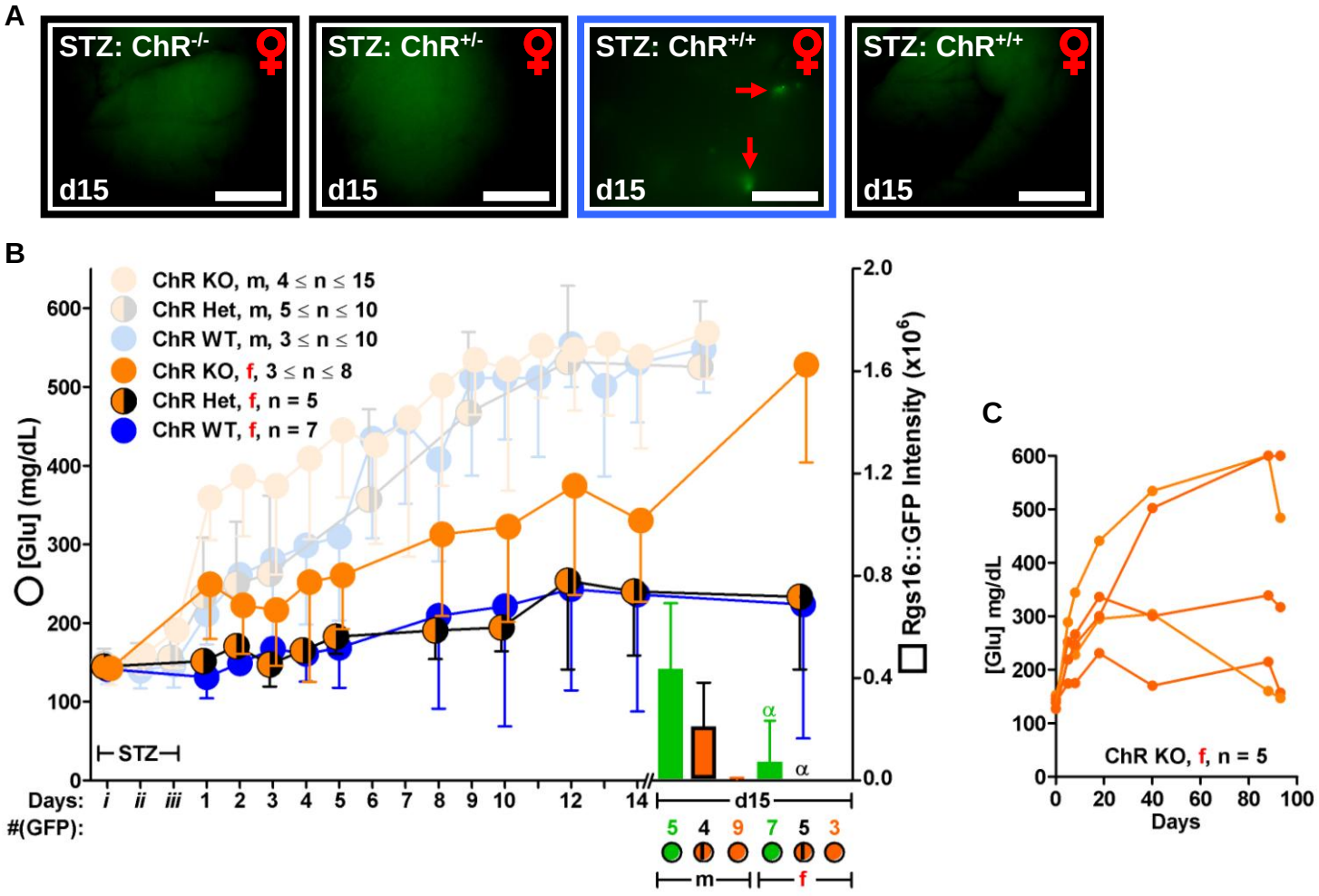

females showed mild hyperglycemia like their WT counterparts (Figure 19B). On the other hand, ChREBP KO females immediately became mildly hyperglycemic and their glucose level progressed above WT or heterozygous females. After two weeks, most ChREBP KO female mice reached moderate to high glucose levels.

Despite chronic hyperglycemia at day 15 post-STZ, ChREBP KO female pancreata did not express Rgs16::GFP (Figure 19A), as we observed in males. ChREBP heterozygous female mice with occasional mild hyperglycemia did not express Rgs16::GFP either. When we followed the glucose levels of ChREBP KO female mice for 3 months, we noticed that mice with mild hyperglycemia could normalize their glucose levels, whereas those with more severe initial hyperglycemia could not (Figure 19C). ChREBP, while preventing Rgs16::GFP induction, might not be an obstacle against regeneration from pre-existing beta cells. Rather, recovery seemed to be dependent on the degree of initial beta cell apoptosis (Le May et al., 2006).

ChREBP's involvement in Rgs16::GFP induction did not seem to make a difference between genders. As in males, ChREBP KO females were all non-expressers, suggesting that "hyperglycemia sensor" dependent GPCR signals might be operated the same way in both genders.

Figure 19: Rgs16::GFP is not turned on in ChREBP KO hyperglycemic females

Representative images of day 15 female pancreata with different ChREBP backgrounds are shown in Panel A. Red arrows indicate GFP+ islets. Symbols at right hand corner indicate gender. Scale bar is 1mm. The glucose curve (scaled to left axis) and day 15 pancreatic GFP levels (scaled to the right axis) of female Rgs16::GFP mice treated with STZ in $ChREBP^{+/+}$ (n = 7), $ChREBP^{+/-}$ (n = 5) and $ChREBP^{-/-}$ (n = 8 for glucose, n = 3 for GFP) background are shown in Panel B. Statistical significances of GFP values between ChR KO and heterozygous males vs. females are calculated with Student's t test (unpaired, two-tailed). $p < 0.05$ (α). Faded glucose curves belong to the male Rgs16::GFP mice different ChREBP genotypes. Error bars are SD. 5 non-GFP $ChREBP^{-/-}$ female individual glucose curves until their sac on day 93 are shown on Panel C.

PART 4: Analysis of Rgs16 in pancreatic ductal adenocarcinoma and testing receptor/ligand candidates

Summary: Rgs16::GFP in islets is a promising reporter for identifying new therapeutics of diabetes. Our studies revealed that Rgs16::GFP was expressed not only in islet beta cells but also in vessel and ductal associated cells (VDAC) early in response to hyperglycemia. VDAC are intriguing because islet progenitor cells have been postulated to reside in pancreatic ducts (Bonner-Weir et al., 2008; Bonner-Weir et al., 2004; Bonner-Weir and Weir, 2005; Hua et al., 2006; Kritzik et al., 1999; Magenheim et al., 2011; Sarvetnick and Gu, 1992; Teitelman and Lee, 1987). During postnatal isletogenesis, Rgs16::GFP expression in VDAC continued until P27, at least two weeks beyond the period of islet expression (Villasenor et al., 2010). Interestingly, this ductal-associated expression of Rgs16::GFP persisted and dramatically expanded in a mouse model of pancreatic ductal adenocarcinoma (PDAC) (Aguirre et al., 2003; Hruban et al., 2001). We initiated Rgs16::GFP expressing primary pancreatic ductal adenocarcinoma cell line to develop screens for GPCR ligands that induce Rgs16. We identified GPCRs in these cells that will guide our future ligand screens.

4.1: Rgs16::GFP starts to express postnatally from the onset of PDAC formation *in vivo*

PDAC has been an important source for ductal cell lines. Our collaborator, R. Brekken, pointed out that the origin of PDAC appeared strikingly similar to VDAC during postnatal development and early hyperglycemia. A mouse model of PDAC had been created to study the disease progression and treatment (Aguirre et al., 2003; Malumbres and Pellicer, 1998). Activating mutations in Kras occur in approximately 90% of human PDAC and are thought to drive cell

proliferation signals (Fischer et al., 2001; Gocke et al., 1997; Moore et al., 2001; Pellise et al., 2003; Smit et al., 1988; Stacey, 1988). A missense mutation ($Kras^{G12D}$) could cause insensitivity of Kras to GAP regulation, conferring it constitutive activity (Farr et al., 1988; Stevens et al., 1988). Researchers obtained mice carrying this allele that were prone to cancer in their tissues (Tuveson and Hingorani, 2005). Using this feature, mouse line with Kras mutation and accompanied pancreas specific tumor suppressor deletion was created by crossing $Kras^{G12D/+}$ mice with pancreas lineage specific *p48::Cre* driven $Ink^{-/-}$ transgenic mouse (Aguirre et al., 2003). The resulting $Kras^{G12D/+}$*; p48::Cre;* $Ink^{-/-}$ mice were later shown to get early pancreatic intraepithelial neoplasms (PanIN) which would give rise to invasive PDAC in young adult mice (Aguirre et al., 2003; Klein et al., 2002; Kloppel and Luttges, 2004; Takaori et al., 2004).

We postulated that if Rgs16::GFP was present in VDAC during postnatal and diabetic islet expansion, it could also be active in ductal cells during PDAC formation. To test the possibility of Rgs16 being involved in ductal cancer, we decided to utilize our reporter mouse in the PDAC model and crossed *Rgs16::GFP*$^{o/o}$ mice with $Kras^{+/-}$*; p48::Cre;* $Ink^{-/-}$ to create *Rgs16::GFP*$^{o/+}$*;* $Kras^{+/-}$*; p48::Cre;* $Ink^{+/-}$ mouse line. By back-crossing the F1 generation, we were able to obtain $Ink^{-/-}$ mice that completely lacked the tumor suppressor in the pancreas. We followed these fast tumor forming mice from their postnatal 3rd week because that was the time when the earliest PanINs would start to form. Pups were sacrificed at P18, P20, and P22. GFP+ VDAC were present throughout the ductal network of the pancreas, in much greater numbers than typical of normal Rgs16::GFP transgenic pups. VDAC were also clustered near early tumor nodules that also expressed GFP+ (Figure 20A). The GFP+ tumors were larger in older mice as clearly reflected in quantifications (Figure 20B). These observations were quite striking because we observed bright GFP+ ducts that included GFP+

Figure 20: Rgs16::GFP is expressed in nascent PDAC lesions at P18 - P22

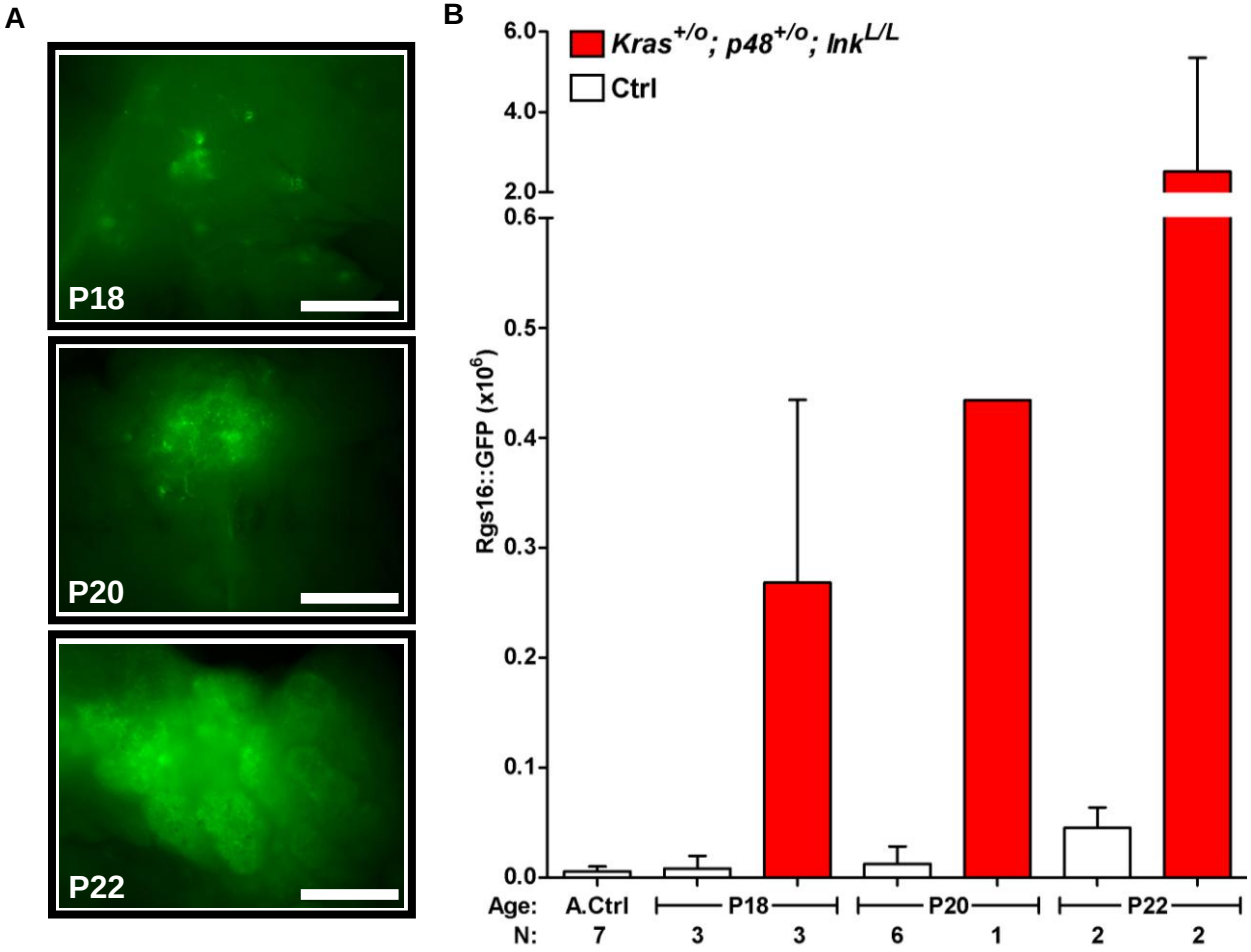

nodules. This bloom of expression was undeniably pronounced at this stage of development where Rgs16::GFP in VDAC was normally declining.

The finding that Rgs16::GFP was expressed in PDAC opened several areas of investigation. One interesting possibility was that PDAC in our mouse model initiated from VDAC that did not become quiescent. Furthermore, if Rgs16::GFP was activated in VDAC during the early response to chronic hyperglycemia, one idea could be these cells would give rise to pancreatic ductal adenocarcinoma in people or animals predisposed to cancer. Our results were in line with a recent observation of Rgs16 gene expression changes in late stage pancreas cancer with lymph node metastasis (Kim et al., 2010). Therefore, we thought about culturing PDAC cells and using them to screen for GPCR ligands that might regulate Rgs16::GFP expression in culture and might have a chance at conveying biological effects in beta cell expansion or pancreatic ductal adenocarcinoma.

4.2: Isolated Rgs16::GFP PDAC primary culture cells express GFP in a serum dependent manner but extinguish over time

We set out to determine if PDAC cells could be used to search for factors that cause Rgs16::GFP expression and gain insight about the GPCR signaling that Rgs16 regulates. Screening primary cancer cells would have great advantages over islets, which are meticulous to isolate and require special expertise (Bonnevie-Nielsen et al., 1983; Gaber and Fraga, 2004; Gordon et al., 1982; Gray et al., 1984; Hahn, 1978; Parr et al., 1980; Rabinovitch et al., 1979). PDAC had

---

Figure 20: Rgs16::GFP is expressed in nascent PDAC lesions at P18 - P22
Pancreatic image samples of *Rgs16::GFP; Kras$^{+/o}$; p48$^{+/o}$; Ink$^{L/L}$* tumor forming mice are shown in Panel A. Scale bar is 0.8mm. ImageJ quantification of tumor bearing and control postnatal mice are compared in Panel B. Adult WT Kras (A.Ctrl) mice are negative control for GFP+ tumors. Error bars are SD.

the advantage of being plentiful, easy to isolate, and maintain in cell culture as a cancer cell line (Lieber et al., 1975; Lohr et al., 1994; Parsa and Marsh, 1976; Rao et al., 1980).

PDAC were isolated from a male *Rgs16::GFP$^{o/+}$; Kras$^{-/+}$; p48::Cre; Ink$^{-/-}$* mouse (L. Rivera). Isolated tumor culture was selected for Rgs16::GFP expressing cells via subcloning by Lee Rivera. As can be seen in Figure 21A, PDAC subclone still had a significant portion of non-GFP expressing cells. Early passages seemed to retain a high proportion of GFP+/gfpNEG cells, but as passage number increased, we noticed a clear depletion of GFP+ population (Figure 21B). The shape, size, and proliferation pattern of both populations seemed similar and did not suggest a difference in cell type origin. We found that Rgs16::GFP expression was dependent on the concentration of the serum in the media (Figure 21C). When grown in 50% FBS for 24hr, the culture was enriched in GFP+ cells. The average brightness of GFP+ cells appeared higher and the cells retained their increased GFP expression after passage. Also, PDAC cells subcutaneously injected to NOD-SCID animals kept their original proportion of Rgs16::GFP expressing population, indicating *in vivo* blood serum does not further induce GFP than tissue culture conditions (Figure 21D) (Shultz et al., 1995).

Rgs16::GFP induction could arise due to GPCR agonists in serum stimulating its transcription. Interestingly, serum type did not seem to make any difference, as the same percentage of FBS or rat serum yielded the same percentage of GFP+ cells when culture for 1 day (data not shown). Even though GFP percentage was an issue and we could not answer the cause of reduction of GFP+ cells, the fact that cells did not switch off Rgs16::GFP completely and could still be induced by culturing in elevated FBS meant that they retained their GFP induction capacity on culture. Therefore PDAC cells could be used for screening of ligands that would induce Rgs16::GFP expression.

Figure 21: Isolated Rgs16::GFP PDAC primary culture cells express GFP in a serum dependent manner but extinguish over time.

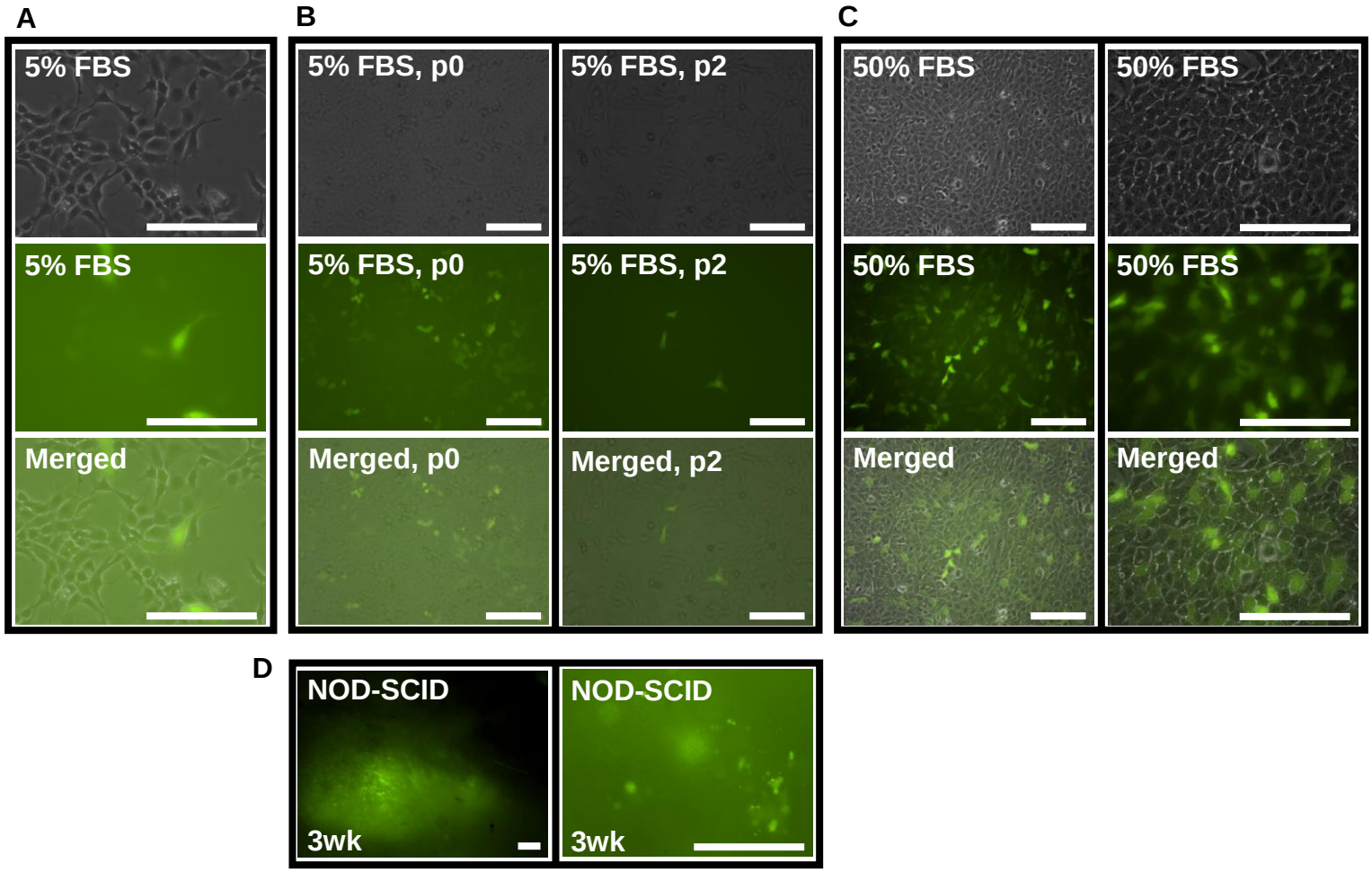

4.3: RNA-Seq analysis of Rgs16::GFP sorted PDAC culture shows gene expression of ductal lineage markers

We characterized PDAC culture cells to determine their potential for identifying GPCRs and ligands relevant to pancreatic biology and disease. Even though PDAC were thought to originate from ducts, the PDAC cells we isolated were from a late stage of tumor, at which point the tumor mass could contain multiple cell types, including various hematopoietic cells and fibroblasts (Aguirre et al., 2003; Bachem et al., 2005; Lohr et al., 1996; Wagner et al., 1998). To assess their progenitor cell capacity, PDAC culture cells were transplanted into the pancreas of NOD-SCID immunocompromised mice (Bosma et al., 1983). Rgs16::GFP was specifically expressed in duct-like structures throughout the transplanted tumor, but not in the stroma, indicating the primary PDAC cells in culture could be predominantly comprised of duct-like progenitor cells (L. Rivera, data not shown). This suggested that PDAC cells either preserved their ductal gene program and formed ducts once they returned to their original environment or signals in pancreas reactivated ductal differentiation in PDAC cells. The best way to know what kind of genes would be active in PDAC culture was to make genome-wide gene expression analysis. We wanted to determine if there was a

---

Figure 21: Isolated Rgs16::GFP PDAC primary culture cells express GFP in a serum dependent manner but extinguish over time
Panel A shows PDAC at ~70% confluency incubated at 5% FBS containing DMEM. Panel B compares the percentage of GFP+ cells of a PDAC sub-clone (3D11-4-F4) obtained by selection for GFP+ cells grown at 5% FBS containing DMEM. Cells on the right column are 2 passages later than those on the left. Bright-field and green channel exposures are 0.3s and 3.0s respectively. Panel C shows PDAC at 100% confluence incubated at 50% FBS containing DMEM under 10x and 20x objective, respectively. Bright-field, fluorescent green channel and composite pictures are ordered from top to bottom. Panel D shows pictures of GFP+ tumor cells obtained 3 weeks after they were injected into NOD-SCID recipients subcutaneously. Scale bar is 0.2mm in all panels.

significant difference between Rgs16::GFP expressing and non-expressing cells in culture. PDAC cells were sorted into GFP+ and gfpNEG populations and their isolated total RNA was used for sequencing (V. Pashkov, C. Shen, G. Swift, UTSW flow cytometry and RNA-Seq core facilities) (Wang et al., 2009).

The RNA-Seq data showed that both GFP+ and gfpNEG populations had considerable similarities in gene expression (data not shown). The GFP+ population expressed 214 genes that were > 1.5-fold higher than in the other population, whereas 587 genes were > 1.5-fold higher in the gfpNEG population. No signaling pathways or metabolic functions clearly discriminated between these cell populations. The highest preferential expression of endogenous genes in GFP+ cells was over 9-fold, whereas several genes were over 50-fold increased in the gfpNEG population. Endogenous Rgs16 was about 2.4 fold up-regulated in the GFP+ group, whereas its value in gfpNEG population was below 1 rpkm. By contrast, Rgs16::GFP gene expression was about 35-fold higher in the GFP+ population over gfpNEG according to qPCR analysis (V. Pashkov, data not shown). This difference in fold expression is probably due to the short half-life of endogenous Rgs16 mRNA relative to GFP. Because Rgs16::GFP in the GFP+ pool responded to 40% FBS in the media, these differences in gene expression might be attributable to factors in the serum.

We characterized PDAC cells for expression of genes specific to the three pancreatic lineages, ducts, acinar and endocrine cells (Figure 22). Six genes from each lineage were selected (recommended by R. MacDonald and G. Swift) (Agbunag and Bar-Sagi, 2004; Duval et al., 2000; Fukuda et al., 2006; Kim and MacDonald, 2002; Lynn et al., 2007; MacDonald et al., 1982; MacDonald et al., 2010; Madsen et al., 1991; Miller et al., 2009; Murata et al., 1968; Rabanal et al., 1992; von Burstin et al., 2010; Yasuda and Coons, 1966; Zhou et al., 1995). As a reference point, we compared expression of this panel of genes in PDAC cells to RNA-Seq data obtained from developing pancreas at e13.5 and e17.5

Figure 22: RNA-Seq analysis of Rgs16::GFP sorted PDAC culture shows gene expression of ductal lineage markers, but not that of acinar or endothelial.

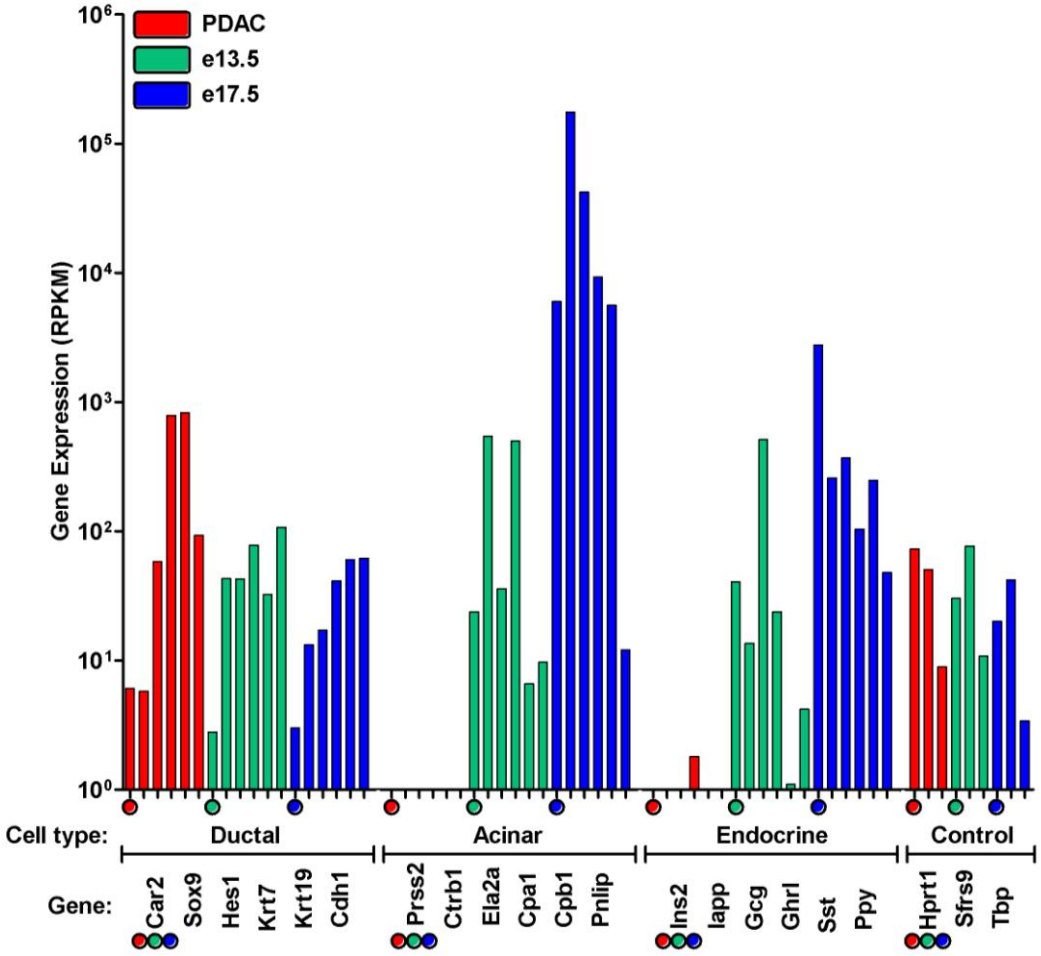

(G. Swift). In the embryonic pancreas, percentages of early ductal and endocrine cell were close to that of acinar during embryogenesis. On the other hand, pancreatic acinar cell percentage was known to continually increase during postnatal development, constituting majority of adult pancreas with more than ~90% cell number (Weir and Bonner-Weir, 1990).

As Figure 22 shows, PDAC and e13.5 and e17.5 pancreas were expressing ductal markers at comparable levels on a logarithmic scale. By contrast, PDAC cells did not express acinar and endocrine marker genes at significant levels. Moreover, even though the comparison was shown with GFP+ population, gene expression values in gfpNEG population were all similar; suggesting that Rgs16::GFP based segregation did not alter cell identity. As expected, housekeeping genes were similarly expressed in all samples.

This RNA-Seq based gene expression comparison indicated that PDAC in tissue culture was reflecting embryonic pancreatic ductal progenitor cells. This characteristic was maintained independently of Rgs16::GFP expression, suggesting that GFP expression loss during passages of PDAC cells was not associated with population-wide changes in cell character. Because PDAC cells exhibited ductal identity in culture, they might be useful for identifying GPCR ligands that act on pancreatic ductal progenitor cells in diabetes and pancreatic cancer.

Figure 22: RNA-Seq analysis of Rgs16::GFP sorted PDAC culture shows gene expression of ductal lineage markers, but not that of acinar or endothelial

RNA-Seq (ERange) data from GFP+ FACS pool of Rgs16::GFP PDAC cells is compared to embryonic (e13.5 and e17.5) whole pancreas RNA-Seq data from MacDonald laboratory. Important ductal, acinar and endocrine markers are compared for their gene expression. Colored dots underneath x-axis indicate first gene in the series. 3 housekeeper genes as expression control are shown at the furthest right. RPKM values are in logarithmic scale.

4.4: Identifying candidate GPCRs and ligands in PDAC based on RNA-Seq analysis

Once we obtained gene expression profiling of PDAC and confirmed that they were mimicking pancreatic ductal cell expression, we wanted to know the entire mouse candidate GPCRs as potential targets of Rgs16 regulation (Alldinger et al., 2005). As shown in Figure 23, there were 55 GPCRs that were expressed in PDAC in a wide spectrum. Several of them were orphans. In addition to these 55, we found 8 GPCRs were likely to be significantly expressed according to BLAST fragment counts and they were depicted in the lower insert of Figure 23. Taking both graphs into account, there were at least 63 GPCRs that were expressed in PDAC populations. If fold difference of RNA was considered, receptors Gpr68 (2.8-fold) and Lgr6 (1.6-fold) were preferentially expressed in GFP+ population, whereas Gpr120 (2.4-fold) was the sole GPCR gene that had gfpNEG favoring expression. When the functions of expressed GPCRs were investigated from published papers, we found that several of them were associated with cancer, stem cell, and other important signaling relevant to proliferation and examples were indicated individually.

The GPCR profiling of PDAC cells identified potentially active GPCR pathways. Although most of the GPCRs we identified were equally expressed in the GFP+ and gfpNEG pool of cells, we identified three receptors which were differentially expressed in the two cell populations. Gpr68 and Lgr6 were orphan receptors and Gpr120 was shown to bind long chain fatty acids (Birchmeier, 2011; Hirasawa et al., 2005; Hsu et al., 2000; Ludwig et al., 2003; Oh et al., 2010; Snippert et al., 2010; Suzuki et al., 2008; Tanaka et al., 2008a; Tanaka et al., 2008b; Xu and Casey, 1996). These receptors were interesting to us because they might initiate signals that regulated Rgs16 levels. To prioritize the GPCRs in PDAC cells, we also conducted an expression analysis in pancreatic islets. We

Figure 23: Identifying candidate GPCRs and ligands in PDAC based on RNA-Seq analysis.

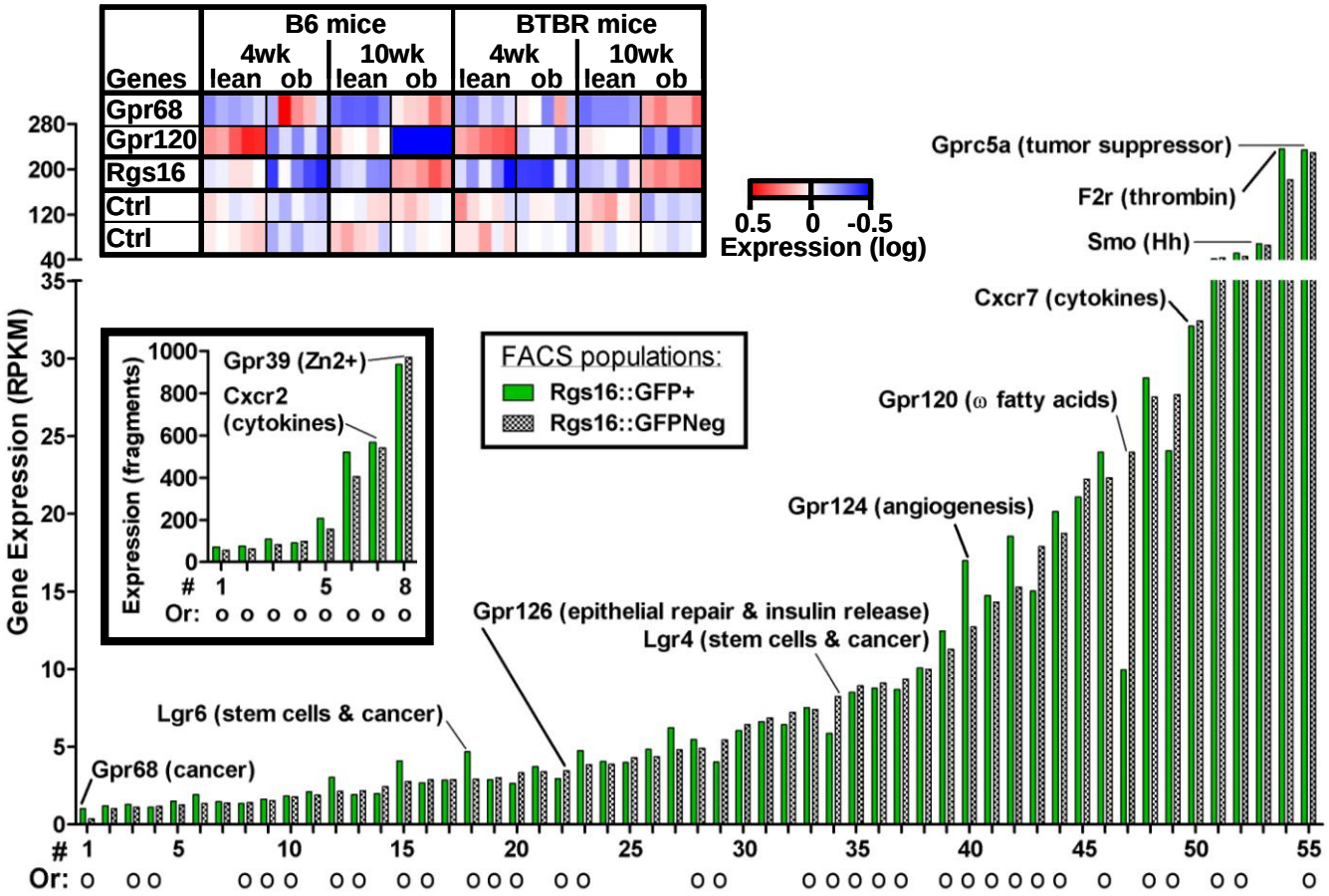

compared the expression differences of 124 GPCRs in an islet database (Keller et al., 2008). Of these, Gpr120 had the highest reduction in islets of 10 week old *ob/ob* mice compared to lean controls. Conversely, Gpr68 was the most highly enriched GPCR, in parallel to the induction of Rgs16 (Figure 23, upper insert).

Coincidentally, Gpr68 and Gpr120 expression changes correlated directly and inversely with Rgs16 in both PDAC culture and expanding beta cells of *ob/ob* mice, respectively. Still, further investigation is required to prove whether these GPCRs are involved in the signaling that Rgs16 regulates.

4.5: Gpr68 putative ligand induces Rgs16::GFP in PDAC in a dose dependent manner

The interesting tendency of Gpr68 to match the expression pattern of Rgs16 in diabetes and cancer stimulated us to give it priority in testing associated ligands in our PDAC model in tissue culture. Data from literature about Gpr68

Figure 23: Identifying candidate GPCRs and ligands in PDAC based on RNA-Seq analysis
GPCR search of the RNA-Seq (ERange) results from Rgs16::GFP BAC containing PDAC cells separated into GFP+ (green bar) and gfpNEG (patterned bar) populations by FACS showed 55 candidate gene expression with RPKM > 1 level for either or both group. Additional 8 GPCRs with sequenced fragment counts 70 or above in either population are also likely to be expressed and depicted in the lower insert. Stem cell, tumor or potentially relevant GPCRs are indicated exclusively. There are 42 orphan receptors (o). Genes are graphed according to increasing gfpNEG RPKM or fragment number value. GFP+ population specific enhanced expresser Gpr68 and gfpNEG population specific enhanced expresser Gpr120 are compared to Rgs16 and 2 other GPCRs (P2ry5 and Gabbr1) as controls in the heat map based on diabetic mouse pancreatic islet expression according to Alan Attie Diabetes Database data on the upper insert. Mouse backgrounds C57BL66 and BTBR, mouse age, and lean or *ob/ob* genotype are shown on the upper part of insert. Heat map log scale is shown to the right of insert. Red color shows increase and blue color shows decrease in expression (Keller et al., 2008).

emphasized its “pH sensing” properties but lacked any structural depiction or ligand binding kinetics elucidating this proposal (Liu et al., 2010; Ludwig et al., 2003; Tomura et al., 2005; Tomura et al., 2008; Xu and Casey, 1996; Yang et al., 2006). Meanwhile, an isoxazole (ISX) derivate was identified to be a putative ligand of Gpr68 (Schneider et al., 2008); J. Schneider, personal communication) (Figure 24C).

We tested this ISX compound in our PDAC cells to determine its effect on Rgs16::GFP expression (Figure 24A). As it can be seen from cell counts in Figure 24B, ISX concentrations below 3.7µM did not have an effect on Rgs16::GFP in PDAC. However, the highest concentrations starting from 11µM showed a dose-dependent increase in the percentage of GFP+ cells within the population, reaching about ~75% of the total PDAC number on the plates (Figure 24B). On the other hand, the general brightness of GFP fluorescence remained similar to background expression of few GFP+ cells seen with lower concentrations and negative control. This would mean the highest ISX dosage of 100µM was enhancing GFP+ proportion of the PDAC population from about 0.1% to 75% without increasing cellular GFP transcription any further than that of an average GFP+ cell of native population.

Induction of PDAC Rgs16::GFP by ISX in a dosage dependent manner laid out a possibility of it being a small molecule which resembles to an endogenous ligand. It also pointed out that if ISX was indeed exerting its effect via binding to GPCRs, Gpr68 could be the receptor through which Rgs16 was induced in the pancreas. If ISX was a true GPCR ligand, it would be an important drug candidate to be used in identifying the role of Rgs16 in pancreatic cancer. Also, ties between PDAC and ductal cells *in vivo* could translate into a probable induction of Rgs16::GFP expression in VDAC by ISX. As ISX emerged as a positive hit of a large scale screening in stem cells, any possible induction of VDAC could also be beneficial to understanding their character. Furthermore,

Figure 24: Gpr68 putative ligand induces Rgs16::GFP in PDAC in a dose dependent manner.

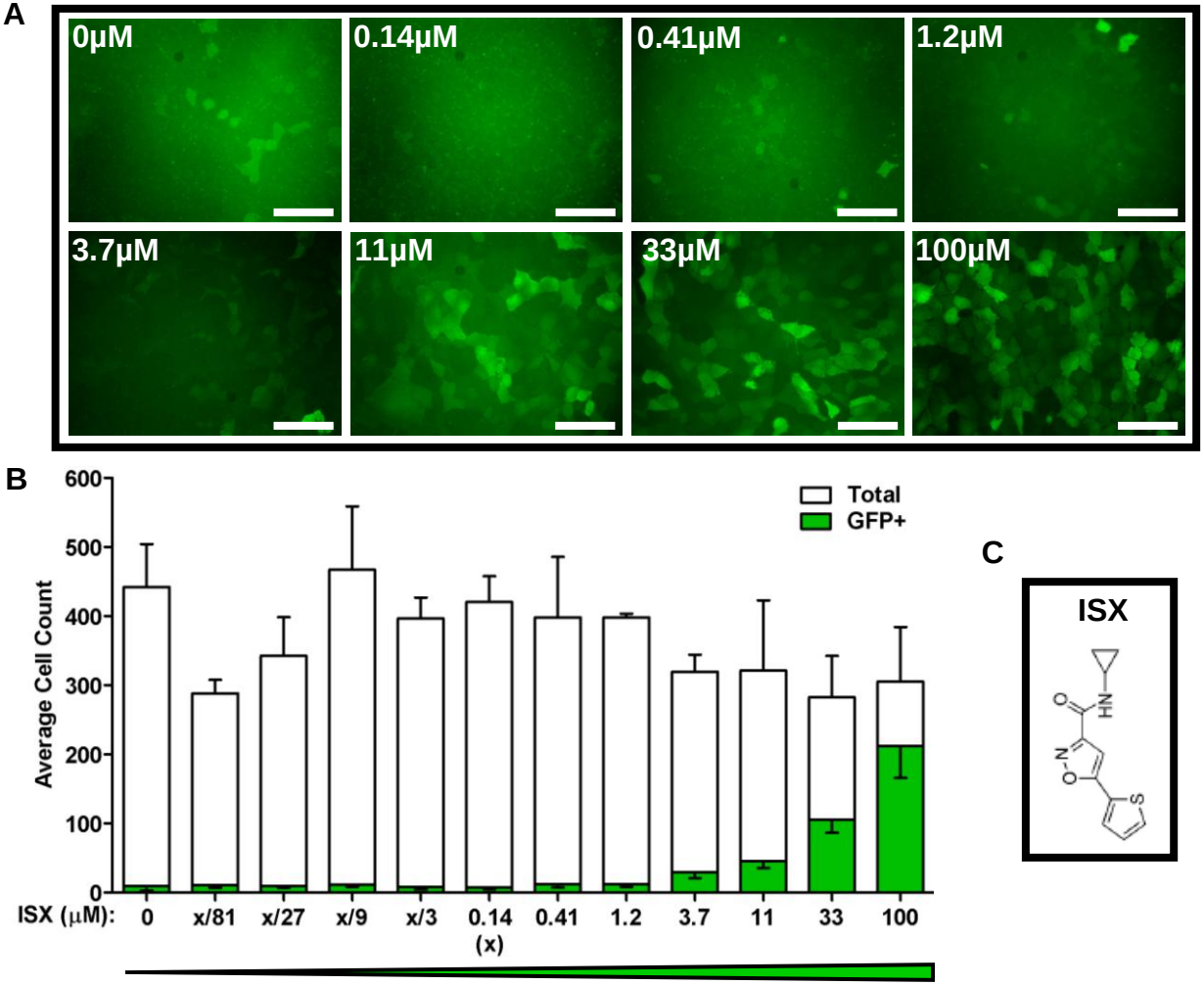

such exciting outcome would stretch to diabetes research due to the positive correlation between Gpr68 and Rgs16 expression in islets we saw in Attie database. No matter how ISX was able to induce Rgs16::GFP, these results showed that gfpNEG PDAC cells were not losing their capacity to induce GFP expression. It became also apparent that in addition to known or predicted endogenous agonists, small molecules deserved attention for testing drugs in PDAC and encouraged us to conduct comprehensive screens.

4.6: HDAC inhibitors induce Rgs16::GFP in PDAC culture

The ISX derivative we used was thought to be a Gpr68 ligand (J. Schneider, personal communication). On the other hand, related ISX compounds have been reported to inhibit histone deacetylases (HDAC) (Schneider et al., 2008; Zhang et al., 2011a). There have been various publications about how chromatin packaging and its regulation played a role in gene transcription (Braunstein et al., 1993; Jones and Wolffe, 1999; McKinsey et al., 2000; Reuter et al., 1990; Shaffer et al., 1993; Steger et al., 1998; Zhang et al., 2002). In general, histone acetylation was shown to enhance gene transcription (Braunstein et al., 1993). Acetylation was argued to eliminate positive charges of histone amino acid residues in close proximity to DNA, weakening bonds between histone subunits

---

Figure 24: Gpr68 putative ligand induces Rgs16::GFP in PDAC in a dose dependent manner
Representative pictures of PDAC with increasing ISX concentrations visualized under 20x objective are shown in Panel A. Scale bar is 0.1mm. Total (white bar) and Rgs16::GFP expressing (green bar) cell counts of PDAC cells grown in 5% FBS DMEM (25mM Glucose) are shown in Panel B. Cells were counted under 40x objective. 100µM starting ISX concentration was diluted in 1:3 ratio for decreasing dosages. Concentrations lower than x = 0.14µM is shown as fraction of x. Error bars are SD. The chemical structure of ISX compound tested is shown in Panel C.

and DNA (Bradbury, 1983; Turner and O'Neill, 1995). Consequently, acetylation manages to bring about dissociation of nucleosomes making target genes accessible to transcription factors and RNA Polymerase II (Hardy et al., 2002; Hirose, 1998). In this way, histone acetyl transferases (HAT) were regarded as transcriptional enhancers, whereas HDACs acted as repressors (Laherty et al., 1997; Siddique et al., 1998; Utley et al., 1998). In recent years, research on gene transcription focused on finding drugs that would affect activity of these enzymes (Balasubramanyam et al., 2003; Dekker and Haisma, 2009). Compounds that can block activity or binding ability of HDACs were termed HDAC inhibitors and scientists had been investigating their function in cancers (Bertrand, 2010; Gui et al., 2004; Kuendgen et al., 2006; Lin et al., 1998; Nagy et al., 1997; Takimoto et al., 2005). While we were thinking that Rgs16 in islets, VDAC or PDAC was induced by external ligands, none of the transcription factors and auxiliary elements was known. We had established Rgs16::GFP PDAC tissue culture system as a way of testing compounds and conditions leading to GFP induction. ISX being the first such molecule causing GFP expression, we thought about expanding the repertoire of tested compounds by incorporating HDAC inhibitors to see if they could facilitate Rgs16 transcription.

HDAC inhibitors romidepsin, trichostatin A, and sodium butyrate were all able to induce Rgs16::GFP robustly under normal culture conditions (Figure 25) (Dangond and Gullans, 1998; Demary et al., 2001; Nakajima et al., 1998; Novogrodsky et al., 1983; Ueda et al., 1994; Yoshida and Beppu, 1988). The number and brightness of GFP+ PDAC cells were similar and in fact exceeded that of the positive control LDR 6020 cells upon addition of each of these compounds (Johnson et al., 2008). The only difference between ISX and these compounds was the morphology of PDAC. While HDAC inhibitors seemed to retain the cubical shape of PDAC, cells would enlarge in response to ISX. Although their classification and specificities were different, GFP induction with

Figure 25: HDAC and DMT inhibitors induce Rgs16::GFP in PDAC culture.

A) PDAC

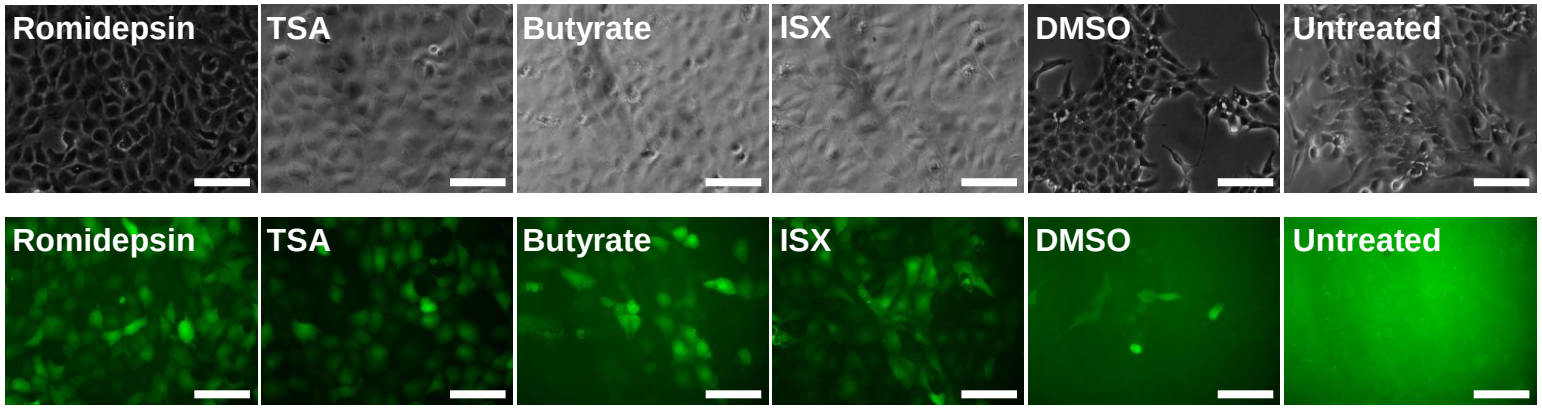

B) LDR 6020

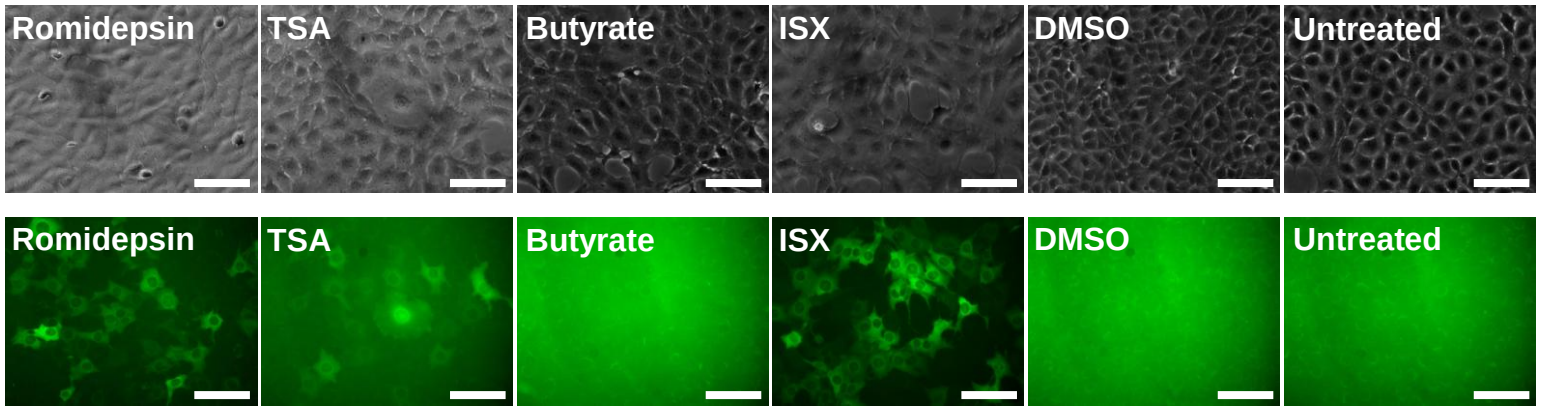

all three of these HDAC inhibitors showed that the promoter region of Rgs16::GFP in PDAC was clearly subject to histone modifications. These results raised the possibility of whether ISX or other activating compounds would be affiliated with histone modifications. This effect of HDAC inhibitors made us question if ISX could be affecting histones rather than acting as a transmembrane receptor ligand. Although we did not test the effect of these HDAC inhibitors *in vivo*, this tissue culture outcome pointed out the various ways of gene induction and reminded us to investigate any inducing compound's mechanism of action separately. We will therefore test siRNA mediated knockdown of Gpr68 to determine to determine if ISX acts via this GPCR or modifies histone acetylation directly in PDAC cells.

4.7: Gpr68 putative ligand does not induce Rgs16::GFP in normal glycemic mice, but enhances expression in STZ model

Induction of Rgs16::GFP by ISX in tissue culture gave us a candidate small molecule that had potential to be an endogenous GPCR ligand mimetic. The molecular effects and the binding kinetics of this compound needed to be tested to confirm if it was acting via a GPCR pathway or not. On the other hand, we wanted to know if this compound can exert its effect during diabetes irrespective of how it stimulated Rgs16::GFP in tissue culture cells. A possible explanation for

---

Figure 25: HDAC and DMT inhibitors induce Rgs16::GFP in PDAC culture
The GFP induction of Rgs16::GFP PDAC and LDR 6020 cells after ~24hr incubation with certain HDAC inhibitors and ISX is shown in representative pictures of Panels A and B, respectively. Both cell types were incubated with Romidepsin (25ng/mL, ~46nM), TSA (400nM), Butyrate (10mM) and ISX (50µM) dissolved in DMSO. DMSO (1µl/ml) and untreated wells serve as negative controls. The bright-field pictures of the cells on the upper row of each panel serve as comparison of cell number, morphology, and confluency. Scale bar is 0.1mm

Rgs16::GFP induction in islets and VDAC during diabetes and in ductal cells during cancer was that it responded to the same GPCR signals in all of these situations. Therefore, if a compound like ISX was able to induce Rgs16::GFP in PDAC, it had a possibility to also exert an effect *in vivo*. With this in mind, we incorporated ISX administration to our fastest and most repeated diabetic mouse model of STZ treatment.

As shown in Figure 26A and B, ISX injected pancreata showed increased GFP in STZ-treated mice at day 12. On the other hand, ISX itself did not induce any Rgs16::GFP in the pancreas of normal glycemic control mice. GFP quantification of day 12 pancreata lacked statistical significance due to low sample size and the experiment needs to be repeated with more mice. Waiting until day 15 post-STZ closed the gap between ISX injected and control groups, suggesting that GFP enhancement at day 12 might be a precocious advancement of beta cell expansion signals (Figure 26C). Neither ISX nor its carbohydrate based carrier seemed to have an effect on glucose levels in any situation. Both STZ and STZ + ISX groups had similar hyperglycemic course. Because STZ was not a regenerative model, any long-term effect of ISX on beta cell expansion needs to be tested in PANIC-ATTAC mice.

We also tested if ISX could enhance VDAC GFP expression in postnatal pups. We chose weanlings over adult because this was the postnatal development period when GFP expression in islets was fading in VDAC and totally absent in islets (Villasenor et al., 2010). Although we could detect GFP expression in some VDAC in these P24 pancreata, ISX did not seem to induce any noticeable VDAC expression (Figure 26D). As these results showed, ISX was not a compound that could induce Rgs16::GFP in islets or VDAC *in vivo* on its own. This might be an important observation if ISX promotes beta cell regeneration in PANIC-ATTAC mice but not pancreatic ductal adenocarcinoma in the PDAC mouse model.

Figure 26: Gpr68 putative ligand does not induce Rgs16::GFP in normal glycemic mice, but enhances expression in STZ model.

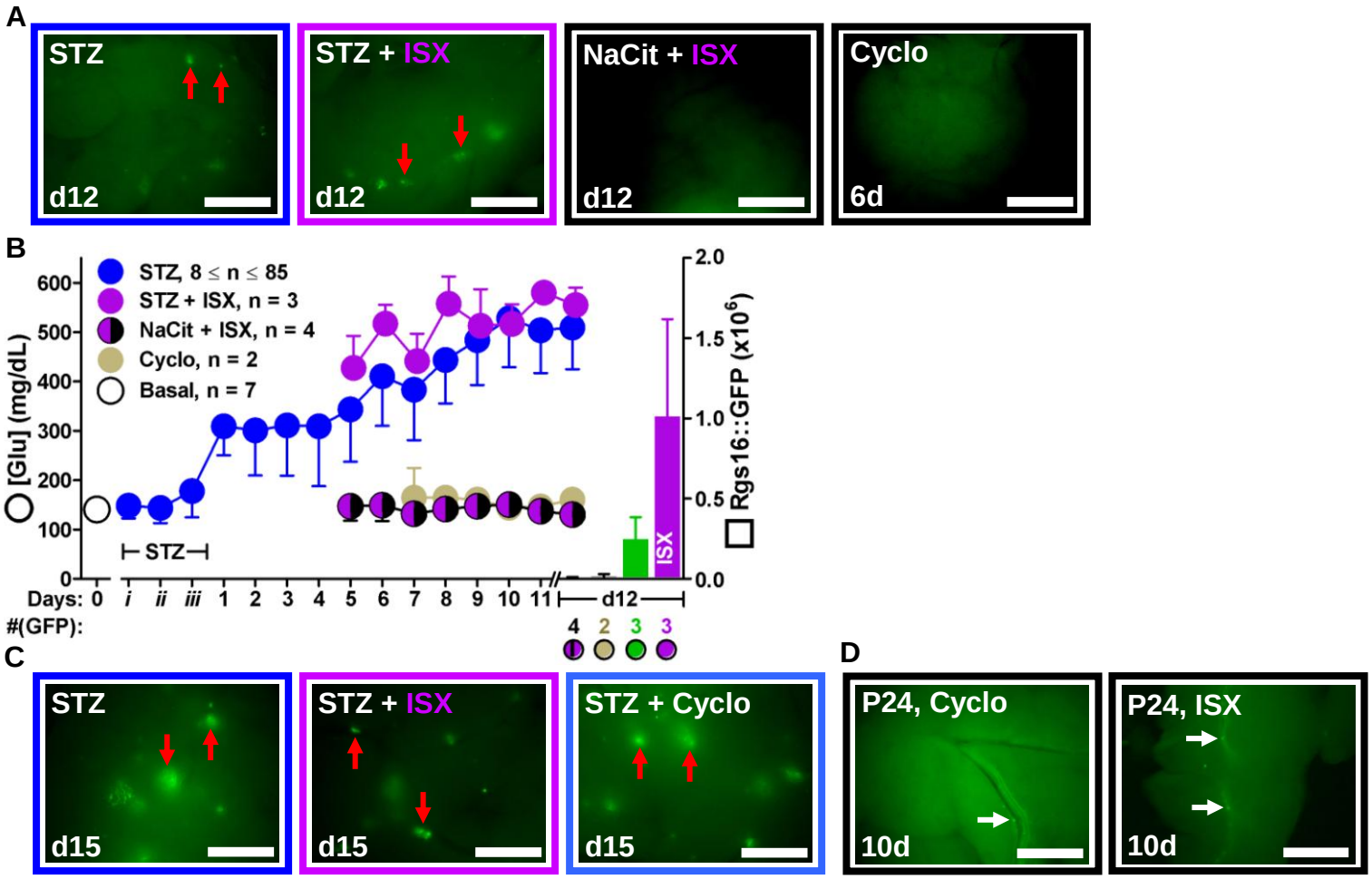

4.8: Type 2 diabetic drug exendin-4 can induce mild pancreatic Rgs16::GFP expression in islets and VDAC

In the last decade, an important focus of type 2 diabetes research was dedicated to drugs that stimulate insulin secretion such as Glucagon-like peptide1 (Glp1) or compounds that enhanced Glp1 mediated effects (Gutniak et al., 1992; Herman et al., 2006; Waget et al., 2011). Glp1 increases insulin secretion, inhibits glucagon release and food intake and slows gastric emptying (Kreymann et al., 1987; Orskov, 1992; Turton et al., 1996; Wettergren et al., 1993). However, it has a very short half-life in blood and is rapidly degraded by Dipeptidylpeptidase-4 (Dpp4) (Ahren and Hughes, 2005; Ahren et al., 2004; Ahren and Schmitz, 2004). Exendin-4 (Exenatide), a stable Glp1 homolog, was isolated from Gila monster's saliva and has been used as a type 2 diabetic drug for humans (Drucker, 1998; Eng et al., 1992; Fehmann et al., 1994; Goke et al., 1993; Raufman et al., 1982; Schepp et al., 1994). Exendin-4 was also shown to stimulate beta cell expansion (Arakawa et al., 2009; Song et al., 2008; Tourrel et al., 2001; Xu et al., 1999a).

Figure 26: Gpr68 putative ligand does not induce Rgs16::GFP in normal glycemic mice, but enhances expression in STZ model
Representative images from day 12 pancreas of male Rgs16::GFP mice treated with STZ only, STZ-treated and injected with ISX starting from day 5, NaCit treated and injected with ISX starting from day 5, and cyclodextrin alone injected for 6 days are shown in Panel A. Red arrows indicate GFP+ islets. Scale bar is 1mm. The glucose curve (scaled to left axis) and day 12 pancreatic GFP levels (scaled to the right axis) of different groups are shown in Panel B. NaCit animals (n = 4) injected with ISX are control for STZ group and cyclodextrin-injected mice are control for ISX. Even though cyclodextrin animals are not pre-treated with NaCit or STZ, their GFP quantification is shown with other groups. Error bars are SD. Panel C compares cyclodextrin- or ISX-injected STZ pre-treated mouse day 15 mouse pancreata to STZ only pancreas. Cyclodextrin was injected for 6 days and ISX for 8 days daily until sacrifice. Panel D compares sample pictures of P24 Rgs16::GFP animals injected daily for 10 days with ISX or cyclodextrin starting from P15. White arrows indicate VDAC. Scale bar is 1mm.

Diabetic mice treated with exendin-4 displayed increased recovery from diabetes along with larger islet size (Wang et al., 2008). We knew that Rgs16::GFP was not induced merely by insulin secretion as it was absent in normal glycemic mice after feeding or repeated glucose injections. Because exendin-4 was reported to stimulate beta cell expansion in mice, we decided to test if this drug was strong enough to induce GFP expression in mice with normal basal glucose level.

When we looked at pancreata 3 days after the daily injection, we noticed faint islet expression (Figure 27C) in the exendin-4 and glucose co-injected group. In addition, this was accompanied by occasional GFP+ VDAC. At day 6 of this procedure, we detected faint GFP+ islets and VDAC not only in the co-injected mice but also in the exendin-4 only group. This suggested that exendin-4 mediated faint pancreatic GFP induction was not dependent on acute hyperglycemia. Even though glucose administrations might have shortened the initial emergence of this low expression, hyperglycemia was not required for any possible exendin-4 effect.

As seen in Figure 27A, exendin-4 alone slightly lowered basal glucose levels of mice at day 1. In addition, glucose and exendin-4 co-injected mice had reduced hyperglycemia than their glucose-injected counterparts, confirming this drug's fast acting effects. At day 6, the effect of daily exendin-4 injections was more pronounced. It again kept basal levels low, but also had a dramatic effect on insulin secretion capacity in the glucose co-injected mice (Figure 27D). Mice co-injected with glucose and exendin-4 had normalized blood glucose levels after 1 hour. It appeared that pancreatic beta cells had adapted to experiencing daily acute hyperglycemia as the glucose only group 1hr post-injection level at day 6 was also lower than that at day 1. Nevertheless, exendin-4 enhanced total insulin secretion capacity of the glucose co-injected group, as both exendin-4 alone and glucose co-injected groups had insulin levels similarly higher than those of glucose alone or PBS groups, confirming previously published data about its

Figure 27: Type 2 diabetic drug exendin-4 can induce mild pancreatic Rgs16::GFP expression in islets and VDAC.

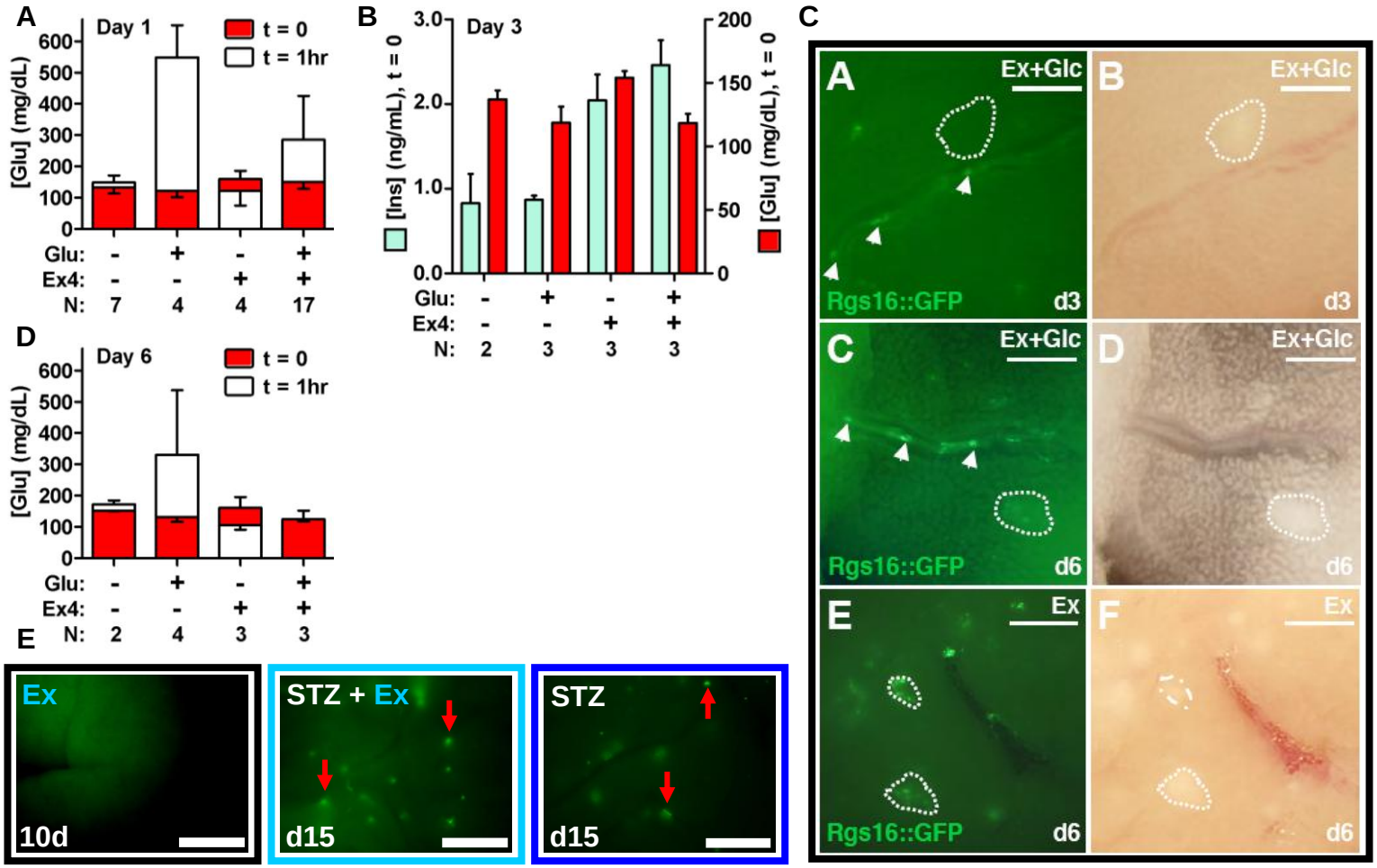

short-term effects (Figure 27B) (Goke et al., 1993). Mild islet and VDAC expression on the other hand hinted to its beta cell expansion stimulating long-lasting effects (Xu et al., 1999a). However, daily exendin-4 injections in STZ model did not result in any quantitative differences at day 15 (Figure 27E). Contrary to ISX, exendin-4 did not induce GFP expression in late passage PDAC either, presumably because the Glp1 receptor was not expressed in either GFP+ or gfpNEG populations of PDAC according to RNA-Seq (data not shown) (Thorens, 1992). Nevertheless, these results suggested that exendin-4 with its long-lasting effects on islets could be used in combination with other compounds that stimulate GFP to identify novel drug combinations to promote beta cell expansion in diabetes.

Figure 27: Type 2 diabetic drug exendin-4 can induce mild pancreatic Rgs16::GFP expression in islets and VDAC

Glucose levels of injection groups at day 1 and day 6 at basal and 1hr post-injection are shown on Panels A and D. Comparison of basal glucose and insulin levels at day 3 is shown on Panel B. All error bars are SD. Day 3 and day 6 pancreatic expression of Rgs16::GFP mice injected with either exendin-4 alone or together with glucose twice daily are shown on Panel C. Scale bar is 100μm. Dotted lines and arrow heads indicate islet margins and VDAC respectively. Pancreas of 10 days long daily exendin-4-injected mouse with or without STZ pre-treatment is compared to STZ-treated pancreas on Panel E. Red arrows indicate GFP+ islets.

DISCUSSION AND FUTURE DIRECTIONS

Using Rgs16 expression as a reporter gene of GPCR signaling in pancreas opens up new directions for diabetes and cancer research. The Rgs16::GFP reporter mouse shows us that this GPCR signaling indicator is expressed during beta cell expansion in embryogenesis, postnatal isletogenesis, pregnancy, and diabetes. Rgs16::GFP is also reactivated in PDAC *in vivo* and can be induced by transcriptional activators in culture. Such critical temporal coincidence of Rgs16::GFP expression and pancreatic transformations suggest the existence of GPCR(s) central to those events that are yet to be identified in islets and ductal cells.

It is known that beta cells can replicate to increase their population and thereby their collective insulin production capacity (Ackermann and Gannon, 2007; Sachdeva and Stoffers, 2009). On the other hand, theories about beta cell expansion include other sources, such as pancreatic ductal cells (Ackermann and Gannon, 2007; Bonner-Weir et al., 2004; Bonner-Weir and Weir, 2005). The idea about an unidentified pancreatic ductal progenitor type contributing to beta cell pool under metabolic demand was especially interesting for interpreting the return of VDAC to pancreas during diabetic conditions (Villasenor et al., 2010). We therefore think studies using the Rgs16::GFP PDAC line can shed light to understanding the nature of VDAC (Bonner-Weir et al., 2008). While several GPCRs are known to be important for insulin secretion and islet maintenance, none of them have been directly and clearly associated with beta cell expansion in response to chronic hyperglycemia, the common feature of both type 1 and type 2 diabetes, as well as PDAC (Ahren, 2009; Sachdeva and Stoffers, 2009). Our PDAC analysis is therefore important in proposing such candidates.

While we pursued Rgs16::GFP gene expression *in vivo* as a GPCR reporter, we did not address Rgs16 function in pancreas. An initial motivation for

our studies in pancreas was the finding that Rgs16 negatively regulated fatty acid oxidation in liver during fasting (Pashkov et al., 2011). Rgs16 KO mice had elevated rates of FA oxidation whereas transgenic expression of Rgs16 in liver inhibited FA oxidation and lowered blood glucose during fasting (Pashkov et al., 2011). Furthermore, Rgs16 transcription, mRNA and protein were rapidly induced in cultured hepatocytes by glucose and dependent on the glucose-responsive transcription factor ChREBP (Pashkov et al., 2011). However, it is unknown if Rgs16 KO mice have any pancreas defect. They have normal glycemia in fed and fasted states, show usual GTT results, and responded to STZ in a normal time course of type 1 diabetic hyperglycemia (Pashkov et al., 2011); data not shown). A pancreatic phenotype in the Rgs16 KO mice could be suppressed by expression of functionally redundant Rgs genes, such as the tandemly duplicated gene, Rgs8. Rgs8 KO mice were also found to be fertile and healthy throughout adulthood without any metabolic abnormalities (Kuwata et al., 2007). The lack of any obvious pancreatic defect in either of the Rgs8 and Rgs16 single KO mouse indicates that these genes were not individually critical for pancreatic islet and duct maturation or function. This came as no surprise as temporal and spatial overlap of Rgs8::GFP and Rgs16::GFP reporter expression in islets during development and diabetes suggested that these Rgs genes might be regulating the same or parallel GPCR signaling. Redundancy of Rgs8 and Rgs16 expression proposed homologous compensation as an explanation for the lack of any identifiable pancreatic phenotype directing endeavors to creating mice with dual gene deletion. The ~43kb distance and consequent low cross-over probability between these two genes prevented making the double KO (dKO) from crossing single Rgs8 and Rgs16 KO mouse.

Rgs8-Rgs16 dKO mouse was made by deleting Rgs8 in the Rgs16 KO background. Johnson, Hammer, and Wilkie laboratories have collaborated to generate a conditional Rgs8 allele in homozygous Rgs16 KO ES cells.

Heterozygous *Rgs8*$^{+/flox}$*; Rgs16*$^{+/-}$ founder mice were obtained. Initial results showed that homozygous whole body dKO mice obtained by driving gene deletion with *Meox2::Cre* construct were viable and fertile. In our preliminary observations, we did not see a significant difference in islet number and distribution of P8 and P12 WT and dKO mice following dithiazone staining (DTZ) (data not shown). Weanlings and young adult mice (3 and 5 weeks of age) had normal insulin levels and exhibited a normal response to GTT (Figure 28C, F, I). To compare the onset and severity of type 2 diabetes, we initiated 60% HF diet and followed their body weight and blood glucose level. These experiments are still ongoing but neither heterozygous nor dKO mice have so far shown a clear deviation from their WT counterparts (Figure 28).

Based on the outcome from our preliminary tests, it can be argued that Rgs8 and Rg16 are not essential genes for pancreas development and function. Even though the GPCR pathways these genes act upon might be critical for beta cell expansion, regulation by Rgs8 and/or Rgs16 does not seem to be indispensible. Other R4 class Rgs genes that are known to be expressed during endocrine development and in beta cells include Rgs4 and Rgs2 (Iankova et al., 2008; Ruiz de Azua et al., 2010; Serafimidis et al., 2011). Rgs4 may be particularly important to delete with Rgs8 and Rgs16, as it is expressed in Ngn3+ progenitor cells and subsequent endocrine cell differentiation (Serafimidis et al., 2011). Rgs4 was reported to regulate beta cell aggregation during isletogenesis (Serafimidis et al., 2011). Perhaps Rgs2 and/or Rgs4 can compensate for the loss of both Rgs8 and Rgs16 under the conditions we have assayed (Iankova et al., 2008; Ruiz de Azua et al., 2010). These genes are separated from each other by more than one megabase on chromosome one, so the triple and quadruple knockouts could be achieved by meiotic recombination (Figure 3A).

ChREBP's involvement in Rgs16::GFP induction during diabetes raised the question of whether it directly regulated transcription at Rgs16 promoter.

Figure 28: Rgs8-Rgs16 dKO mice on 60% fat diet for 16 weeks

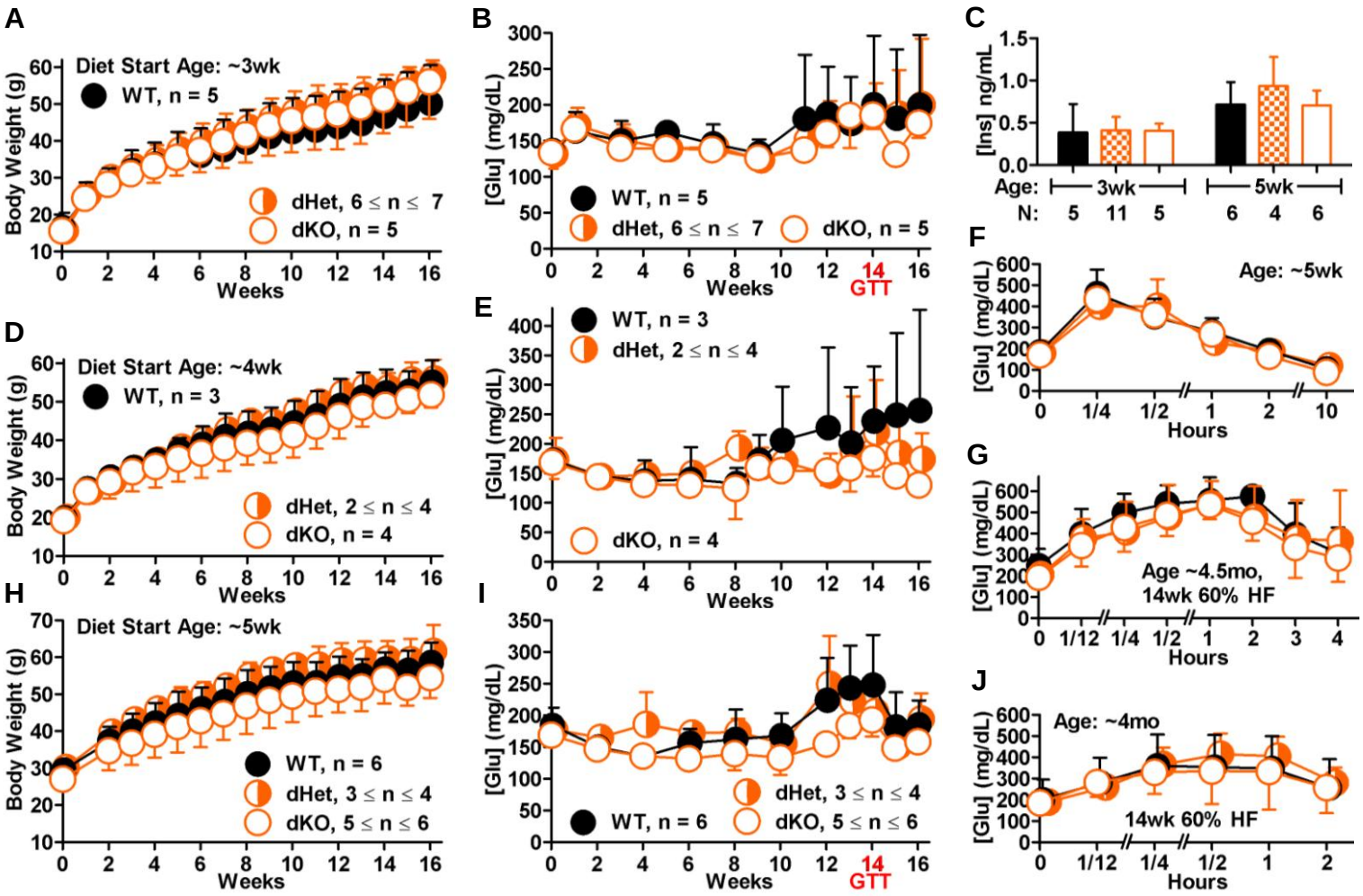

Tissue culture transfection experiments done with 5' 2.6kb and 4.3kb Rgs16 promoter luciferase constructs using various cell lines did not indicate an enhancement of transcription by ChREBP with or without its partner Mlx (Ma et al., 2006; Ma et al., 2005; Stoeckman et al., 2004); data not shown). Recent ChREBP ChIP-Seq data from the HepG2 liver cell line showed its binding within transcription start site of various glucose regulated genes, some of which previously unknown (Jeong et al., 2011). However, the absence of any close peaks within any R4 Rgs genes suggests that it exerts its effect on Rgs16 via regulating other factors (Jeong et al., 2011). Emerging data about ChREBP's involvement in regulation of several gene expression in islets suggests it might induce Rgs16 transcription during beta cell expansion signals (Boergesen et al., 2011; da Silva Xavier et al., 2006; da Silva Xavier et al., 2010). On the other hand, the requirement for many days of hyperglycemia prior to initial expression of Rgs16::GFP in islets and the heterogeneous distribution of Rgs16::GFP within islets and among beta cells belonging to the same islet indicate a possibility of ChREBP being involved in a sensor that relays signals to the pancreas. This model can be tested by crossing Rgs16::GFP transgenic mice to beta cell or neuronal-specific ChREBP KO mice. Also, it would be interesting to test Rgs16::GFP induction during recovery in PANIC-ATTAC with ChREBP KO

Figure 28: Rgs8-Rgs16 dKO mouse glucose, insulin, body weight measurements

Mice with *Rgs8*$^{+/+}$*; Rgs16*$^{+/+}$, *Rgs8*$^{+/-}$*; Rgs16*$^{+/-}$, and *Rgs8*$^{-/-}$*; Rgs16*$^{-/-}$ genotypes are given 60% HF diet starting from approximately 3, 4, and 5 weeks of age. Panels A, D, H show weekly body weight measurements of these 3 different age groups. Panels B, E, I show the bi-weekly glucose measurements of these mice. GTT weeks are indicated below x-axis. Panels C shows the basal insulin values of 3wk and 5wk old mice before starting with 60% HF diet. 4 additional dHet mice that contributed to insulin values were later discarded. GTT values (2g/kg glucose) of 5wk old group before starting 60% HF diet and 14 weeks afterwards are shown in Panel F and J, whereas GTT values (1g/kg glucose) of mice at 14th week of 60% HF diet started at 3wk of age is shown in Panel G.

background. If ChREBP is central for GPCR signal relay or response in the islets, then Rgs16::GFP expression could be lost in both type 1 and type 2 diabetes. Despite partial alleviation of obesity driven type 2 diabetes in ChREBP KO mice (Iizuka et al., 2006), it is important to see if Rgs16::GFP is still induced in *ob/ob; ChREBP*$^{-/-}$ mice.

As it appears that ChREBP does not directly bind to and regulate Rgs16 transcription, Rgs16 promoter and 5' upstream region should be tested for sites that bind pancreatic transcription factors. Several bHLH transcription factor binding sites (E-box elements) occur in and around the Rgs16 gene (Figure 29) (Doi et al., 2011; Stuebe et al., 2008). Deletion promoter constructs including these elements need to be tested for any transcription factor binding in tissue culture using PDAC tumor cells or insulinoma lines such as Min6 and Ins1 (Hohmeier and Newgard, 2004; Ishihara et al., 1993; Nakashima et al., 2009).

The GPCR genes we identify from RNA-Seq analysis in PDAC are the primary candidates through which Rgs16 is feedback induced. Their known and predicted ligands need to be tested in the PDAC tumor culture. In addition, induction via small molecules like ISX encourages us to test other such compounds in a high throughput screen (HTS) (Schneider et al., 2008). We have already determined culture conditions to screen compounds in 384-well plates. Initial tests with ISX in PDAC cells grown in regular media were successful in inducing Rgs16::GFP and provide us a proof of principle for testing large compound libraries available in HTS facility.

We have also determined *in vivo* assay conditions for testing GPCR ligands or small molecules that can emerge from HTS. Rapid hyperglycemia followed by gradual Rgs16::GFP expression in type 1 diabetic mouse models provides us valuable animal testing grounds. Short term drug effects can be pursued in STZ treatment protocol we have established in Rgs16::GFP mice, whereas *Rgs16::GFP; PANIC-ATTAC* is suitable for longer term outcome of

Figure 29: Rgs16 plasmid map to test putative promoter elements

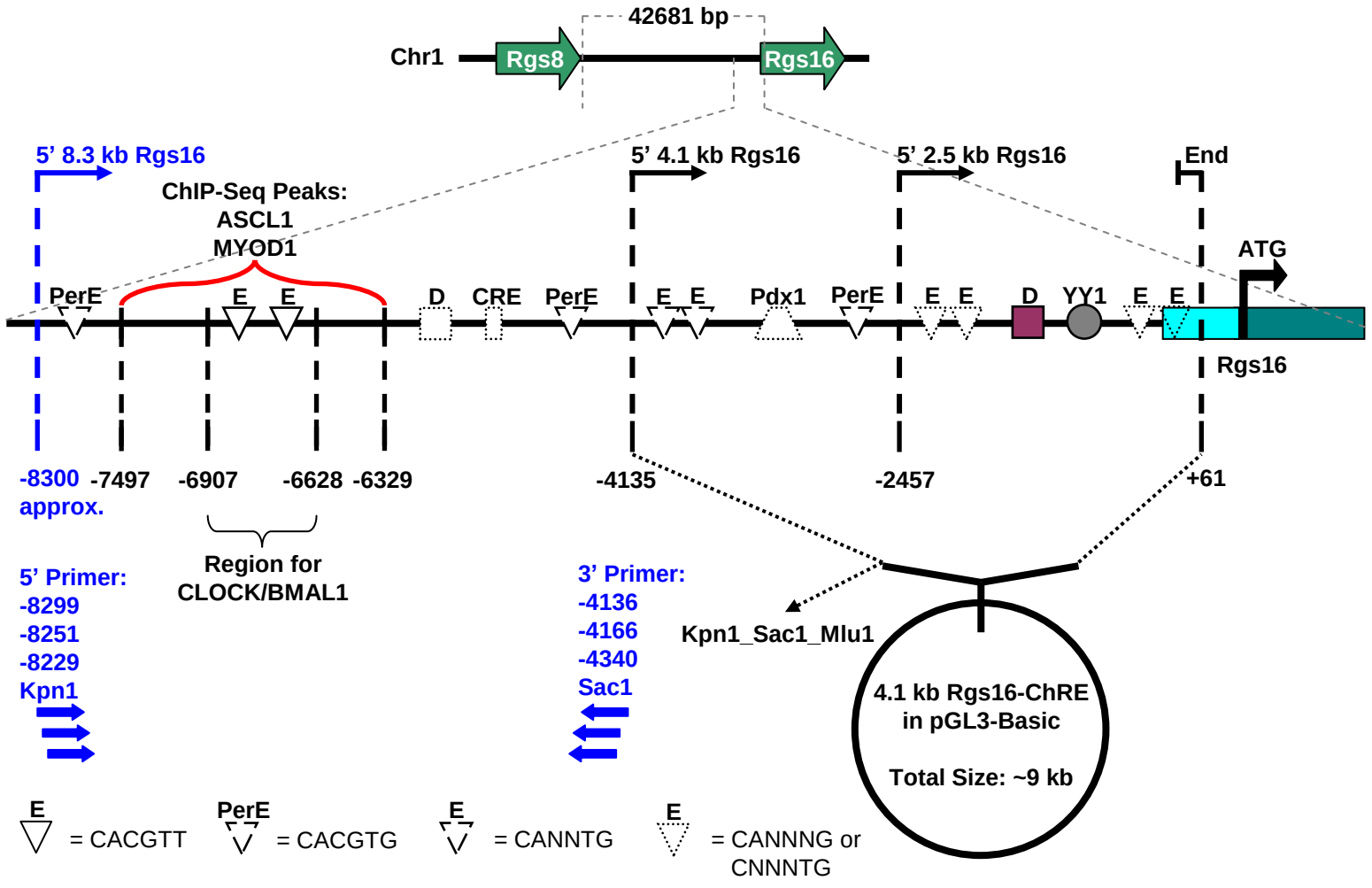

compounds that can facilitate pancreas regeneration and recovery from hyperglycemia.

Our findings suggest there is a yet to be identified connection between a "hyperglycemia sensor" that would link chronic elevation in blood glucose concentration to activation of Rgs16::GFP expression in beta cells. Our hypothesis is that this "hyperglycemia sensor" controls the relay of beta cell expansion signals either directly or via other pathways. The mechanism of this sensor has great potential to create exciting angles for diabetes research. Analysis of islet Rgs16::GFP expression in diabetic pancreas thus lays out the basis of future studies aimed at understanding important GPCR pathways of islet biology. We hope that our work establishes the fundamental principles of pancreatic Rgs16 expression and tissue culture testing conditions that will be utilized during scientific journey towards future discoveries of islet biology and diabetes.

Figure 29: Rgs16 plasmid map to test putative promoter elements
Putative Rgs16 promoter elements based on consensus sequence match or literature are shown. Dashed elements are based on consensus sequence match and lack any supporting data. Numbers are according to the transcription start site, whereas thick angled arrow shows translation start site. The current long and short 5' promoter constructs are indicated above the DNA strand with black angled arrows. The suggested primers to extend the long constructs are indicated below DNA strand with their 5' and 3' start sites for forward and reverse primers, respectively. The approximate 5' start site of the planned new construct is indicated with blue angled arrow above the strand. The current basic vector with the promoter inserts is shown as a circle with the 5' restriction endonuclease sites. Binding site abbreviations are PerE: Single perfect E-box, E: Single E-box or E-box-like, D: D-box, CRE: cAMP Response Element, Pdx1: Pancreatic and duodenal homeobox1, and YY1: Yingyang1 (Doi et al., 2011; Stuebe et al., 2008).

ACKNOWLEDGEMENTS

We thank all our collaborators and colleagues for their support and contribution in various steps of projects. Without their help, we would not be able to accomplish the tasks mentioned in this work.

This dissertation relied primarily on the transgenic Rgs16::GFP reporter mouse that was created by Mary E. Hatten's group and her collaborators. Without her acceptance to add Rgs16 and Rgs8 genes into the transgenic mouse pool during gene expression atlas development, we wouldn't be able to find out their involvement in pancreas. We thank Mary E. Hatten and her collaborators for making and kindly sharing these mice with us.

Ondine Cleaver and her former student Alethia Villasenor together with Thomas Wilkie characterized embryonic and postnatal expression of Rgs16::GFP in the transgenic mice. Insulin, glucagon, and pancreas progenitor marker staining on pancreatic sections was done by Alethia Villasenor. She also visualized part of Rgs16::GFP expression in *ob/ob* mice. We utilized Ondine Cleaver's fluorescence microscope for visualizing all of the Rgs16::GFP mice we have gone though in our studies. Everybody in Cleaver laboratory was helpful. We thank Ondine Cleaver and Alethia Villasenor for their collaboration and support. We also thank everybody else from Cleaver laboratory for their assistance and discussion.

Rolf Brekken and his former student Lee Rivera together with Thomas Wilkie identified Rgs16::GFP expression in the PDAC mouse model. Isolation of tumor, subcloning of Rgs16::GFP expressing cells, and preparation of PDAC tissue culture was accomplished by Lee Rivera. Transplantation of PDAC into recipient NOD-SCID animals, isolation of grown tumor, sectioning and visualization of duct-like structure were done by Lee Rivera as well. He also contributed to immunohistochemistry staining of pancreas slides taken from postnatal mice. Juliet Carbon genotyped PDAC mice. We used Rolf Brekken's

fluorescent microscope to visualize PDAC in native culture and upon administration of several compounds we tested. Michael Dellinger also contributed to our cancer studies with genotyping and discussion. We thank Rolf Brekken, Lee Rivera, Juliet Carbon, Michael Dellinger, and other members of Brekken laboratory for their help.

Zhao Wang formerly from Philipp Scherer laboratory together with Thomas Wilkie found out Rgs16::GFP expression in PANIC-ATTAC mice. PANIC-ATTAC mouse line was obtained from Scherer laboratory. Zhao genotyped PANIC-ATTAC mice and visualized antibody stained pancreatic slides after sectioning them. Ingrid Wernstedt-Asterholm from Scherer laboratory measured insulin levels of type 1 and type 2 diabetic mice as well as young Rgs8-Rgs16 dKO mice. We thank Zhao Wang and Ingrid Wernstedt-Asterholm for their help in PANIC-ATTAC studies and insulin measurements. We thank Philipp Scherer for his discussion and scientific and financial support in our studies.

PDAC RNA-Seq raw data analysis and calculation of gene expression values was done by Chengcheng Shen formerly from Raymond MacDonald laboratory. Galvin Swift from MacDonald laboratory helped with genomic list compilation. Embryonic and adult pancreatic RNA-Seq data belongs to Galwin Swift from MacDonald laboratory. Pancreatic lineage markers for comparison of RNA-Seq data were suggested by Raymond MacDonald and Galvin Swift. We thank Raymond MacDonald, Galvin Swift and Chengcheng Shen for their help in RNA-Seq studies. We thank Raymond Macdonald, Galvin Swift and the remainder of MacDonald laboratory members for their support in our discussions.

Alex Artyukhin formerly from Steven Altschuler/Lani Wu laboratory showed us how to do pancreatic image quantification. He quantified GFP from PDAC culture experiments (data not shown) and thought us how to do Matlab graphical presentation. We thank Alex Artyukhin for his discussion and assistance in setting-up GFP quantification method.

Rgs8-Rgs16 dKO mentioned was created primarily by Jane Johnson and Robert Hammer laboratories. Thomas Wilkie and Jane Johnson initiated the joint task and supervised the project. Joshua Chang from Johnson laboratory made vector construct and verified its integrity with the help of Trisha Savage. Robert Hammer laboratory prepared embryonic stem cells and conducted homologous recombination. Lauren Dickel from Johnson laboratory performed genotyping of dKO mouse crosses. Jane Johnson provided guidance and support during all steps. We thank Jane Johnson, Robert Hammer, Joshua Chang, Trisha Savage, Lauren Dickel, and other Johnson and Hammer laboratory members for their contributions.

ISX compound and information about via personal communication were obtained from Jay Schneider. We thank Jay Schneider and his laboratory for assistance.

384-well plate assay of PDAC cells were set-up together with Mridula Vishwanath from UTSW HTS facility (data not shown). We thank Mridula Vishwanath and facility director Bruce Posner for their assistance.

During these projects, Victor Pashkov formerly from Thomas Wilkie laboratory helped me with discussions, provided reagents, recipes, protocols and thought me bench-work and tissue culture techniques. Victor genotyped Rgs16 and ChREBP KO mice, discovered Rgs16::GFP induction properties of ISX in PDAC culture, set-up ISX dose-response experiment and tested it in PDAC simultaneously. Victor also did qPCR analysis of Rgs16 and Gpr68 expression in PDAC and insulinoma cells (data not shown). He prepared PDAC cells before FACS, obtained total RNA from GFP+ and gfpNEG populations after sorting and has oversaw RNA-Seq data creation. Victor provided advice and guidance on many experiments and topics and became a reliable laboratory fellow while he was in Wilkie laboratory. We thank Victor Pashkov for all his work and support he gave all these years in the laboratory.

All the projects, tests, findings, and progress described in this work and beyond have been possible by one person: Thomas Wilkie. Tom has planned, initiated, supervised, organized, and participated in all of the biological questions we asked and oversaw and guided in majority of experiments realized to date. Tom started Rgs16::GFP transgenic mouse crosses with *ob/ob*, PANIC-ATTAC, ChREBP KO, and PDAC mouse models and maintained them throughout the studies. He made connections with our past and current collaborators, gathered resources, set-up assays, stimulated endeavors, interpreted outcomes, proposed ideas, and laid out next steps. As the principal investigator of the laboratory and central research administrator of our diabetic and cancer studies involving pancreas, he moved our research forward. Tom directly helped me with mouse experiments and sacrificed all the animals for pancreatic studies by himself. He thought me several techniques, showed hands-on demonstrations of mouse handling, enhanced my expertise with laboratory tests, and gave a hand in most or all the pancreas dissections, visualizations, mouse injections. Tom guided and supervised me during preparation, execution, and analysis of experiments, oral and written presentations, joint tasks with collaborations, and ideas for projects. He supported me as a mentor, colleague, partner, friend and made me progress in my graduate studies. His contributions to my research training shaped most of the knowledge and experiences I gained to date. I am grateful to Tom for all the time he spent with me during our interactions and joint work on experiments. I will remember all the insight, inspiration, perspective, courage, support, and mentorship he gave me in his laboratory and hope to become a science person that he would be proud of. Tom, thank you for everything you have done for me.

BIBLIOGRAPHY

Ackermann, A.M., and Gannon, M. (2007). Molecular regulation of pancreatic beta-cell mass development, maintenance, and expansion. J Mol Endocrinol *38*, 193-206.

Ackermann, S., Hiller, S., Osswald, H., Losle, M., Grenz, A., and Hambrock, A. (2009). 17beta-Estradiol modulates apoptosis in pancreatic beta-cells by specific involvement of the sulfonylurea receptor (SUR) isoform SUR1. J Biol Chem *284*, 4905-4913.

Agbunag, C., and Bar-Sagi, D. (2004). Oncogenic K-ras drives cell cycle progression and phenotypic conversion of primary pancreatic duct epithelial cells. Cancer Res *64*, 5659-5663.

Aguirre, A.J., Bardeesy, N., Sinha, M., Lopez, L., Tuveson, D.A., Horner, J., Redston, M.S., and DePinho, R.A. (2003). Activated Kras and Ink4a/Arf deficiency cooperate to produce metastatic pancreatic ductal adenocarcinoma. Genes Dev *17*, 3112-3126.

Ahren, B. (2009). Islet G protein-coupled receptors as potential targets for treatment of type 2 diabetes. Nat Rev Drug Discov *8*, 369-385.

Ahren, B., and Hughes, T.E. (2005). Inhibition of dipeptidyl peptidase-4 augments insulin secretion in response to exogenously administered glucagon-like peptide-1, glucose-dependent insulinotropic polypeptide, pituitary adenylate cyclase-activating polypeptide, and gastrin-releasing peptide in mice. Endocrinology *146*, 2055-2059.

Ahren, B., Landin-Olsson, M., Jansson, P.A., Svensson, M., Holmes, D., and Schweizer, A. (2004). Inhibition of dipeptidyl peptidase-4 reduces glycemia, sustains insulin levels, and reduces glucagon levels in type 2 diabetes. J Clin Endocrinol Metab *89*, 2078-2084.

Ahren, B., and Schmitz, O. (2004). GLP-1 receptor agonists and DPP-4 inhibitors in the treatment of type 2 diabetes. Horm Metab Res *36*, 867-876.

Alberts, B., Johnson, A., Lewis, J., Raff, M., Roberts, K., and Walter, P. (2007) Molecular Biology of the Cell. 5th ed. (New York, Garland Science).

Alldinger, I., Dittert, D., Peiper, M., Fusco, A., Chiappetta, G., Staub, E., Lohr, M., Jesnowski, R., Baretton, G., Ockert, D., Saeger, H.D., Grutzmann, R., and Pilarsky, C. (2005). Gene expression analysis of pancreatic cell lines reveals genes overexpressed in pancreatic cancer. Pancreatology *5*, 370-379.

Anastasi, A., Erspamer, V., and Endean, R. (1967). Isolation and structure of caerulein, an active decapeptide from the skin of Hyla caerulea. Experientia *23*, 699-700.

Anastasi, A., Erspamer, V., and Endean, R. (1968). Isolation and amino acid sequence of caerulein, the active decapeptide of the skin of hyla caerulea. Arch Biochem Biophys *125*, 57-68.

Arakawa, M., Ebato, C., Mita, T., Hirose, T., Kawamori, R., Fujitani, Y., and Watada, H. (2009). Effects of exendin-4 on glucose tolerance, insulin secretion, and beta-cell proliferation depend on treatment dose, treatment duration and meal contents. Biochem Biophys Res Commun *390*, 809-814.

Arees, E.A., and Mayer, J. (1967). Anatomical connections between medial and lateral regions of the hypothalamus concerned with food intake. Science *157*, 1574-1575.

Bachem, M.G., Schunemann, M., Ramadani, M., Siech, M., Beger, H., Buck, A., Zhou, S., Schmid-Kotsas, A., and Adler, G. (2005). Pancreatic carcinoma cells induce fibrosis by stimulating proliferation and matrix synthesis of stellate cells. Gastroenterology *128*, 907-921.

Balasubramanyam, K., Swaminathan, V., Ranganathan, A., and Kundu, T.K. (2003). Small molecule modulators of histone acetyltransferase p300. J Biol Chem *278*, 19134-19140.

Balhuizen, A., Kumar, R., Amisten, S., Lundquist, I., and Salehi, A. (2010). Activation of G protein-coupled receptor 30 modulates hormone secretion and counteracts cytokine-induced apoptosis in pancreatic islets of female mice. Mol Cell Endocrinol *320*, 16-24.

Bansal, G., Druey, K.M., and Xie, Z. (2007). R4 RGS proteins: regulation of G-protein signaling and beyond. Pharmacol Ther *116*, 473-495.

Banting, F.G. and Best, C.H. (1922). The internal secretion of the pancreas. J Lab Clin Med *7*, 251–266

Barber, M., Kasturi, B.S., Austin, M.E., Patel, K.P., MohanKumar, S.M., and MohanKumar, P.S. (2003). Diabetes-induced neuroendocrine changes in rats: role of brain monoamines, insulin and leptin. Brain Res *964*, 128-135.

Beadling, C., Druey, K.M., Richter, G., Kehrl, J.H., and Smith, K.A. (1999). Regulators of G protein signaling exhibit distinct patterns of gene expression and target G protein specificity in human lymphocytes. J Immunol *162*, 2677-2682.

Beattie, G., Lannom, R., Lipsick, J., Kaplan, N.O., and Osler, A.G. (1980). Streptozotocin-induced diabetes in athymic and conventional BALB/c mice. Diabetes *29*, 146-150.

Bell, G.I., and Polonsky, K.S. (2001). Diabetes mellitus and genetically programmed defects in beta-cell function. Nature *414*, 788-791.

Benzo, C.A. (1983). Minireview. The hypothalamus and blood glucose regulation. Life Sci *32*, 2509-2515.

Berman, D.M., Wilkie, T.M., and Gilman, A.G. (1996). GAIP and RGS4 are GTPase-activating proteins for the Gi subfamily of G protein alpha subunits. Cell *86*, 445-452.

Bernstein, L.S., Grillo, A.A., Loranger, S.S., and Linder, M.E. (2000). RGS4 binds to membranes through an amphipathic alpha -helix. J Biol Chem *275*, 18520-18526.

Bertrand, P. (2010). Inside HDAC with HDAC inhibitors. Eur J Med Chem *45*, 2095-2116.

Bertuzzi, F., Marzorati, S., and Secchi, A. (2006). Islet cell transplantation. Curr Mol Med *6*, 369-374.

Bestetti, G., and Rossi, G.L. (1980). Hypothalamic lesions in rats with long-term streptozotocin-induced diabetes mellitus. A semiquantitative light- and electron-microscopic study. Acta Neuropathol *52*, 119-127.

Birchmeier, W. (2011). Stem cells: Orphan receptors find a home. Nature *476*, 287-288.

Bluestone, J.A., Herold, K., and Eisenbarth, G. (2010). Genetics, pathogenesis and clinical interventions in type 1 diabetes. Nature *464*, 1293-1300.

Boergesen, M., Poulsen, L.C., Schmidt, S.F., Frigerio, F., Maechler, P., and Mandrup, S. (2011). ChREBP mediates glucose repression of peroxisome proliferator-activated receptor alpha expression in pancreatic beta-cells. J Biol Chem *286*, 13214-13225.

Bollen, M., Keppens, S., and Stalmans, W. (1998). Specific features of glycogen metabolism in the liver. Biochem J *336 (Pt 1)*, 19-31.

Bonner-Weir, S., Inada, A., Yatoh, S., Li, W.C., Aye, T., Toschi, E., and Sharma, A. (2008). Transdifferentiation of pancreatic ductal cells to endocrine beta-cells. Biochem Soc Trans *36*, 353-356.

Bonner-Weir, S., Toschi, E., Inada, A., Reitz, P., Fonseca, S.Y., Aye, T., and Sharma, A. (2004). The pancreatic ductal epithelium serves as a potential pool of progenitor cells. Pediatr Diabetes *5 Suppl 2*, 16-22.

Bonner-Weir, S., and Weir, G.C. (2005). New sources of pancreatic beta-cells. Nat Biotechnol *23*, 857-861.

Bonnevie-Nielsen, V., Skovgaard, L.T., and Lernmark, A. (1983). beta-Cell function relative to islet volume and hormone content in the isolated perfused mouse pancreas. Endocrinology *112*, 1049-1056.

Bonnevie-Nielsen, V., Steffes, M.W., and Lernmark, A. (1981). A major loss in islet mass and B-cell function precedes hyperglycemia in mice given multiple low doses of streptozotocin. Diabetes *30*, 424-429.

Borowiak, M. (2010). The new generation of beta-cells: replication, stem cell differentiation, and the role of small molecules. Rev Diabet Stud *7*, 93-104.

Bosma, G.C., Custer, R.P., and Bosma, M.J. (1983). A severe combined immunodeficiency mutation in the mouse. Nature *301*, 527-530.

Bradbury, E.M. (1983). Conformations and flexibilities of histones and high mobility group (HMG) proteins in chromatin structure and function. Ciba Found Symp *93*, 246-270.

Braunstein, M., Rose, A.B., Holmes, S.G., Allis, C.D., and Broach, J.R. (1993). Transcriptional silencing in yeast is associated with reduced nucleosome acetylation. Genes Dev *7*, 592-604.

Brosky, G., and Logothetopoulos, J. (1969). Streptozotocin diabetes in the mouse and guinea pig. Diabetes *18*, 606-611.

Burchett, S.A., Bannon, M.J., and Granneman, J.G. (1999). RGS mRNA expression in rat striatum: modulation by dopamine receptors and effects of repeated amphetamine administration. J Neurochem *72*, 1529-1533.

Burchett, S.A., Volk, M.L., Bannon, M.J., and Granneman, J.G. (1998). Regulators of G protein signaling: rapid changes in mRNA abundance in response to amphetamine. J Neurochem *70*, 2216-2219.

Campfield, L.A., Smith, F.J., and Burn, P. (1996). The OB protein (leptin) pathway--a link between adipose tissue mass and central neural networks. Horm Metab Res *28*, 619-632.

Casey, P.J., and Gilman, A.G. (1988). G protein involvement in receptor-effector coupling. J Biol Chem *263*, 2577-2580.

Cha-Molstad, H., Saxena, G., Chen, J., and Shalev, A. (2009). Glucose-stimulated expression of Txnip is mediated by carbohydrate response element-binding protein, p300, and histone H4 acetylation in pancreatic beta cells. J Biol Chem *284*, 16898-16905.

Chakir, K., Zhu, W., Tsang, S., Woo, A.Y., Yang, D., Wang, X., Zeng, X., Rhee, M.H., Mende, U., Koitabashi, N., Takimoto, E., Blumer, K.J., Lakatta, E.G., Kass, D.A., and Xiao, R.P. (2011). RGS2 is a primary terminator of beta-adrenergic receptor-mediated G(i) signaling. J Mol Cell Cardiol *50*, 1000-1007.

Chalfie, M., Tu, Y., Euskirchen, G., Ward, W.W., and Prasher, D.C. (1994). Green fluorescent protein as a marker for gene expression. Science *263*, 802-805.

Chance, R.E., Ellis, R.M., and Bromer, W.W. (1968). Porcine proinsulin: characterization and amino acid sequence. Science *161*, 165-167.

Chang, L., Chiang, S.H., and Saltiel, A.R. (2004). Insulin signaling and the regulation of glucose transport. Mol Med *10*, 65-71.

Chen, C., Seow, K.T., Guo, K., Yaw, L.P., and Lin, S.C. (1999). The membrane association domain of RGS16 contains unique amphipathic features that are conserved in RGS4 and RGS5. J Biol Chem *274*, 19799-19806.

Chen, L., Alam, T., Johnson, J.H., Hughes, S., Newgard, C.B., and Unger, R.H. (1990). Regulation of beta-cell glucose transporter gene expression. Proc Natl Acad Sci U S A *87*, 4088-4092.

Chen, Z., Wells, C.D., Sternweis, P.C., and Sprang, S.R. (2001). Structure of the rgRGS domain of p115RhoGEF. Nat Struct Biol *8*, 805-809.

Cherrington, A.D. (1999). Banting Lecture 1997. Control of glucose uptake and release by the liver in vivo. Diabetes *48*, 1198-1214.

Cherrington, A.D., Sindelar, D., Edgerton, D., Steiner, K., and McGuinness, O.P. (2002). Physiological consequences of phasic insulin release in the normal animal. Diabetes *51 Suppl 1,* S103-108.

Chin, L., Pomerantz, J., and DePinho, R.A. (1998). The INK4a/ARF tumor suppressor: one gene--two products--two pathways. Trends Biochem Sci *23*, 291-296.

Cook, M.J. (1965). The Anatomy of the Laboratory Mouse. 1st ed. (New York, Academic Press)

Cotton, M., and Claing, A. (2009). G protein-coupled receptors stimulation and the control of cell migration. Cell Signal *21,* 1045-1053.

Couzin-Frankel, J. (2011). Clinical studies. Trying to reset the clock on type 1 diabetes. Science *333*, 819-821.

Cowie, C.C., Rust, K.F., Ford, E.S., Eberhardt, M.S., Byrd-Holt, D.D., Li ,C., Williams, D.E., Gregg, E.W., Bainbridge, K.E., Saydah, S.H., Geiss, L.S. (2009). Full accounting of diabetes and prediabetes in the U.S. population in 1988–1994 and 2005–2006. Diabetes Care *32,* 287–294.

da Silva Xavier, G., Rutter, G.A., Diraison, F., Andreolas, C., and Leclerc, I. (2006). ChREBP binding to fatty acid synthase and L-type pyruvate kinase genes is stimulated by glucose in pancreatic beta-cells. J Lipid Res *47,* 2482-2491.

da Silva Xavier, G., Sun, G., Qian, Q., Rutter, G.A., and Leclerc, I. (2010). ChREBP regulates Pdx-1 and other glucose-sensitive genes in pancreatic beta-cells. Biochem Biophys Res Commun *402,* 252-257.

Dangond, F., and Gullans, S.R. (1998). Differential expression of human histone deacetylase mRNAs in response to immune cell apoptosis induction by trichostatin A and butyrate. Biochem Biophys Res Commun *247,* 833-837.

Davenport, D., and Nicol, J.A.C. (1955). Luminescence of hydromedusae. Proc R Soc London Ser B *144*, 399-411.

Davies, M.N., O'Callaghan, B.L., and Towle, H.C. (2008). Glucose activates ChREBP by increasing its rate of nuclear entry and relieving repression of its transcriptional activity. J Biol Chem *283*, 24029-24038.

De Caro, G., Endean, R., Erspamer, V., and Roseghini, M. (1968). Occurrence of caerulein in extracts of the skin of Hyla caerulea and other Australian hylids. Br J Pharmacol Chemother *33*, 48-58.

De Vries, L., Mousli, M., Wurmser, A., and Farquhar, M.G. (1995). GAIP, a protein that specifically interacts with the trimeric G protein G alpha i3, is a member of a protein family with a highly conserved core domain. Proc Natl Acad Sci U S A *92*, 11916-11920.

Dekker, F.J., and Haisma, H.J. (2009). Histone acetyl transferases as emerging drug targets. Drug Discov Today *14*, 942-948.

Delaere, F., Magnan, C., and Mithieux, G. (2010). Hypothalamic integration of portal glucose signals and control of food intake and insulin sensitivity. Diabetes Metab *36*, 257-262.

Demary, K., Wong, L., and Spanjaard, R.A. (2001). Effects of retinoic acid and sodium butyrate on gene expression, histone acetylation and inhibition of proliferation of melanoma cells. Cancer Lett *163*, 103-107.

Dessauer, C.W., Posner, B.A., and Gilman, A.G. (1996). Visualizing signal transduction: receptors, G-proteins, and adenylate cyclases. Clin Sci (Lond) *91*, 527-537.

Dittmer, S., Sahin, M., Pantlen, A., Saxena, A., Toutzaris, D., Pina, A.L., Geerts, A., Golz, S., and Methner, A. (2008). The constitutively active orphan G-protein-coupled receptor GPR39 protects from cell death by increasing secretion of pigment epithelium-derived growth factor. J Biol Chem *283*, 7074-7081.

Dohlman, H.G., Apaniesk, D., Chen, Y., Song, J., and Nusskern, D. (1995). Inhibition of G-protein signaling by dominant gain-of-function mutations in Sst2p, a pheromone desensitization factor in Saccharomyces cerevisiae. Mol Cell Biol *15*, 3635-3643.

Doi, M., Ishida, A., Miyake, A., Sato, M., Komatsu, R., Yamazaki, F., Kimura, I., Tsuchiya, S., Kori, H., Seo, K., Yamaguchi, Y., Matsuo, M., Fustin, J.M., Tanaka, R., Santo, Y., Yamada, H., Takahashi, Y., Araki, M., Nakao, K., Aizawa, S., Kobayashi, M., Obrietan, K., Tsujimoto, G., and Okamura, H. (2011). Circadian

regulation of intracellular G-protein signalling mediates intercellular synchrony and rhythmicity in the suprachiasmatic nucleus. Nat Commun *2*, 327.

Drucker, D.J. (1998). Glucagon-like peptides. Diabetes *47*, 159-169.

Dryer, L., and Berghard, A. (1999). Odorant receptors: a plethora of G-protein-coupled receptors. Trends Pharmacol Sci *20*, 413-417.

Duval, J.V., Savas, L., and Banner, B.F. (2000). Expression of cytokeratins 7 and 20 in carcinomas of the extrahepatic biliary tract, pancreas, and gallbladder. Arch Pathol Lab Med *124*, 1196-1200.

Emanuel, C.F. (1960). Some physical properties of deoxyribonucleic acids dissolved in a high-salt medium: salt hyperchromicity. Biochim Biophys Acta *42*, 91-98.

Eng, J., Kleinman, W.A., Singh, L., Singh, G., and Raufman, J.P. (1992). Isolation and characterization of exendin-4, an exendin-3 analogue, from Heloderma suspectum venom. Further evidence for an exendin receptor on dispersed acini from guinea pig pancreas. J Biol Chem *267*, 7402-7405.

Eszlinger, M., Holzapfel, H.P., Voigt, C., Arkenau, C., and Paschke, R. (2004). RGS 2 expression is regulated by TSH and inhibits TSH receptor signaling. Eur J Endocrinol *151*, 383-390.

Ettinghausen, S.E., Schwartzentruber, D.J., and Sindelar, W.F. (1995). Evolving strategies for the treatment of adenocarcinoma of the pancreas. A review. J Clin Gastroenterol *21*, 48-60.

Farr, C.J., Saiki, R.K., Erlich, H.A., McCormick, F., and Marshall, C.J. (1988). Analysis of RAS gene mutations in acute myeloid leukemia by polymerase chain reaction and oligonucleotide probes. Proc Natl Acad Sci U S A *85*, 1629-1633.

Fehmann, H.C., Jiang, J., Schweinfurth, J., Wheeler, M.B., Boyd, A.E., 3rd, and Goke, B. (1994). Stable expression of the rat GLP-I receptor in CHO cells: activation and binding characteristics utilizing GLP-I(7-36)-amide, oxyntomodulin, exendin-4, and exendin(9-39). Peptides *15*, 453-456.

Ferguson, S.S., and Caron, M.G. (1998). G protein-coupled receptor adaptation mechanisms. Semin Cell Dev Biol *9*, 119-127.

Fischer, C., Buthe, J., Nollau, P., Hollerbach, S., Schulmann, K., Schmiegel, W., Wagener, C., and Tschentscher, P. (2001). Enrichment of mutant KRAS alleles in

pancreatic juice by subtractive iterative polymerase chain reaction. Lab Invest *81*, 827-831.

Fong, C.W., Zhang, Y., Neo, S.Y., and Lin, S.C. (2000). Specific induction of RGS16 (regulator of G-protein signalling 16) mRNA by protein kinase C in CEM leukaemia cells is mediated via tumour necrosis factor alpha in a calcium-sensitive manner. Biochem J *352 Pt 3*, 747-753.

Foster, D.W. (1984). Banting lecture 1984. From glycogen to ketones--and back. Diabetes *33*, 1188-1199.

Frankel, B.J., Atwater, I., and Grodsky, G.M. (1981). Calcium affects insulin release and membrane potential in islet beta-cells. Am J Physiol *240*, C64-72.

Fredriksson, R., Lagerstrom, M.C., Lundin, L.G., and Schioth, H.B. (2003). The G-protein-coupled receptors in the human genome form five main families. Phylogenetic analysis, paralogon groups, and fingerprints. Mol Pharmacol *63*, 1256-1272.

Freissmuth, M., Casey, P.J., and Gilman, A.G. (1989). G proteins control diverse pathways of transmembrane signaling. FASEB J *3*, 2125-2131.

Friedman, J.M. (2000). Obesity in the new millennium. Nature *404*, 632-634.

Friedman, J.M. (2009). Obesity: Causes and control of excess body fat. Nature *459*, 340-342.

Friedman, J.M., and Halaas, J.L. (1998). Leptin and the regulation of body weight in mammals. Nature *395*, 763-770.

Fukuda, A., Kawaguchi, Y., Furuyama, K., Kodama, S., Horiguchi, M., Kuhara, T., Koizumi, M., Boyer, D.F., Fujimoto, K., Doi, R., Kageyama, R., Wright, C.V., and Chiba, T. (2006). Ectopic pancreas formation in Hes1 -knockout mice reveals plasticity of endodermal progenitors of the gut, bile duct, and pancreas. J Clin Invest *116*, 1484-1493.

Gaber, A.O., and Fraga, D. (2004). Advances in long-term islet culture: the Memphis experience. Cell Biochem Biophys *40*, 49-54.

Gaillard, I., Rouquier, S., and Giorgi, D. (2004). Olfactory receptors. Cell Mol Life Sci *61*, 456-469.

Ganda, O.P., Rossini, A.A., and Like, A.A. (1976). Studies on streptozotocin diabetes. Diabetes *25*, 595-603.

Gannon, M. (2001). Molecular genetic analysis of diabetes in mice. Trends Genet *17*, S23-28.

Gao, N., Le Lay, J., Qin, W., Doliba, N., Schug, J., Fox, A.J., Smirnova, O., Matschinsky, F.M., and Kaestner, K.H. (2010). Foxa1 and Foxa2 maintain the metabolic and secretory features of the mature beta-cell. Mol Endocrinol *24*, 1594-1604.

Garnier, M., Zaratin, P.F., Ficalora, G., Valente, M., Fontanella, L., Rhee, M.H., Blumer, K.J., and Scheideler, M.A. (2003). Up-regulation of regulator of G protein signaling 4 expression in a model of neuropathic pain and insensitivity to morphine. J Pharmacol Exp Ther *304*, 1299-1306.

Gerich, J.E. (1993). Control of glycaemia. Baillieres Clin Endocrinol Metab *7*, 551-586.

Gilman, A.G. (1984). G proteins and dual control of adenylate cyclase. Cell *36*, 577-579.

Gilman, A.G. (1987). G proteins: transducers of receptor-generated signals. Annu Rev Biochem *56*, 615-649.

Giorelli, M., Livrea, P., Defazio, G., Iacovelli, L., Capobianco, L., Picascia, A., Sallese, M., Martino, D., Aniello, M.S., Trojano, M., and De Blasi, A. (2002). Interferon beta-1a counteracts effects of activation on the expression of G-protein-coupled receptor kinases 2 and 3, beta-arrestin-1, and regulators of G-protein signalling 2 and 16 in human mononuclear leukocytes. Cell Signal *14*, 673-678.

Girish, V., and Vijayalakshmi, A. (2004). Affordable image analysis using NIH Image/ImageJ. Indian J Cancer *41*, 47.

Gocke, C.D., Dabbs, D.J., Benko, F.A., and Silverman, J.F. (1997). KRAS oncogene mutations suggest a common histogenetic origin for pleomorphic giant cell tumor of the pancreas, osteoclastoma of the pancreas, and pancreatic duct adenocarcinoma. Hum Pathol *28*, 80-83.

Goke, R., Fehmann, H.C., Linn, T., Schmidt, H., Krause, M., Eng, J., and Goke, B. (1993). Exendin-4 is a high potency agonist and truncated exendin-(9-39)-amide an antagonist at the glucagon-like peptide 1-(7-36)-amide receptor of insulin-secreting beta-cells. J Biol Chem *268*, 19650-19655.

Gold, S.J., Han, M.H., Herman, A.E., Ni, Y.G., Pudiak, C.M., Aghajanian, G.K., Liu, R.J., Potts, B.W., Mumby, S.M., and Nestler, E.J. (2003). Regulation of RGS proteins by chronic morphine in rat locus coeruleus. Eur J Neurosci *17*, 971-980.

Gold, S.J., Ni, Y.G., Dohlman, H.G., and Nestler, E.J. (1997). Regulators of G-protein signaling (RGS) proteins: region-specific expression of nine subtypes in rat brain. J Neurosci *17*, 8024-8037.

Gong, S., Zheng, C., Doughty, M.L., Losos, K., Didkovsky, N., Schambra, U.B., Nowak, N.J., Joyner, A., Leblanc, G., Hatten, M.E., and Heintz, N. (2003). A gene expression atlas of the central nervous system based on bacterial artificial chromosomes. Nature *425*, 917-925.

Gordon, D.A., Toledo-Pereyra, L.H., and MacKenzie, G.H. (1982). Preservation for transplantation: a review of techniques of islet cell culture and storage. J Surg Res *32*, 182-193.

Grafstein-Dunn, E., Young, K.H., Cockett, M.I., and Khawaja, X.Z. (2001). Regional distribution of regulators of G-protein signaling (RGS) 1, 2, 13, 14, 16, and GAIP messenger ribonucleic acids by in situ hybridization in rat brain. Brain Res Mol Brain Res *88*, 113-123.

Grant, S.L., Lassegue, B., Griendling, K.K., Ushio-Fukai, M., Lyons, P.R., and Alexander, R.W. (2000). Specific regulation of RGS2 messenger RNA by angiotensin II in cultured vascular smooth muscle cells. Mol Pharmacol *57*, 460-467.

Gray, D.W., McShane, P., Grant, A., and Morris, P.J. (1984). A method for isolation of islets of Langerhans from the human pancreas. Diabetes *33*, 1055-1061.

Gromada, J., Franklin, I., and Wollheim, C.B. (2007). Alpha-cells of the endocrine pancreas: 35 years of research but the enigma remains. Endocr Rev *28*, 84-116.

Gui, C.Y., Ngo, L., Xu, W.S., Richon, V.M., and Marks, P.A. (2004). Histone deacetylase (HDAC) inhibitor activation of p21WAF1 involves changes in promoter-associated proteins, including HDAC1. Proc Natl Acad Sci U S A *101*, 1241-1246.

Gukovsky, I., Gukovskaya, A.S., Blinman, T.A., Zaninovic, V., and Pandol, S.J. (1998). Early NF-kappaB activation is associated with hormone-induced pancreatitis. Am J Physiol *275*, G1402-1414.

Gunaje, J.J., Bahrami, A.J., Schwartz, S.M., Daum, G., and Mahoney, W.M., Jr. (2011). PDGF-dependent regulation of regulator of G protein signaling-5 expression and vascular smooth muscle cell functionality. Am J Physiol Cell Physiol *301*, C478-489.

Guney, M.A., and Gannon, M. (2009). Pancreas cell fate. Birth Defects Res C Embryo Today *87*, 232-248.

Gutniak, M., Orskov, C., Holst, J.J., Ahren, B., and Efendic, S. (1992). Antidiabetogenic effect of glucagon-like peptide-1 (7-36)amide in normal subjects and patients with diabetes mellitus. N Engl J Med *326*, 1316-1322.

Hahn, H.J. (1978). [The isolated islet of Langerhans, a model for insulin secretion in vitro]. Endokrinologie *71*, 308-324.

Hamann, A., and Matthaei, S. (1996). Regulation of energy balance by leptin. Exp Clin Endocrinol Diabetes *104*, 293-300.

Hardy, S., Brand, M., Mittler, G., Yanagisawa, J., Kato, S., Meisterernst, M., and Tora, L. (2002). TATA-binding protein-free TAF-containing complex (TFTC) and p300 are both required for efficient transcriptional activation. J Biol Chem *277*, 32875-32882.

Heim, R., Cubitt, A.B., and Tsien, R.Y. (1995). Improved green fluorescence. Nature *373*, 663-664.

Heintz, N. (2001). BAC to the future: the use of bac transgenic mice for neuroscience research. Nat Rev Neurosci *2*, 861-870.

Hellman, B. (1975). The significance of calcium for glucose stimulation of insulin release. Endocrinology *97*, 392-398.

Hendriks-Balk, M.C., Hajji, N., van Loenen, P.B., Michel, M.C., Peters, S.L., and Alewijnse, A.E. (2009). Sphingosine-1-phosphate regulates RGS2 and RGS16 mRNA expression in vascular smooth muscle cells. Eur J Pharmacol *606*, 25-31.

Hepler, J.R. (1999). Emerging roles for RGS proteins in cell signalling. Trends Pharmacol Sci *20*, 376-382.

Hepler, J.R., and Gilman, A.G. (1992). G proteins. Trends Biochem Sci *17*, 383-387.

Herman, G.A., Bergman, A., Liu, F., Stevens, C., Wang, A.Q., Zeng, W., Chen, L., Snyder, K., Hilliard, D., Tanen, M., Tanaka, W., Meehan, A.G., Lasseter, K., Dilzer, S., Blum, R., and Wagner, J.A. (2006). Pharmacokinetics and pharmacodynamic effects of the oral DPP-4 inhibitor sitagliptin in middle-aged obese subjects. J Clin Pharmacol *46*, 876-886.

Heximer, S.P., Lim, H., Bernard, J.L., and Blumer, K.J. (2001). Mechanisms governing subcellular localization and function of human RGS2. J Biol Chem *276*, 14195-14203.

Hirasawa, A., Tsumaya, K., Awaji, T., Katsuma, S., Adachi, T., Yamada, M., Sugimoto, Y., Miyazaki, S., and Tsujimoto, G. (2005). Free fatty acids regulate gut incretin glucagon-like peptide-1 secretion through GPR120. Nat Med *11*, 90-94.

Hirose, S. (1998). Chromatin remodeling and transcription. J Biochem *124*, 1060-1064.

Hohmeier, H.E., and Newgard, C.B. (2004). Cell lines derived from pancreatic islets. Mol Cell Endocrinol *228*, 121-128.

Hollinger, S., and Hepler, J.R. (2002). Cellular regulation of RGS proteins: modulators and integrators of G protein signaling. Pharmacol Rev *54*, 527-559.

Hotamisligil, G.S. (2006). Inflammation and metabolic disorders. Nature *444*, 860-867.

Hruban, R.H., Adsay, N.V., Albores-Saavedra, J., Compton, C., Garrett, E.S., Goodman, S.N., Kern, S.E., Klimstra, D.S., Kloppel, G., Longnecker, D.S., Luttges, J., and Offerhaus, G.J. (2001). Pancreatic intraepithelial neoplasia: a new nomenclature and classification system for pancreatic duct lesions. Am J Surg Pathol *25*, 579-586.

Hsu, H.C., Yang, P., Wang, J., Wu, Q., Myers, R., Chen, J., Yi, J., Guentert, T., Tousson, A., Stanus, A.L., Le, T.V., Lorenz, R.G., Xu, H., Kolls, J.K., Carter, R.H., Chaplin, D.D., Williams, R.W., and Mountz, J.D. (2008). Interleukin 17-producing T helper cells and interleukin 17 orchestrate autoreactive germinal center development in autoimmune BXD2 mice. Nat Immunol *9*, 166-175.

Hsu, S.Y., Kudo, M., Chen, T., Nakabayashi, K., Bhalla, A., van der Spek, P.J., van Duin, M., and Hsueh, A.J. (2000). The three subfamilies of leucine-rich repeat-containing G protein-coupled receptors (LGR): identification of LGR6 and LGR7 and the signaling mechanism for LGR7. Mol Endocrinol *14*, 1257-1271.

Hua, H., Zhang, Y.Q., Dabernat, S., Kritzik, M., Dietz, D., Sterling, L., and Sarvetnick, N. (2006). BMP4 regulates pancreatic progenitor cell expansion through Id2. J Biol Chem *281*, 13574-13580.

Huang, J., Pashkov, V., Kurrasch, D.M., Yu, K., Gold, S.J., and Wilkie, T.M. (2006). Feeding and fasting controls liver expression of a regulator of G protein signaling (Rgs16) in periportal hepatocytes. Comp Hepatol *5*, 8.

Huang, S.W., and Taylor, G.E. (1981). Immune insulitis and antibodies to nucleic acids induced with streptozotocin in mice. Clin Exp Immunol *43*, 425-429.

Hughes, S.D., Johnson, J.H., Quaade, C., and Newgard, C.B. (1992). Engineering of glucose-stimulated insulin secretion and biosynthesis in non-islet cells. Proc Natl Acad Sci U S A *89*, 688-692.

Hunt, T.W., Fields, T.A., Casey, P.J., and Peralta, E.G. (1996). RGS10 is a selective activator of G alpha i GTPase activity. Nature *383*, 175-177.

Iankova, I., Chavey, C., Clape, C., Colomer, C., Guerineau, N.C., Grillet, N., Brunet, J.F., Annicotte, J.S., and Fajas, L. (2008). Regulator of G protein signaling-4 controls fatty acid and glucose homeostasis. Endocrinology *149*, 5706-5712.

Iizuka, K., Bruick, R.K., Liang, G., Horton, J.D., and Uyeda, K. (2004). Deficiency of carbohydrate response element-binding protein (ChREBP) reduces lipogenesis as well as glycolysis. Proc Natl Acad Sci U S A *101*, 7281-7286.

Iizuka, K., Miller, B., and Uyeda, K. (2006). Deficiency of carbohydrate-activated transcription factor ChREBP prevents obesity and improves plasma glucose control in leptin-deficient (ob/ob) mice. Am J Physiol Endocrinol Metab *291*, E358-364.

Ikemoto, S., Takahashi, M., Tsunoda, N., Maruyama, K., Itakura, H., and Ezaki, O. (1996). High-fat diet-induced hyperglycemia and obesity in mice: differential effects of dietary oils. Metabolism *45*, 1539-1546.

Ingi, T., Krumins, A.M., Chidiac, P., Brothers, G.M., Chung, S., Snow, B.E., Barnes, C.A., Lanahan, A.A., Siderovski, D.P., Ross, E.M., Gilman, A.G., and

Worley, P.F. (1998). Dynamic regulation of RGS2 suggests a novel mechanism in G-protein signaling and neuronal plasticity. J Neurosci *18*, 7178-7188.

Ishihara, H., Asano, T., Tsukuda, K., Katagiri, H., Inukai, K., Anai, M., Kikuchi, M., Yazaki, Y., Miyazaki, J.I., and Oka, Y. (1993). Pancreatic beta cell line MIN6 exhibits characteristics of glucose metabolism and glucose-stimulated insulin secretion similar to those of normal islets. Diabetologia *36*, 1139-1145.

Ishii, S., Iizuka, K., Miller, B.C., and Uyeda, K. (2004). Carbohydrate response element binding protein directly promotes lipogenic enzyme gene transcription. Proc Natl Acad Sci U S A *101*, 15597-15602.

Itoh, M., Odagiri, M., Abe, H., and Saitoh, O. (2001). RGS8 protein is distributed in dendrites and cell body of cerebellar Purkinje cell. Biochem Biophys Res Commun *287*, 223-228.

Iwai, K., Koike, M., Ohshima, S., Miyatake, K., Uchiyama, Y., Saeki, Y., and Ishii, M. (2007). RGS18 acts as a negative regulator of osteoclastogenesis by modulating the acid-sensing OGR1/NFAT signaling pathway. J Bone Miner Res *22*, 1612-1620.

Iwaki, S., Lu, Y., Xie, Z., and Druey, K.M. (2011). p53 negatively regulates RGS13 protein expression in immune cells. J Biol Chem *286*, 22219-22226.

Jeong, Y.S., Kim, D., Lee, Y.S., Kim, H.J., Han, J.Y., Im, S.S., Chong, H.K., Kwon, J.K., Cho, Y.H., Kim, W.K., Osborne, T.F., Horton, J.D., Jun, H.S., Ahn, Y.H., Ahn, S.M., and Cha, J.Y. (2011). Integrated expression profiling and genome-wide analysis of ChREBP targets reveals the dual role for ChREBP in glucose-regulated gene expression. PLoS One *6*, e22544.

Johnson, R.L., Huang, W., Jadhav, A., Austin, C.P., Inglese, J., and Martinez, E.D. (2008). A quantitative high-throughput screen identifies potential epigenetic modulators of gene expression. Anal Biochem *375*, 237-248.

Jonasson, O., and Hoversten, G.H. (1978). Replacement of pancreatic beta cells as treatment for diabetes mellitus: a review. Surg Annu *10*, 1-21.

Jones, P.L., and Wolffe, A.P. (1999). Relationships between chromatin organization and DNA methylation in determining gene expression. Semin Cancer Biol *9*, 339-347.

Kabashima, T., Kawaguchi, T., Wadzinski, B.E., and Uyeda, K. (2003). Xylulose 5-phosphate mediates glucose-induced lipogenesis by xylulose 5-phosphate-

activated protein phosphatase in rat liver. Proc Natl Acad Sci U S A *100*, 5107-5112.

Kanatsuka, A., Makino, H., Sakurada, M., Hashimoto, N., Yamaguchi, T., and Yoshida, S. (1987). Biphasic insulin response to high glucose and a role of protons and calcium. Endocrinology *120*, 77-82.

Kardestuncer, T., Wu, H., Lim, A.L., and Neer, E.J. (1998). Cardiac myocytes express mRNA for ten RGS proteins: changes in RGS mRNA expression in ventricular myocytes and cultured atria. FEBS Lett *438*, 285-288.

Kawaguchi, T., Osatomi, K., Yamashita, H., Kabashima, T., and Uyeda, K. (2002). Mechanism for fatty acid "sparing" effect on glucose-induced transcription: regulation of carbohydrate-responsive element-binding protein by AMP-activated protein kinase. J Biol Chem *277*, 3829-3835.

Kawaguchi, T., Takenoshita, M., Kabashima, T., and Uyeda, K. (2001). Glucose and cAMP regulate the L-type pyruvate kinase gene by phosphorylation/dephosphorylation of the carbohydrate response element binding protein. Proc Natl Acad Sci U S A *98*, 13710-13715.

Keller, M.P., Choi, Y., Wang, P., Davis, D.B., Rabaglia, M.E., Oler, A.T., Stapleton, D.S., Argmann, C., Schueler, K.L., Edwards, S., Steinberg, H.A., Chaibub Neto, E., Kleinhanz, R., Turner, S., Hellerstein, M.K., Schadt, E.E., Yandell, B.S., Kendziorski, C., and Attie, A.D. (2008). A gene expression network model of type 2 diabetes links cell cycle regulation in islets with diabetes susceptibility. Genome Res *18*, 706-716.

Kikutani, H., and Makino, S. (1992). The murine autoimmune diabetes model: NOD and related strains. Adv Immunol *51*, 285-322.

Kim, J.H., Lee, J.Y., Lee, K.T., Lee, J.K., Lee, K.H., Jang, K.T., Heo, J.S., Choi, S.H., and Rhee, J.C. (2010). RGS16 and FosB underexpressed in pancreatic cancer with lymph node metastasis promote tumor progression. Tumour Biol *31*, 541-548.

Kim, S.K., and MacDonald, R.J. (2002). Signaling and transcriptional control of pancreatic organogenesis. Curr Opin Genet Dev *12*, 540-547.

Klein, W.M., Hruban, R.H., Klein-Szanto, A.J., and Wilentz, R.E. (2002). Direct correlation between proliferative activity and dysplasia in pancreatic

intraepithelial neoplasia (PanIN): additional evidence for a recently proposed model of progression. Mod Pathol *15*, 441-447.

Kleuss, C., Raw, A.S., Lee, E., Sprang, S.R., and Gilman, A.G. (1994). Mechanism of GTP hydrolysis by G-protein alpha subunits. Proc Natl Acad Sci U S A *91*, 9828-9831.

Klinger, S., Poussin, C., Debril, M.B., Dolci, W., Halban, P.A., and Thorens, B. (2008). Increasing GLP-1-induced beta-cell proliferation by silencing the negative regulators of signaling cAMP response element modulator-alpha and DUSP14. Diabetes *57*, 584-593.

Kloppel, G., and Luttges, J. (2004). The pathology of ductal-type pancreatic carcinomas and pancreatic intraepithelial neoplasia: insights for clinicians. Curr Gastroenterol Rep *6*, 111-118.

Klover, P.J., and Mooney, R.A. (2004). Hepatocytes: critical for glucose homeostasis. Int J Biochem Cell Biol *36*, 753-758.

Koelle, M.R., and Horvitz, H.R. (1996). EGL-10 regulates G protein signaling in the C. elegans nervous system and shares a conserved domain with many mammalian proteins. Cell *84*, 115-125.

Kreymann, B., Williams, G., Ghatei, M.A., and Bloom, S.R. (1987). Glucagon-like peptide-1 7-36: a physiological incretin in man. Lancet *2*, 1300-1304.

Kritzik, M.R., Jones, E., Chen, Z., Krakowski, M., Krahl, T., Good, A., Wright, C., Fox, H., and Sarvetnick, N. (1999). PDX-1 and Msx-2 expression in the regenerating and developing pancreas. J Endocrinol *163*, 523-530.

Kroeze, W.K., Douglas S.J., and Bryan R.L. (2003). G-protein-coupled receptors at a glance. J Cell Sci *116*, 4867-4869.

Krumins, A.M., Barker, S.A., Huang, C., Sunahara, R.K., Yu, K., Wilkie, T.M., Gold, S.J., and Mumby, S.M. (2004). Differentially regulated expression of endogenous RGS4 and RGS7. J Biol Chem *279*, 2593-2599.

Kuendgen, A., Schmid, M., Schlenk, R., Knipp, S., Hildebrandt, B., Steidl, C., Germing, U., Haas, R., Dohner, H., and Gattermann, N. (2006). The histone deacetylase (HDAC) inhibitor valproic acid as monotherapy or in combination with all-trans retinoic acid in patients with acute myeloid leukemia. Cancer *106*, 112-119.

Kumar, R., Balhuizen, A., Amisten, S., Lundquist, I., and Salehi, A. (2011). Insulinotropic and antidiabetic effects of 17beta-estradiol and the GPR30 agonist G-1 on human pancreatic islets. Endocrinology *152*, 2568-2579.

Kuo, C.Y., Hsu, C.T., Ho, C.S., Su, T.E., Wu, M.H., and Wang, C.J. (2011). Accuracy and precision evaluation of seven self-monitoring blood glucose systems. Diabetes Technol Ther *13*, 596-600.

Kuwata, H., Nakao, K., Harada, T., Matsuda, I., and Aiba, A. (2007). Generation of RGS8 null mutant mice by Cre/loxP system. Kobe J Med Sci *53*, 275-281.

Lacy, P.E. (1957). Electron microscopic identification of different cell types in the islets of Langerhans of the guinea pig, rat, rabbit and dog. Anat Rec *128*, 255-267.

Lacy, P.E. (1961). Electron microscopy of the beta cell of the pancreas. Am J Med *31*, 851-859.

Lacy, P.E. (1972). The secretion of insulin. Diabetes *21*, 510.

Lacy, P.E. (1975). Endocrine secretory mechanisms. A review. Am J Pathol *79*, 170-188.

Lacy, P.E. (1995). Islet cell transplantation for insulin-dependent diabetes. Hosp Pract (Minneap) *30*, 41-45.

Lacy, P.E., Davie, J.M., and Finke, E.H. (1980). Effect of culture on islet rejection. Diabetes *29 Suppl 1*, 93-97.

Laherty, C.D., Yang, W.M., Sun, J.M., Davie, J.R., Seto, E., and Eisenman, R.N. (1997). Histone deacetylases associated with the mSin3 corepressor mediate mad transcriptional repression. Cell *89*, 349-356.

Lammert, E., Cleaver, O., and Melton, D. (2003). Role of endothelial cells in early pancreas and liver development. Mech Dev *120*, 59-64.

Lampel, M., and Kern, H.F. (1977). Acute interstitial pancreatitis in the rat induced by excessive doses of a pancreatic secretagogue. Virchows Arch A Pathol Anat Histol *373*, 97-117.

Langerhans, P. (1869). [Contributions to the microscopic anatomy of the pancreas]. (Berlin, Gustav Lange).

Le May, C., Chu, K., Hu, M., Ortega, C.S., Simpson, E.R., Korach, K.S., Tsai, M.J., and Mauvais-Jarvis, F. (2006). Estrogens protect pancreatic beta-cells from apoptosis and prevent insulin-deficient diabetes mellitus in mice. Proc Natl Acad Sci U S A *103*, 9232-9237.

Leiter, E.H. (1982). Multiple low-dose streptozotocin-induced hyperglycemia and insulitis in C57BL mice: influence of inbred background, sex, and thymus. Proc Natl Acad Sci U S A *79*, 630-634.

Leloup, C., Orosco, M., Serradas, P., Nicolaidis, S., and Penicaud, L. (1998). Specific inhibition of GLUT2 in arcuate nucleus by antisense oligonucleotides suppresses nervous control of insulin secretion. Brain Res Mol Brain Res *57*, 275-280.

Li, J., Peet, G.W., Balzarano, D., Li, X., Massa, P., Barton, R.W., and Marcu, K.B. (2001). Novel NEMO/IkappaB kinase and NF-kappa B target genes at the pre-B to immature B cell transition. J Biol Chem *276*, 18579-18590.

Liang, X.D., Guo, Y.Y., Sun, M., Ding, Y., Wang, N., Yuan, L., and De, W. (2011). Streptozotocin-induced expression of Ngn3 and Pax4 in neonatal rat pancreatic alpha-cells. World J Gastroenterol *17*, 2812-2820.

Lieber, M., Mazzetta, J., Nelson-Rees, W., Kaplan, M., and Todaro, G. (1975). Establishment of a continuous tumor-cell line (panc-1) from a human carcinoma of the exocrine pancreas. Int J Cancer *15*, 741-747.

Like, A.A., Appel, M.C., Williams, R.M., and Rossini, A.A. (1978). Streptozotocin-induced pancreatic insulitis in mice. Morphologic and physiologic studies. Lab Invest *38*, 470-486.

Like, A.A., and Rossini, A.A. (1976). Streptozotocin-induced pancreatic insulitis: new model of diabetes mellitus. Science *193*, 415-417.

Lin, R.J., Nagy, L., Inoue, S., Shao, W., Miller, W.H., Jr., and Evans, R.M. (1998). Role of the histone deacetylase complex in acute promyelocytic leukaemia. Nature *391*, 811-814.

Liu, J.P., Komachi, M., Tomura, H., Mogi, C., Damirin, A., Tobo, M., Takano, M., Nochi, H., Tamoto, K., Sato, K., and Okajima, F. (2010). Ovarian cancer G protein-coupled receptor 1-dependent and -independent vascular actions to acidic pH in human aortic smooth muscle cells. Am J Physiol Heart Circ Physiol *299*, H731-742.

Liu, S., Le May, C., Wong, W.P., Ward, R.D., Clegg, D.J., Marcelli, M., Korach, K.S., and Mauvais-Jarvis, F. (2009). Importance of extranuclear estrogen receptor-alpha and membrane G protein-coupled estrogen receptor in pancreatic islet survival. Diabetes *58*, 2292-2302.

Liu, S., and Mauvais-Jarvis, F. (2009). Rapid, nongenomic estrogen actions protect pancreatic islet survival. Islets *1*, 273-275.

Liu, S., and Mauvais-Jarvis, F. (2010). Minireview: Estrogenic protection of beta-cell failure in metabolic diseases. Endocrinology *151*, 859-864.

Lohmann, K. (1929). [On the pyrophosphate fraction in muscle]. Naturwissenschaften *17*, 624-625.

Lohr, M., Trautmann, B., Gottler, M., Peters, S., Zauner, I., Maier, A., Kloppel, G., Liebe, S., and Kreuser, E.D. (1996). Expression and function of receptors for extracellular matrix proteins in human ductal adenocarcinomas of the pancreas. Pancreas *12*, 248-259.

Lohr, M., Trautmann, B., Gottler, M., Peters, S., Zauner, I., Maillet, B., and Kloppel, G. (1994). Human ductal adenocarcinomas of the pancreas express extracellular matrix proteins. Br J Cancer *69*, 144-151.

Ludwig, M.G., Vanek, M., Guerini, D., Gasser, J.A., Jones, C.E., Junker, U., Hofstetter, H., Wolf, R.M., and Seuwen, K. (2003). Proton-sensing G-protein-coupled receptors. Nature *425*, 93-98.

Luo, X., Popov, S., Bera, A.K., Wilkie, T.M., and Muallem, S. (2001). RGS proteins provide biochemical control of agonist-evoked [Ca2+]i oscillations. Mol Cell *7*, 651-660.

Lynn, F.C., Smith, S.B., Wilson, M.E., Yang, K.Y., Nekrep, N., and German, M.S. (2007). Sox9 coordinates a transcriptional network in pancreatic progenitor cells. Proc Natl Acad Sci U S A *104*, 10500-10505.

Ma, L., Robinson, L.N., and Towle, H.C. (2006). ChREBP*Mlx is the principal mediator of glucose-induced gene expression in the liver. J Biol Chem *281*, 28721-28730.

Ma, L., Tsatsos, N.G., and Towle, H.C. (2005). Direct role of ChREBP.Mlx in regulating hepatic glucose-responsive genes. J Biol Chem *280*, 12019-12027.

MacDonald, R.J., Stary, S.J., and Swift, G.H. (1982). Two similar but nonallelic rat pancreatic trypsinogens. Nucleotide sequences of the cloned cDNAs. J Biol Chem *257*, 9724-9732.

MacDonald, R.J., Swift, G.H., and Real, F.X. (2010). Transcriptional control of acinar development and homeostasis. Prog Mol Biol Transl Sci *97*, 1-40.

Madsen, O.D., Nielsen, J.H., Michelsen, B., Westermark, P., Betsholtz, C., Nishi, M., and Steiner, D.F. (1991). Islet amyloid polypeptide and insulin expression are controlled differently in primary and transformed islet cells. Mol Endocrinol *5*, 143-148.

Maeda, T., Imanishi, Y., and Palczewski, K. (2003). Rhodopsin phosphorylation: 30 years later. Prog Retin Eye Res *22*, 417-434.

Magenheim, J., Klein, A.M., Stanger, B.Z., Ashery-Padan, R., Sosa-Pineda, B., Gu, G., and Dor, Y. (2011). Ngn3(+) endocrine progenitor cells control the fate and morphogenesis of pancreatic ductal epithelium. Dev Biol *359*, 26-36.

Malumbres, M., and Pellicer, A. (1998). RAS pathways to cell cycle control and cell transformation. Front Biosci *3*, d887-912.

Mansford, K.R., and Opie, L. (1968). Comparison of metabolic abnormalities in diabetes mellitus induced by streptozotocin or by alloxan. Lancet *1*, 670-671.

Marks, J.L., Waite, K., and Li, M. (1993). Effects of streptozotocin-induced diabetes mellitus and insulin treatment on neuropeptide Y mRNA in the rat hypothalamus. Diabetologia *36*, 497-502.

Mathis, D., Vence, L., and Benoist, C. (2001). beta-Cell death during progression to diabetes. Nature *414*, 792-798.

Matschinsky, F.M. (2005). Glucokinase, glucose homeostasis, and diabetes mellitus. Curr Diab Rep *5*, 171-176.

Matschinsky, F.M., and Collins, H.W. (1997). Essential biochemical design features of the fuel-sensing system in pancreatic beta-cells. Chem Biol *4*, 249-257.

McCoy, K.L., and Hepler, J.R. (2009). Regulators of G protein signaling proteins as central components of G protein-coupled receptor signaling complexes. Prog Mol Biol Transl Sci *86*, 49-74.

McEvoy, R.C., Andersson, J., Sandler, S., and Hellerstrom, C. (1984). Multiple low-dose streptozotocin-induced diabetes in the mouse. Evidence for stimulation of a cytotoxic cellular immune response against an insulin-producing beta cell line. J Clin Invest *74*, 715-722.

McKinsey, T.A., Zhang, C.L., Lu, J., and Olson, E.N. (2000). Signal-dependent nuclear export of a histone deacetylase regulates muscle differentiation. Nature *408*, 106-111.

Meyerhof, O. (1927). Recent Investigations on the Aerobic and an-Aerobic Metabolism of Carbohydrates. J Gen Physiol *8*, 531-542.

Miles, R.R., Sluka, J.P., Santerre, R.F., Hale, L.V., Bloem, L., Boguslawski, G., Thirunavukkarasu, K., Hock, J.M., and Onyia, J.E. (2000). Dynamic regulation of RGS2 in bone: potential new insights into parathyroid hormone signaling mechanisms. Endocrinology *141*, 28-36.

Miller, K., Kim, A., Kilimnik, G., Jo, J., Moka, U., Periwal, V., and Hara, M. (2009). Islet formation during the neonatal development in mice. PLoS One *4*, e7739.

Mittmann, C., Schuler, C., Chung, C.H., Hoppner, G., Nose, M., Kehrl, J.H., and Wieland, T. (2001). Evidence for a short form of RGS3 preferentially expressed in the human heart. Naunyn Schmiedebergs Arch Pharmacol *363*, 456-463.

Mixon, M.B., Lee, E., Coleman, D.E., Berghuis, A.M., Gilman, A.G., and Sprang, S.R. (1995). Tertiary and quaternary structural changes in Gi alpha 1 induced by GTP hydrolysis. Science *270*, 954-960.

Miyawaki, K., Yamada, Y., Yano, H., Niwa, H., Ban, N., Ihara, Y., Kubota, A., Fujimoto, S., Kajikawa, M., Kuroe, A., Tsuda, K., Hashimoto, H., Yamashita, T., Jomori, T., Tashiro, F., Miyazaki, J., and Seino, Y. (1999). Glucose intolerance caused by a defect in the entero-insular axis: a study in gastric inhibitory polypeptide receptor knockout mice. Proc Natl Acad Sci U S A *96*, 14843-14847.

Mojsov, S., Heinrich, G., Wilson, I.B., Ravazzola, M., Orci, L., and Habener, J.F. (1986). Preproglucagon gene expression in pancreas and intestine diversifies at the level of post-translational processing. J Biol Chem *261*, 11880-11889.

Moller, D.E. (2001). New drug targets for type 2 diabetes and the metabolic syndrome. Nature *414*, 821-827.

Moore, P.S., Sipos, B., Orlandini, S., Sorio, C., Real, F.X., Lemoine, N.R., Gress, T., Bassi, C., Kloppel, G., Kalthoff, H., Ungefroren, H., Lohr, M., and Scarpa, A. (2001). Genetic profile of 22 pancreatic carcinoma cell lines. Analysis of K-ras, p53, p16 and DPC4/Smad4. Virchows Arch *439*, 798-802.

Mortazavi, A., Williams, B.A., McCue, K., Schaeffer, L., and Wold, B. (2008). Mapping and quantifying mammalian transcriptomes by RNA-Seq. Nat Methods *5*, 621-628.

Murata, F., Yokota, S., and Nagata, T. (1968). Electron microscopic demonstration of lipase in the pancreatic acinar cells of mice. Histochemie *13*, 215-222.

Nagalakshmi, U., Wang, Z., Waern, K., Shou, C., Raha, D., Gerstein, M., and Snyder, M. (2008). The transcriptional landscape of the yeast genome defined by RNA sequencing. Science *320*, 1344-1349.

Nagy, L., Kao, H.Y., Chakravarti, D., Lin, R.J., Hassig, C.A., Ayer, D.E., Schreiber, S.L., and Evans, R.M. (1997). Nuclear receptor repression mediated by a complex containing SMRT, mSin3A, and histone deacetylase. Cell *89*, 373-380.

Nakagawa, T., Minami, M., and Satoh, M. (2001). Up-regulation of RGS4 mRNA by opioid receptor agonists in PC12 cells expressing cloned mu- or kappa-opioid receptors. Eur J Pharmacol *433*, 29-36.

Nakajima, H., Kim, Y.B., Terano, H., Yoshida, M., and Horinouchi, S. (1998). FR901228, a potent antitumor antibiotic, is a novel histone deacetylase inhibitor. Exp Cell Res *241*, 126-133.

Nakashima, K., Kanda, Y., Hirokawa, Y., Kawasaki, F., Matsuki, M., and Kaku, K. (2009). MIN6 is not a pure beta cell line but a mixed cell line with other pancreatic endocrine hormones. Endocr J *56*, 45-53.

Nason, R.W., Rajotte, R.V., and Warnock, G.L. (1988). Pancreatic islet cell transplantation: past, present and future. Diabetes Res *7*, 1-11.

Natochin, M., McEntaffer, R.L., and Artemyev, N.O. (1998). Mutational analysis of the Asn residue essential for RGS protein binding to G-proteins. J Biol Chem *273*, 6731-6735.

Nauck, M.A., Baller, B., and Meier, J.J. (2004). Gastric inhibitory polypeptide and glucagon-like peptide-1 in the pathogenesis of type 2 diabetes. Diabetes *53 Suppl 3*, S190-196.

Neitzel, K.L., and Hepler, J.R. (2006). Cellular mechanisms that determine selective RGS protein regulation of G protein-coupled receptor signaling. Semin Cell Dev Biol *17*, 383-389.

Ngarmukos, C., Baur, E.L., and Kumagai, A.K. (2001). Co-localization of GLUT1 and GLUT4 in the blood-brain barrier of the rat ventromedial hypothalamus. Brain Res *900*, 1-8.

Ni, Y.G., Gold, S.J., Iredale, P.A., Terwilliger, R.Z., Duman, R.S., and Nestler, E.J. (1999). Region-specific regulation of RGS4 (Regulator of G-protein-signaling protein type 4) in brain by stress and glucocorticoids: in vivo and in vitro studies. J Neurosci *19*, 3674-3680.

Niederau, C., Ferrell, L.D., and Grendell, J.H. (1985). Caerulein-induced acute necrotizing pancreatitis in mice: protective effects of proglumide, benzotript, and secretin. Gastroenterology *88*, 1192-1204.

Niederau, C., and Grendell, J.H. (1999). Role of cholecystokinin in the development and progression of acute pancreatitis and the potential of therapeutic application of cholecystokinin receptor antagonists. Digestion *60 Suppl 1*, 69-74.

Nishio, T., Toyoda, Y., Hiramatsu, M., Chiba, T., and Miwa, I. (2006). Decline in glucokinase activity in the arcuate nucleus of streptozotocin-induced diabetic rats. Biol Pharm Bull *29*, 216-219.

Noguchi, H. (2007). Stem cells for the treatment of diabetes. Endocr J *54*, 7-16.

Noguchi, H. (2010). Production of pancreatic beta-cells from stem cells. Curr Diabetes Rev *6*, 184-190.

Nomoto, S., Adachi, K., Yang, L.X., Hirata, Y., Muraguchi, S., and Kiuchi, K. (1997). Distribution of RGS4 mRNA in mouse brain shown by in situ hybridization. Biochem Biophys Res Commun *241*, 281-287.

Noordeen, N.A., Khera, T.K., Sun, G., Longbottom, E.R., Pullen, T.J., da Silva Xavier, G., Rutter, G.A., and Leclerc, I. (2010). Carbohydrate-responsive element-binding protein (ChREBP) is a negative regulator of ARNT/HIF-1beta gene expression in pancreatic islet beta-cells. Diabetes *59*, 153-160.

Novogrodsky, A., Dvir, A., Ravid, A., Shkolnik, T., Stenzel, K.H., Rubin, A.L., and Zaizov, R. (1983). Effect of polar organic compounds on leukemic cells. Butyrate-induced partial remission of acute myelogenous leukemia in a child. Cancer *51*, 9-14.

Nuttall, F.Q., Gilboe, D.P., Gannon, M.C., Niewoehner, C.B., and Tan, A.W. (1988). Regulation of glycogen synthesis in the liver. Am J Med *85*, 77-85.

Oh, D.Y., Talukdar, S., Bae, E.J., Imamura, T., Morinaga, H., Fan, W., Li, P., Lu, W.J., Watkins, S.M., and Olefsky, J.M. (2010). GPR120 is an omega-3 fatty acid receptor mediating potent anti-inflammatory and insulin-sensitizing effects. Cell *142*, 687-698.

Oliver, E.H., Sartin, J.L., Dieberg, G., Rahe, C.H., Marple, D.N., and Kemppainen, R.J. (1989). Effects of acute insulin deficiency on catecholamine and indoleamine content and catecholamine turnover in microdissected hypothalamic nuclei in streptozotocin-diabetic rats. Acta Endocrinol (Copenh) *120*, 343-350.

Orskov, C. (1992). Glucagon-like peptide-1, a new hormone of the entero-insular axis. Diabetologia *35*, 701-711.

Paik, S.G., Fleischer, N., and Shin, S.I. (1980). Insulin-dependent diabetes mellitus induced by subdiabetogenic doses of streptozotocin: obligatory role of cell-mediated autoimmune processes. Proc Natl Acad Sci U S A *77*, 6129-6133.

Pajvani, U.B., Trujillo, M.E., Combs, T.P., Iyengar, P., Jelicks, L., Roth, K.A., Kitsis, R.N., and Scherer, P.E. (2005). Fat apoptosis through targeted activation of caspase 8: a new mouse model of inducible and reversible lipoatrophy. Nat Med *11*, 797-803.

Panetta, R., Guo, Y., Magder, S., and Greenwood, M.T. (1999). Regulators of G-protein signaling (RGS) 1 and 16 are induced in response to bacterial lipopolysaccharide and stimulate c-fos promoter expression. Biochem Biophys Res Commun *259*, 550-556.

Park, E.S., Echetebu, C.O., Soloff, S., and Soloff, M.S. (2002). Oxytocin stimulation of RGS2 mRNA expression in cultured human myometrial cells. Am J Physiol Endocrinol Metab *282*, E580-584.

Parr, E.L., Bowen, K.M., and Lafferty, K.J. (1980). Cellular changes in cultured mouse thyroid glands and islets of Langerhans. Transplantation *30*, 135-141.

Parsa, I., and Marsh, W.H. (1976). An in vitro model of pancreatic carcinoma. Morphology and in vivo growth. Am J Pathol *84*, 469-478.

Pashkov, V., Huang, J., Parameswara, V.K., Kedzierski, W., Kurrasch, D.M., Tall, G.G., Esser, V., Gerard, R.D., Uyeda, K., Towle, H.C., and Wilkie, T.M.

(2011). Regulator of G protein signaling (RGS16) inhibits hepatic fatty acid oxidation in a carbohydrate response element-binding protein (ChREBP)-dependent manner. J Biol Chem *286*, 15116-15125.

Pellise, M., Castells, A., Gines, A., Sole, M., Mora, J., Castellvi-Bel, S., Rodriguez-Moranta, F., Fernandez-Esparrach, G., Llach, J., Bordas, J.M., Navarro, S., and Pique, J.M. (2003). Clinical usefulness of KRAS mutational analysis in the diagnosis of pancreatic adenocarcinoma by means of endosonography-guided fine-needle aspiration biopsy. Aliment Pharmacol Ther *17*, 1299-1307.

Pennington, S.R. (1987). G proteins and diabetes. Nature *327*, 188-189.

Pepperl, D.J., Shah-Basu, S., VanLeeuwen, D., Granneman, J.G., and MacKenzie, R.G. (1998). Regulation of RGS mRNAs by cAMP in PC12 cells. Biochem Biophys Res Commun *243*, 52-55.

Perrier, P., Martinez, F.O., Locati, M., Bianchi, G., Nebuloni, M., Vago, G., Bazzoni, F., Sozzani, S., Allavena, P., and Mantovani, A. (2004). Distinct transcriptional programs activated by interleukin-10 with or without lipopolysaccharide in dendritic cells: induction of the B cell-activating chemokine, CXC chemokine ligand 13. J Immunol *172*, 7031-7042.

Polak, J.M., Bloom, S., Coulling, I., and Pearse, A.G. (1971). Immunofluorescent localization of enteroglucagon cells in the gastrointestinal tract of the dog. Gut *12*, 311-318.

Polonsky, K.S., Sturis, J., and Bell, G.I. (1996). Seminars in Medicine of the Beth Israel Hospital, Boston. Non-insulin-dependent diabetes mellitus - a genetically programmed failure of the beta cell to compensate for insulin resistance. N Engl J Med *334*, 777-783.

Popov, S., Yu, K., Kozasa, T., and Wilkie, T.M. (1997). The regulators of G protein signaling (RGS) domains of RGS4, RGS10, and GAIP retain GTPase activating protein activity in vitro. Proc Natl Acad Sci U S A *94*, 7216-7220.

Prasher, D.C., Eckenrode, V.K., Ward, W.W., Prendergast, F.G., and Cormier, M.J. (1992). Primary structure of the Aequorea victoria green-fluorescent protein. Gene *111*, 229-233.

Quesada, I., Tuduri, E., Ripoll, C., and Nadal, A. (2008). Physiology of the pancreatic alpha-cell and glucagon secretion: role in glucose homeostasis and diabetes. J Endocrinol *199*, 5-19.

Rabanal, R., Fondevila, D., Vargas, A., Ramis, A., Badiola, J., and Ferrer, L. (1992). Immunocytochemical detection of amylase, carboxypeptidase A, carcinoembryonic antigen and alpha 1-antitrypsin in carcinomas of the exocrine pancreas of the dog. Res Vet Sci *52*, 217-223.

Rabinovitch, A., Russell, T., and Mintz, D.H. (1979). Factors from fibroblasts promote pancreatic islet B cell survival in tissue culture. Diabetes *28*, 1108-1113.

Rao, K.N., Takahashi, S., and Shinozuka, H. (1980). Acinar cell carcinoma of the rat pancreas grown in cell culture and in nude mice. Cancer Res *40*, 592-597.

Raufman, J.P., Jensen, R.T., Sutliff, V.E., Pisano, J.J., and Gardner, J.D. (1982). Actions of Gila monster venom on dispersed acini from guinea pig pancreas. Am J Physiol *242*, G470-474.

Regard, J.B., Kataoka, H., Cano, D.A., Camerer, E., Yin, L., Zheng, Y.W., Scanlan, T.S., Hebrok, M., and Coughlin, S.R. (2007). Probing cell type-specific functions of Gi in vivo identifies GPCR regulators of insulin secretion. J Clin Invest *117*, 4034-4043.

Regard, J.B., Sato, I.T., and Coughlin, S.R. (2008). Anatomical profiling of G protein-coupled receptor expression. Cell *135*, 561-571.

Reif, K., and Cyster, J.G. (2000). RGS molecule expression in murine B lymphocytes and ability to down-regulate chemotaxis to lymphoid chemokines. J Immunol *164*, 4720-4729.

Rerup, C.C. (1970). Drugs producing diabetes through damage of the insulin secreting cells. Pharmacol Rev *22*, 485-518.

Reuter, G., Giarre, M., Farah, J., Gausz, J., Spierer, A., and Spierer, P. (1990). Dependence of position-effect variegation in Drosophila on dose of a gene encoding an unusual zinc-finger protein. Nature *344*, 219-223.

Riekenberg, S., Farhat, K., Debarry, J., Heine, H., Jung, G., Wiesmuller, K.H., and Ulmer, A.J. (2009). Regulators of G-protein signalling are modulated by bacterial lipopeptides and lipopolysaccharide. FEBS J *276*, 649-659.

Romero, D.G., Plonczynski, M.W., Gomez-Sanchez, E.P., Yanes, L.L., and Gomez-Sanchez, C.E. (2006). RGS2 is regulated by angiotensin II and functions as a negative feedback of aldosterone production in H295R human adrenocortical cells. Endocrinology *147*, 3889-3897.

Rosenbaum, D.M., Rasmussen, S.G., and Kobilka, B.K. (2009). The structure and function of G-protein-coupled receptors. Nature *459*, 356-363.

Ross, E.M., and Wilkie, T.M. (2000). GTPase-activating proteins for heterotrimeric G proteins: regulators of G protein signaling (RGS) and RGS-like proteins. Annu Rev Biochem *69*, 795-827.

Rossini, A.A., Like, A.A., Chick, W.L., Appel, M.C., and Cahill, G.F., Jr. (1977). Studies of streptozotocin-induced insulitis and diabetes. Proc Natl Acad Sci U S A *74*, 2485-2489.

Rossini, A.A., Williams, R.M., Appel, M.C., and Like, A.A. (1978). Sex differences in the multiple-dose streptozotocin model of diabetes. Endocrinology *103*, 1518-1520.

Ruiz de Azua, I., Scarselli, M., Rosemond, E., Gautam, D., Jou, W., Gavrilova, O., Ebert, P.J., Levitt, P., and Wess, J. (2010). RGS4 is a negative regulator of insulin release from pancreatic beta-cells in vitro and in vivo. Proc Natl Acad Sci U S A *107*, 7999-8004.

Sachdeva, M.M., and Stoffers, D.A. (2009). Minireview: Meeting the demand for insulin: molecular mechanisms of adaptive postnatal beta-cell mass expansion. Mol Endocrinol *23*, 747-758.

Saitoh, O., Masuho, I., Terakawa, I., Nomoto, S., Asano, T., and Kubo, Y. (2001). Regulator of G protein signaling 8 (RGS8) requires its NH2 terminus for subcellular localization and acute desensitization of G protein-gated K+ channels. J Biol Chem *276*, 5052-5058.

Saltiel, A.R. (2001). New perspectives into the molecular pathogenesis and treatment of type 2 diabetes. Cell *104*, 517-529.

San Roman, J.I., De Dios, I., Manso, M.A., Calvo, J.J., and Lopez, M.A. (1990). Caerulein-induced acute pancreatitis in the rat. Pancreatic secretory response to cholecystokinin. Arch Int Physiol Biochim *98*, 237-243.

Saraste, M. (1999). Oxidative phosphorylation at the fin de siecle. Science *283*, 1488-1493.

Sarvetnick, N.E., and Gu, D. (1992). Regeneration of pancreatic endocrine cells in interferon-gamma transgenic mice. Adv Exp Med Biol *321*, 85-89; discussion 91-83.

Sassmann, A., Gier, B., Grone, H.J., Drews, G., Offermanns, S., and Wettschureck, N. (2010). The Gq/G11-mediated signaling pathway is critical for autocrine potentiation of insulin secretion in mice. J Clin Invest *120*, 2184-2193.

Sasson, R., Dantes, A., Tajima, K., and Amsterdam, A. (2003). Novel genes modulated by FSH in normal and immortalized FSH-responsive cells: new insights into the mechanism of FSH action. FASEB J *17*, 1256-1266.

Sasson, R., Rimon, E., Dantes, A., Cohen, T., Shinder, V., Land-Bracha, A., and Amsterdam, A. (2004). Gonadotrophin-induced gene regulation in human granulosa cells obtained from IVF patients. Modulation of steroidogenic genes, cytoskeletal genes and genes coding for apoptotic signalling and protein kinases. Mol Hum Reprod *10*, 299-311.

Schepp, W., Schmidtler, J., Riedel, T., Dehne, K., Schusdziarra, V., Holst, J.J., Eng, J., Raufman, J.P., and Classen, M. (1994). Exendin-4 and exendin-(9-39)NH2: agonist and antagonist, respectively, at the rat parietal cell receptor for glucagon-like peptide-1-(7-36)NH2. Eur J Pharmacol *269*, 183-191.

Schnedl, W.J., Ferber, S., Johnson, J.H., and Newgard, C.B. (1994). STZ transport and cytotoxicity. Specific enhancement in GLUT2-expressing cells. Diabetes *43*, 1326-1333.

Schneider, J.W., Gao, Z., Li, S., Farooqi, M., Tang, T.S., Bezprozvanny, I., Frantz, D.E., and Hsieh, J. (2008). Small-molecule activation of neuronal cell fate. Nat Chem Biol *4*, 408-410.

Seki, N., Sugano, S., Suzuki, Y., Nakagawara, A., Ohira, M., Muramatsu, M., Saito, T., and Hori, T. (1998). Isolation, tissue expression, and chromosomal assignment of human RGS5, a novel G-protein signaling regulator gene. J Hum Genet *43*, 202-205.

Serafimidis, I., Heximer, S., Beis, D., and Gavalas, A. (2011). GPCR signaling and S1P play a phylogenetically conserved role in endocrine pancreas morphogenesis. Mol Cell Biol.

Shaffer, C.D., Wallrath, L.L., and Elgin, S.C. (1993). Regulating genes by packaging domains: bits of heterochromatin in euchromatin? Trends Genet *9*, 35-37.

Shimabukuro, M., Koyama, K., Chen, G., Wang, M.Y., Trieu, F., Lee, Y., Newgard, C.B., and Unger, R.H. (1997). Direct antidiabetic effect of leptin through triglyceride depletion of tissues. Proc Natl Acad Sci U S A *94*, 4637-4641.

Shimomura, O., Johnson, F.H., and Saiga, Y. (1962). Extraction, purification and properties of aequorin, a bioluminescent protein from the luminous hydromedusan, Aequorea. J Cell Comp Physiol *59*, 223-239.

Shultz, L.D., Schweitzer, P.A., Christianson, S.W., Gott, B., Schweitzer, I.B., Tennent, B., McKenna, S., Mobraaten, L., Rajan, T.V., Greiner, D.L., and et al. (1995). Multiple defects in innate and adaptive immunologic function in NOD/LtSz-scid mice. J Immunol *154*, 180-191.

Siddique, H., Zou, J.P., Rao, V.N., and Reddy, E.S. (1998). The BRCA2 is a histone acetyltransferase. Oncogene *16*, 2283-2285.

Siderovski, D.P., Heximer, S.P., and Forsdyke, D.R. (1994). A human gene encoding a putative basic helix-loop-helix phosphoprotein whose mRNA increases rapidly in cycloheximide-treated blood mononuclear cells. DNA Cell Biol *13*, 125-147.

Siegel, E.G., Wollheim, C.B., Kikuchi, M., Renold, A.E., and Sharp, G.W. (1980). Dependency of cyclic AMP-induced insulin release on intra- and extracellular calcium in rat islets of Langerhans. J Clin Invest *65*, 233-241.

Sierra, D.A., Gilbert, D.J., Householder, D., Grishin, N.V., Yu, K., Ukidwe, P., Barker, S.A., He, W., Wensel, T.G., Otero, G., Brown, G., Copeland, N.G., Jenkins, N.A., and Wilkie, T.M. (2002). Evolution of the regulators of G-protein signaling multigene family in mouse and human. Genomics *79*, 177-185.

Sierra, D.A., Popov, S., and Wilkie, T.M. (2000). Regulators of G-protein signaling in receptor complexes. Trends Cardiovasc Med *10*, 263-268.

Singh, R.K., Shi, J., Zemaitaitis, B.W., and Muma, N.A. (2007). Olanzapine increases RGS7 protein expression via stimulation of the Janus tyrosine kinase-signal transducer and activator of transcription signaling cascade. J Pharmacol Exp Ther *322*, 133-140.

Sipos, B., Moser, S., Kalthoff, H., Torok, V., Lohr, M., and Kloppel, G. (2003). A comprehensive characterization of pancreatic ductal carcinoma cell lines: towards the establishment of an in vitro research platform. Virchows Arch *442*, 444-452.

Smit, V.T., Boot, A.J., Smits, A.M., Fleuren, G.J., Cornelisse, C.J., and Bos, J.L. (1988). KRAS codon 12 mutations occur very frequently in pancreatic adenocarcinomas. Nucleic Acids Res *16*, 7773-7782.

Snippert, H.J., Haegebarth, A., Kasper, M., Jaks, V., van Es, J.H., Barker, N., van de Wetering, M., van den Born, M., Begthel, H., Vries, R.G., Stange, D.E., Toftgard, R., and Clevers, H. (2010). Lgr6 marks stem cells in the hair follicle that generate all cell lineages of the skin. Science *327*, 1385-1389.

Song, W.J., Schreiber, W.E., Zhong, E., Liu, F.F., Kornfeld, B.D., Wondisford, F.E., and Hussain, M.A. (2008). Exendin-4 stimulation of cyclin A2 in beta-cell proliferation. Diabetes *57*, 2371-2381.

Sonksen, P.H., Judd, S.L., and Lowy, C. (1978). Home monitoring of blood-glucose. Method for improving diabetic control. Lancet *1*, 729-732.

Spiegelman, B.M., and Flier, J.S. (2001). Obesity and the regulation of energy balance. Cell *104*, 531-543.

Srinivasa, S.P., Bernstein, L.S., Blumer, K.J., and Linder, M.E. (1998). Plasma membrane localization is required for RGS4 function in Saccharomyces cerevisiae. Proc Natl Acad Sci U S A *95*, 5584-5589.

Stacey, D.W. (1988). The ras pathway: a model for the control of proliferation in animal cells. Adv Exp Med Biol *234*, 141-167.

Steger, D.J., Eberharter, A., John, S., Grant, P.A., and Workman, J.L. (1998). Purified histone acetyltransferase complexes stimulate HIV-1 transcription from preassembled nucleosomal arrays. Proc Natl Acad Sci U S A *95*, 12924-12929.

Stein, C.J., and Colditz, G.A. (2004). The epidemic of obesity. J Clin Endocrinol Metab *89*, 2522-2525.

Stevens, C.W., Manoharan, T.H., and Fahl, W.E. (1988). Characterization of mutagen-activated cellular oncogenes that confer anchorage independence to human fibroblasts and tumorigenicity to NIH 3T3 cells: sequence analysis of an enzymatically amplified mutant HRAS allele. Proc Natl Acad Sci U S A *85*, 3875-3879.

Stoeckman, A.K., Ma, L., and Towle, H.C. (2004). Mlx is the functional heteromeric partner of the carbohydrate response element-binding protein in glucose regulation of lipogenic enzyme genes. J Biol Chem *279*, 15662-15669.

Stuebe, S., Wieland, T., Kraemer, E., Stritzky, A., Schroeder, D., Seekamp, S., Vogt, A., Chen, C.K., and Patten, M. (2008). Sphingosine-1-phosphate and endothelin-1 induce the expression of rgs16 protein in cardiac myocytes by transcriptional activation of the rgs16 gene. Naunyn Schmiedebergs Arch Pharmacol *376*, 363-373.

Sumi, S. (2011). Regenerative medicine for insulin deficiency: creation of pancreatic islets and bioartificial pancreas. J Hepatobiliary Pancreat Sci *18*, 6-12.

Sutherland, E.W., and De Duve, C. (1948). Origin and distribution of the hyperglycemic-glycogenolytic factor of the pancreas. J Biol Chem *175*, 663-674.

Suzuki, T., Igari, S., Hirasawa, A., Hata, M., Ishiguro, M., Fujieda, H., Itoh, Y., Hirano, T., Nakagawa, H., Ogura, M., Makishima, M., Tsujimoto, G., and Miyata, N. (2008). Identification of G protein-coupled receptor 120-selective agonists derived from PPARgamma agonists. J Med Chem *51*, 7640-7644.

Takaori, K., Hruban, R.H., Maitra, A., and Tanigawa, N. (2004). Pancreatic intraepithelial neoplasia. Pancreas *28*, 257-262.

Takata, Y., Liu, J., Yin, F., Collins, A.R., Lyon, C.J., Lee, C.H., Atkins, A.R., Downes, M., Barish, G.D., Evans, R.M., Hsueh, W.A., and Tangirala, R.K. (2008). PPARdelta-mediated antiinflammatory mechanisms inhibit angiotensin II-accelerated atherosclerosis. Proc Natl Acad Sci U S A *105*, 4277-4282.

Takeda, J., Seino, Y., Tanaka, K., Fukumoto, H., Kayano, T., Takahashi, H., Mitani, T., Kurono, M., Suzuki, T., Tobe, T., and et al. (1987). Sequence of an intestinal cDNA encoding human gastric inhibitory polypeptide precursor. Proc Natl Acad Sci U S A *84*, 7005-7008.

Takesono, A., Zahner, J., Blumer, K.J., Nagao, T., and Kurose, H. (1999). Negative regulation of alpha2-adrenergic receptor-mediated Gi signalling by a novel pathway. Biochem J *343 Pt 1*, 77-85.

Takimoto, R., Kato, J., Terui, T., Takada, K., Kuroiwa, G., Wu, J., Ohnuma, H., Takahari, D., Kobune, M., Sato, Y., Takayama, T., Matsunaga, T., and Niitsu, Y. (2005). Augmentation of antitumor effects of p53 gene therapy by combination with HDAC inhibitor. Cancer Biol Ther *4*, 421-428.

Taminato, T., Seino, Y., Goto, Y., Inoue, Y., and Kadowaki, S. (1977). Synthetic gastric inhibitory polypeptide. Stimulatory effect on insulin and glucagon secretion in the rat. Diabetes *26*, 480-484.

Tanaka, T., Katsuma, S., Adachi, T., Koshimizu, T.A., Hirasawa, A., and Tsujimoto, G. (2008a). Free fatty acids induce cholecystokinin secretion through GPR120. Naunyn Schmiedebergs Arch Pharmacol *377*, 523-527.

Tanaka, T., Yano, T., Adachi, T., Koshimizu, T.A., Hirasawa, A., and Tsujimoto, G. (2008b). Cloning and characterization of the rat free fatty acid receptor GPR120: in vivo effect of the natural ligand on GLP-1 secretion and proliferation of pancreatic beta cells. Naunyn Schmiedebergs Arch Pharmacol *377*, 515-522.

Tateishi, K., He, J., Taranova, O., Liang, G., D'Alessio, A.C., and Zhang, Y. (2008). Generation of insulin-secreting islet-like clusters from human skin fibroblasts. J Biol Chem *283*, 31601-31607.

Taymans, J.M., Leysen, J.E., and Langlois, X. (2003). Striatal gene expression of RGS2 and RGS4 is specifically mediated by dopamine D1 and D2 receptors: clues for RGS2 and RGS4 functions. J Neurochem *84*, 1118-1127.

Teitelman, G., and Lee, J.K. (1987). Cell lineage analysis of pancreatic islet development: glucagon and insulin cells arise from catecholaminergic precursors present in the pancreatic duct. Dev Biol *121*, 454-466.

Tesmer, J.J., Berman, D.M., Gilman, A.G., and Sprang, S.R. (1997). Structure of RGS4 bound to AlF4--activated G(i alpha1): stabilization of the transition state for GTP hydrolysis. Cell *89*, 251-261.

Thorens, B. (1992). Expression cloning of the pancreatic beta cell receptor for the gluco-incretin hormone glucagon-like peptide 1. Proc Natl Acad Sci U S A *89*, 8641-8645.

Thorens, B. (2001). GLUT2 in pancreatic and extra-pancreatic gluco-detection (review). Mol Membr Biol *18*, 265-273.

Thorens, B. (2008). Glucose sensing and the pathogenesis of obesity and type 2 diabetes. Int J Obes (Lond) *32 Suppl 6*, S62-71.

Thyssen, S., Arany, E., and Hill, D.J. (2006). Ontogeny of regeneration of beta-cells in the neonatal rat after treatment with streptozotocin. Endocrinology *147*, 2346-2356.

Tomura, H., Wang, J.Q., Komachi, M., Damirin, A., Mogi, C., Tobo, M., Kon, J., Misawa, N., Sato, K., and Okajima, F. (2005). Prostaglandin I(2) production and cAMP accumulation in response to acidic extracellular pH through OGR1 in human aortic smooth muscle cells. J Biol Chem *280*, 34458-34464.

Tomura, H., Wang, J.Q., Liu, J.P., Komachi, M., Damirin, A., Mogi, C., Tobo, M., Nochi, H., Tamoto, K., Im, D.S., Sato, K., and Okajima, F. (2008). Cyclooxygenase-2 expression and prostaglandin E2 production in response to acidic pH through OGR1 in a human osteoblastic cell line. J Bone Miner Res *23*, 1129-1139.

Tourrel, C., Bailbe, D., Meile, M.J., Kergoat, M., and Portha, B. (2001). Glucagon-like peptide-1 and exendin-4 stimulate beta-cell neogenesis in streptozotocin-treated newborn rats resulting in persistently improved glucose homeostasis at adult age. Diabetes *50*, 1562-1570.

Trujillo, M.E., Pajvani, U.B., and Scherer, P.E. (2005). Apoptosis through targeted activation of caspase 8 ("ATTAC-mice"): novel mouse models of inducible and reversible tissue ablation. Cell Cycle *4*, 1141-1145.

Tsien, R.Y. (1998). The green fluorescent protein. Annu Rev Biochem *67*, 509-544.

Tsunoda, N., Ikemoto, S., Takahashi, M., Maruyama, K., Watanabe, H., Goto, N., and Ezaki, O. (1998). High-monounsaturated fat diet-induced obesity and diabetes in C57BL/6J mice. Metabolism *47*, 724-730.

Turner, B.M., and O'Neill, L.P. (1995). Histone acetylation in chromatin and chromosomes. Semin Cell Biol *6*, 229-236.

Turton, M.D., O'Shea, D., Gunn, I., Beak, S.A., Edwards, C.M., Meeran, K., Choi, S.J., Taylor, G.M., Heath, M.M., Lambert, P.D., Wilding, J.P., Smith, D.M., Ghatei, M.A., Herbert, J., and Bloom, S.R. (1996). A role for glucagon-like peptide-1 in the central regulation of feeding. Nature *379*, 69-72.

Tuveson, D.A., and Hingorani, S.R. (2005). Ductal pancreatic cancer in humans and mice. Cold Spring Harb Symp Quant Biol *70*, 65-72.

Ueda, H., Manda, T., Matsumoto, S., Mukumoto, S., Nishigaki, F., Kawamura, I., and Shimomura, K. (1994). FR901228, a novel antitumor bicyclic depsipeptide produced by Chromobacterium violaceum No. 968. III. Antitumor activities on experimental tumors in mice. J Antibiot (Tokyo) *47*, 315-323.

Unger, R.H. (1971). Pancreatic glucagon in health and disease. Adv Intern Med *17*, 265-288.

Unger, R.H. (1978). Role of glucagon in the pathogenesis of diabetes: the status of the controversy. Metabolism *27*, 1691-1709.

Unger, R.H. (1985). Glucagon physiology and pathophysiology in the light of new advances. Diabetologia *28*, 574-578.

Utley, R.T., Ikeda, K., Grant, P.A., Cote, J., Steger, D.J., Eberharter, A., John, S., and Workman, J.L. (1998). Transcriptional activators direct histone acetyltransferase complexes to nucleosomes. Nature *394*, 498-502.

Vanti, W.B., Nguyen, T., Cheng, R., Lynch, K.R., George, S.R., and O'Dowd, B.F. (2003). Novel human G-protein-coupled receptors. Biochem Biophys Res Commun *305*, 67-71.

Vassilatis, D.K., Hohmann, J.G., Zeng, H., Li, F., Ranchalis, J.E., Mortrud, M.T., Brown, A., Rodriguez, S.S., Weller, J.R., Wright, A.C., Bergmann, J.E., and Gaitanaris, G.A. (2003). The G protein-coupled receptor repertoires of human and mouse. Proc Natl Acad Sci U S A *100*, 4903-4908.

Vavra, J.J., Deboer, C., Dietz, A., Hanka, L.J., and Sokolski, W.T. (1959). Streptozotocin, a new antibacterial antibiotic. Antibiot Annu *7*, 230-235.

Villasenor, A., Wang, Z.V., Rivera, L.B., Ocal, O., Asterholm, I.W., Scherer, P.E., Brekken, R.A., Cleaver, O., and Wilkie, T.M. (2010). Rgs16 and Rgs8 in embryonic endocrine pancreas and mouse models of diabetes. Dis Model Mech *3*, 567-580.

von Burstin, J., Reichert, M., Wescott, M.P., and Rustgi, A.K. (2010). The pancreatic and duodenal homeobox protein PDX-1 regulates the ductal specific keratin 19 through the degradation of MEIS1 and DNA binding. PLoS One *5*, e12311.

Vranic, M. (1992). Banting Lecture: glucose turnover. A key to understanding the pathogenesis of diabetes (indirect effects of insulin). Diabetes *41*, 1188-1206.

Waget, A., Cabou, C., Masseboeuf, M., Cattan, P., Armanet, M., Karaca, M., Castel, J., Garret, C., Payros, G., Maida, A., Sulpice, T., Holst, J.J., Drucker, D.J., Magnan, C., and Burcelin, R. (2011). Physiological and pharmacological mechanisms through which the DPP-4 inhibitor sitagliptin regulates glycemia in mice. Endocrinology *152*, 3018-3029.

Wagner, M., Luhrs, H., Kloppel, G., Adler, G., and Schmid, R.M. (1998). Malignant transformation of duct-like cells originating from acini in transforming growth factor transgenic mice. Gastroenterology *115*, 1254-1262.

Walford, S., Gale, E.A., Allison, S.P., and Tattersall, R.B. (1978). Self-monitoring of blood-glucose. Improvement of diabetic control. Lancet *1*, 732-735.

Wang, J., Ducret, A., Tu, Y., Kozasa, T., Aebersold, R., and Ross, E.M. (1998). RGSZ1, a Gz-selective RGS protein in brain. Structure, membrane association, regulation by Galphaz phosphorylation, and relationship to a Gz gtpase-activating protein subfamily. J Biol Chem *273*, 26014-26025.

Wang, R.N., Bouwens, L., and Kloppel, G. (1994). Beta-cell proliferation in normal and streptozotocin-treated newborn rats: site, dynamics and capacity. Diabetologia *37*, 1088-1096.

Wang, Z., Gerstein, M., and Snyder, M. (2009). RNA-Seq: a revolutionary tool for transcriptomics. Nat Rev Genet *10*, 57-63.

Wang, Z.V., Mu, J., Schraw, T.D., Gautron, L., Elmquist, J.K., Zhang, B.B., Brownlee, M., and Scherer, P.E. (2008). PANIC-ATTAC: a mouse model for inducible and reversible beta-cell ablation. Diabetes *57*, 2137-2148.

Watson, N., Linder, M.E., Druey, K.M., Kehrl, J.H., and Blumer, K.J. (1996). RGS family members: GTPase-activating proteins for heterotrimeric G-protein alpha-subunits. Nature *383*, 172-175.

Weir, G.C., and Bonner-Weir, S. (1990). Islets of Langerhans: the puzzle of intraislet interactions and their relevance to diabetes. J Clin Invest *85*, 983-987.

Wellen, K.E., and Hotamisligil, G.S. (2005). Inflammation, stress, and diabetes. J Clin Invest *115*, 1111-1119.

Wettergren, A., Schjoldager, B., Mortensen, P.E., Myhre, J., Christiansen, J., and Holst, J.J. (1993). Truncated GLP-1 (proglucagon 78-107-amide) inhibits gastric and pancreatic functions in man. Dig Dis Sci *38*, 665-673.

Wheatley, M., Hawtin, S.R., Wesley, V.J., Howard, H.C., Simms, J., Miles, A., McEwan, K., and Parslow, R.A. (2003). Agonist binding to peptide hormone receptors. Biochem Soc Trans *31*, 35-39.

Wild, S., Roglic, G., Green, A., Sicree, R., and King, H. (2004). Global prevalence of diabetes: estimates for the year 2000 and projections for 2030. Diabetes Care *27*, 1047-1053.

Wilkie, T.M., and Kinch, L. (2005). New roles for Galpha and RGS proteins: communication continues despite pulling sisters apart. Curr Biol *15*, R843-854.

Willemer, S., Elsasser, H.P., and Adler, G. (1992). Hormone-induced pancreatitis. Eur Surg Res *24 Suppl 1*, 29-39.

Xiao, S.H., Reagan, J.D., Lee, P.H., Fu, A., Schwandner, R., Zhao, X., Knop, J., Beckmann, H., and Young, S.W. (2008). High throughput screening for orphan and liganded GPCRs. Comb Chem High Throughput Screen *11*, 195-215.

Xie, S., Li, J., Wang, J.H., Wu, Q., Yang, P., Hsu, H.C., Smythies, L.E., and Mountz, J.D. (2010). IL-17 activates the canonical NF-kappaB signaling pathway in autoimmune B cells of BXD2 mice to upregulate the expression of regulators of G-protein signaling 16. J Immunol *184*, 2289-2296.

Xu, G., Stoffers, D.A., Habener, J.F., and Bonner-Weir, S. (1999a). Exendin-4 stimulates both beta-cell replication and neogenesis, resulting in increased beta-cell mass and improved glucose tolerance in diabetic rats. Diabetes *48*, 2270-2276.

Xu, X., Zeng, W., Popov, S., Berman, D.M., Davignon, I., Yu, K., Yowe, D., Offermanns, S., Muallem, S., and Wilkie, T.M. (1999b). RGS proteins determine signaling specificity of Gq-coupled receptors. J Biol Chem *274*, 3549-3556.

Xu, Y., and Casey, G. (1996). Identification of human OGR1, a novel G protein-coupled receptor that maps to chromosome 14. Genomics *35*, 397-402.

Yamashita, H., Takenoshita, M., Sakurai, M., Bruick, R.K., Henzel, W.J., Shillinglaw, W., Arnot, D., and Uyeda, K. (2001). A glucose-responsive transcription factor that regulates carbohydrate metabolism in the liver. Proc Natl Acad Sci U S A *98*, 9116-9121.

Yang, M., Mailhot, G., Birnbaum, M.J., MacKay, C.A., Mason-Savas, A., and Odgren, P.R. (2006). Expression of and role for ovarian cancer G-protein-coupled receptor 1 (OGR1) during osteoclastogenesis. J Biol Chem *281*, 23598-23605.

Yang, S., Chen, W., Stashenko, P., and Li, Y.P. (2007). Specificity of RGS10A as a key component in the RANKL signaling mechanism for osteoclast differentiation. J Cell Sci *120*, 3362-3371.

Yang, X.W., Model, P., and Heintz, N. (1997). Homologous recombination based modification in Escherichia coli and germline transmission in transgenic mice of a bacterial artificial chromosome. Nat Biotechnol *15*, 859-865.

Yasuda, K., and Coons, A.H. (1966). Localization by immunofluroescence of amylase, trypsinogen and chymotrypsinogen in the acinar cells of the pig pancreas. J Histochem Cytochem *14*, 303-313.

Yechoor, V., and Chan, L. (2010). Minireview: beta-cell replacement therapy for diabetes in the 21st century: manipulation of cell fate by directed differentiation. Mol Endocrinol *24*, 1501-1511.

Yoshida, M., and Beppu, T. (1988). Reversible arrest of proliferation of rat 3Y1 fibroblasts in both the G1 and G2 phases by trichostatin A. Exp Cell Res *177*, 122-131.

Yowe, D., Weich, N., Prabhudas, M., Poisson, L., Errada, P., Kapeller, R., Yu, K., Faron, L., Shen, M., Cleary, J., Wilkie, T.M., Gutierrez-Ramos, C., and Hodge, M.R. (2001). RGS18 is a myeloerythroid lineage-specific regulator of G-protein-signalling molecule highly expressed in megakaryocytes. Biochem J *359*, 109-118.

Zeng, W., Xu, X., Popov, S., Mukhopadhyay, S., Chidiac, P., Swistok, J., Danho, W., Yagaloff, K.A., Fisher, S.L., Ross, E.M., Muallem, S., and Wilkie, T.M. (1998). The N-terminal domain of RGS4 confers receptor-selective inhibition of G protein signaling. J Biol Chem *273*, 34687-34690.

Zhang, C.L., McKinsey, T.A., Chang, S., Antos, C.L., Hill, J.A., and Olson, E.N. (2002). Class II histone deacetylases act as signal-responsive repressors of cardiac hypertrophy. Cell *110*, 479-488.

Zhang, L., Li, P., Hsu, T., Aguilar, H.R., Frantz, D.E., Schneider, J.W., Bachoo, R.M., and Hsieh, J. (2011a). Small-molecule blocks malignant astrocyte proliferation and induces neuronal gene expression. Differentiation *81*, 233-242.

Zhang, P., Su, J., King, M.E., Maldonado, A.E., Park, C., and Mende, U. (2011b). Regulator of G protein signaling 2 is a functionally important negative regulator of angiotensin II-induced cardiac fibroblast responses. Am J Physiol Heart Circ Physiol *301*, H147-156.

Zhang, Y., Proenca, R., Maffei, M., Barone, M., Leopold, L., and Friedman, J.M. (1994). Positional cloning of the mouse obese gene and its human homologue. Nature *372*, 425-432.

Zhao, T.J., Liang, G., Li, R.L., Xie, X., Sleeman, M.W., Murphy, A.J., Valenzuela, D.M., Yancopoulos, G.D., Goldstein, J.L., and Brown, M.S. (2010). Ghrelin O-acyltransferase (GOAT) is essential for growth hormone-mediated survival of calorie-restricted mice. Proc Natl Acad Sci U S A *107*, 7467-7472.

Zhou, H., Sziegoleit, A., and Fischer, H.P. (1995). Immunocytochemical localization of elastase 1 in human pancreas. Histochem Cell Biol *103*, 103-109.

Zimmerman, S.E., Smith, F.P., and Schein, P.S. (1981). Chemotherapy of pancreatic carcinoma. Cancer *47*, 1724-1728.

Zimmet, P., Alberti, K.G., and Shaw, J. (2001). Global and societal implications of the diabetes epidemic. Nature *414*, 782-787.

Zou, M.X., Roy, A.A., Zhao, Q., Kirshenbaum, L.A., Karmazyn, M., and Chidiac, P. (2006). RGS2 is upregulated by and attenuates the hypertrophic effect of alpha1-adrenergic activation in cultured ventricular myocytes. Cell Signal *18*, 1655-1663.